FINAL REPORT

Electroactive Polymers as Environmentally Benign Coating Replacements for Cadmium Plating on High Strength Steels

SERDP Project WP-1411

JUNE 2008

Dr. Peter Zarras
Dr. David J. Irvin
Naval Air Warfare Center Weapons Division

Strategic Environmental Research and Development Program

Report Documentation Page

Form Approved
OMB No. 0704-0188

1. REPORT DATE	2. REPORT TYPE	3. DATES COVERED
JUN 2008		**00-00-2008 to 00-00-2008**

4. TITLE AND SUBTITLE	5a. CONTRACT NUMBER
Electroactive Polymers as Environmentally Benign Coating Replacements for Cadmium Plating on High Strength Steels	5b. GRANT NUMBER
	5c. PROGRAM ELEMENT NUMBER
6. AUTHOR(S)	5d. PROJECT NUMBER
	5e. TASK NUMBER
	5f. WORK UNIT NUMBER
7. PERFORMING ORGANIZATION NAME(S) AND ADDRESS(ES) **Naval Air Warfare Center,Weapons Division,1 Administration Circle,China Lake,CA,93555**	8. PERFORMING ORGANIZATION REPORT NUMBER
9. SPONSORING/MONITORING AGENCY NAME(S) AND ADDRESS(ES)	10. SPONSOR/MONITOR'S ACRONYM(S)
	11. SPONSOR/MONITOR'S REPORT NUMBER(S)

12. DISTRIBUTION/AVAILABILITY STATEMENT
Approved for public release; distribution unlimited

13. SUPPLEMENTARY NOTES

14. ABSTRACT

15. SUBJECT TERMS

16. SECURITY CLASSIFICATION OF:			17. LIMITATION OF ABSTRACT	18. NUMBER OF PAGES	19a. NAME OF RESPONSIBLE PERSON
a. REPORT **unclassified**	b. ABSTRACT **unclassified**	c. THIS PAGE **unclassified**	**Same as Report (SAR)**	**99**	

Table of Contents

List of Figures

List of Tables

List of Acronyms

ASTM	American Society for Testing and Materials
ATR-FTIR	Attenuated total reflectance FTIR
BAM-PPV	Poly-2,5(bis-N-methyl-N-hexylamino)phenylene vinylene
7-BHN	7-bromoheptanitrile
DI water	deionized water
DSC	Differential scanning calorimetry
DMSO-d_6	deuterated dimethysulfoxide
DoD	Department of Defense
EAP	electroactive polymer
EC	equivalent circuit
EDOT	3,4-ethylenedioxyrthiophene
EDS	Energy dispersive spectroscopy
EIS	electrochemical impedance spectroscopy
FC	ferric citrate
FO	ferric oxalate
FA	ferric acetylacetonate
FTIR	Fourier transform infrared spectroscopy
GPC	Gel Permeation chromatography
HCl	hydrogen chloride
HMIS	Hazardous Materials Identification System
IC	Ion Chromatography
ICP-AES	Inductively Coupled Plasma Atomic Emission Spectroscopy
IPA	isopropyl alcohol
IVD Aluminum	ion vapor deposited aluminum
KOH	potassium hydroxide
KSC	Kennedy Space Center
ksi	thousand pounds per square inch
LANL	Los Alamos National Laboratory
MS	mass spectroscopy
3MT	3-methylthiophene
3MOT	3-methoxythiophene
NAWCWD	Naval Air Warfare Center Weapons Division
NLS	non-line-of sight
NaOH	sodium hydoxide
NR	no reaction
NMR	nuclear magnetic resonance
NFS	notched fracture strength
NFPA	National Fire Protection Agency
OCP	open circuit potential
PANI	poylaniline
P3HT	poly(3-hexylthiophene)

P3MT	poly(3-methylthiophene)
P3PPA	poly(3-pyrrol-1-yl) propanoic acid
P(7-PHA)	poly(7-pyrrol-1-yl)heptanoic acid
3PPA	3-(pyrrol-1-yl) propanoic acid
3PPN	3-(Pyrrol-1-yl) proprionitrile
7-PHN	7-pyrrol-1-yl-heptanitrile
7-PHA	7-pyrrol-1-yl-heptanoic acid
ppb	part per billion
ppm	parts per million
QBSD	Quadrapole backscatter detector
RDE	Rotating disk electrode
SEM	scanning electron microscope/microscopy
SERDP	Strategic Environmental Research and Development Program
TC	thiophene acetic acid
TD-MS	Thermal desorption-mass spectrometry
TGA	Thermal Gravometric Analysis
THF	Tertrahydrofuran
Triton B	benzyltrimethylammonium hydroxide
TP	thiophene methyl phosphonate
TYZOR 131	organic titanate ($Ti(OCH(CH_3)_2)_4$)

Acknowledgements

The financial support of the Department of Defense Strategic Environmental Research and Development Program (SERDP), under the direction of Mr. Bradley Smith, Executive Director, Dr. Jeffrey Marqusee, Technical Director, and Mr. Charles Pellerin, Weapons Systems and Platforms Program Manager is gratefully acknowledged.

The work performed under this SERDP Exploratory Development (SEED) project was conducted at the Naval Air Warfare Center Weapons Division (NAVAIR-WD). Dr. Peter Zarras led monthly and yearly reporting. Dr. Peter Zarras and Dr. David J. Irvin led the synthetic efforts and directed the overall project. Dr. Samantha Hawkins, Dr. Lawrence Baldwin and Dr. Kara D. Lormand characterized all samples using FTIR, NMR and MS. Dr. Andrew Guenthner led the work on incorporating mico-and nano-particles into the polymer film. Meghan Baronowski, Marc Pepi, Joe Hibbs and John Baronowski devised the test matrix and tested for lubricity/galling on EAP coated high strength steel samples. Mr. Chad Waltz examined EAP coated high strength steel coupons using a combination of EDS/SEM and tested for film thickness and adhesion. Dr. Lou Raymond and Dr. Tony Chau performed all hydrogen embrittlement studies and defect tolerance testing on EAP coated high strength steel samples. Dr. Florian Mansfeld and Dr. Esra Kus used EIS to measure the corrosion performance of EAP coated 3x3 high strength steel samples.

Section I

Executive Summary

Despite environmental hazards, cadmium (Cd) is still widely used in the plating industry (especially for fasteners) because of its unique combination of properties. There is no drop-in replacement for Cd-plated high-strength steels, but commercial zinc (Zn) and aluminum (Al)-filled polymers deposited by the dip-spin coating technique have shown initial promise. Although they are quite effective, the coating tends to clog fastener threads, and their torque characteristics tend to change over the course of multiple assemblies. This is a serious drawback for aerospace and other DoD applications where weapon systems require periodic strip-down and maintenance. In order to meet the environmental challenge of replacing Cd on high strength steel substrates without the loss of performance, a novel approach using electro-active polymers (EAP's) as the corrosion inhibition layer has been investigated.

All of the objectives of this SERDP SEED have been accomplished successfully. The synthesis and characterization of new monomers and the synthesis, using electroless deposition techniques and electropolymerization of EAPs that adhere to steel substrates has been completed. Both electropolymerization and electroless deposition are non-line-of-sight (NLS) techniques for coating EAPs onto steel plates and other geometries. The characterization of critical coating properties, using a combination of standard methods for fastener performance such as galling testing and hydrogen embrittlement testing, along with an evaluation of corrosion performance using impedance spectroscopy and neutral salt fog testing, EDS/SEM, has also been completed.

The results (summarized below) demonstrate that the program has achieved all of the objectives

- The new polymeric materials contain no heavy metals (Cd, Cr, Ni, Zn, Cu, etc.).
- New and known monomers, polymers and co-polymers were prepared and processed to produce thin films on steel substrates.
- Thiophene-based co-polymers with adhesion promoting groups have been formed into good quality films by solvent casting and exhibit good adhesion properties.
- Aqueous electroless deposition (NLS technique) of pyrrole-based polymers containing adhesion promoting groups has been demonstrated.
- The EAP electroless deposition coating process does not introduce hydrogen into the specimens nor lead to hydrogen enbrittlement during environmental exposure.
- EAP polymers with hard particle additives have measured galling resistance values of 6000-8000 psi, not as good as cadmium but superior to coatings such as IVD aluminum
- Several polymer coated samples containing the pyrrole monomer with a long-chain aliphatic group have passed the military requirement of 96 hrs neutral salt fog testing. The essential characteristics of the EAPs that have passed the neutral salt fog testing is the improved film quality.

In conclusion, the program has resulted in the acquisition of basic knowledge regarding synthesis techniques and the relationship between material composition and critical coating properties in EAPs for potential replacement of cadmium coatings onto high strength steels.

Section II

Objective: In order to meet the environmental challenge of replacing cadmium (Cd) on high strength steel substrates without the loss of performance, a novel approach using EAPs was investigated. The objectives include: (a) synthesis and characterization of new monomers; (b) synthesis, using electroless deposition techniques, of EAPs that will adhere to steel substrates and demonstrate NLS coating onto steel plates and fasteners; (c) demonstration of comparable corrosion resistance using accelerated weathering tests (Neutral Salt Fog ASTM B117) with Cd-plated high-strength steel coupons as control samples, measurement of barrier properties using electrochemical impedance spectroscopy (EIS) and examination for evidence of passivation of steel substrates using a combination of scanning electron microscopy (SEM) with energy-dispersive spectroscopy (EDS); and finally (d) measurement of other critical coating properties using a combination of standard methods for fastener performance such as galling testing (ASTM G98) and hydrogen embrittlement testing (ASTM F519 and F1624).

Section III

Background: The extensive use of cadmium in industrial operations such as smelting and refining of zinc, lead, copper ores, electroplating, welding, manufacture of pigments, plastic stabilizers and nickel-cadmium batteries has resulted in worker exposure to cadmium [1]. Cadmium exposure can result in pulmonary carcinogenesis, tumors of the prostate, testes and hematopoietic system [2,3]. Cadmium that is released into the environment through human endeavors can contaminate food, water and air. Cadmium can leach through soils into the groundwater where it can bind to river sediment and bioaccumulate. Cadmium does not break down in the environment and can accumulate in the food chain. Cadmium is a carcinogen and a tetragen and is highly regulated by the EPA [4].

Despite these environmental hazards, Cd is still widely used in the plating industry (especially for fasteners) because of its unique combination of properties. Cadmium plating has a unique combination of properties that makes it highly attractive for military use [5]. Several high-strength steels used by the military and commonly cadmium-plated for fastener applications include, but are not limited to the following: AISI 4340, Hy-Tuf™ (an AISI 4340 derivative created by Crucible Specialty Metals), Aermet® 100, E4340, M50, 300M, PH 13-8Mo stainless steel, and maraging Grades 200-250.

The most common method of electroplating cadmium onto high strength steel is the alkaline cyanide bath. While this technology ranks as one of the oldest for cadmium plating, it is also the most forgiving and reliable plating solution, and presently proposed replacements have difficulty in matching its performance (See Table 1) [6-12]. As stated earlier there are no drop-in replacements for Cd-plated high-strength steels, but the Dacromet, Geomet and Magni families of coatings have shown initial promise. These materials are commercial Zn and Al-filled polymers deposited by the dip-spin coating technique, and are often used for automotive applications. Although they are quite effective, the coating tends to clog fastener threads, creating installation problems. In addition, their torque characteristics tend to change over the course of multiple assemblies. This is not a problem for cars but it is a serious drawback for aerospace and other DoD applications where weapon systems require periodic strip-down and maintenance.

Table 1: Cadmium Replacements Suggested by Military, Commercial or Governmental Working Groups for High Strength Steel Fasteners [6-12]

Proposed Replacement	Organization	Possible Limitations
Ion vapor deposited (IVD) aluminum	Air Force	Line-of-sight process, holes not thoroughly coated
Sputtered aluminum	Air Force	Coating tends to gall
Tin/Zinc electroplating	Air Force	Difficult to control process
Zinc/nickel electroplating	Army	Nickel is an EPA regulated material; requires special chromate treatment
Tin/zinc electroplating	Army	Difficult to control process
Stainless steel with no coating	Army	Corrosion of carbon steel (galvanic effect)
Electroplated zinc	Army	Voluminous white corrosion products
SermeTel®(Sermatech Inc)	Navy	Performance hindered by complex geometries
Zinc/nickel with E-coat topcoat	Navy	Performance hindered by complex geometries
Zinc electroplate-alkaline bath	Navy	Better than acid-bath zinc
Zinc electroplate-acid bath	Navy	Does not perform as well as alkaline bath zinc plating
Dacromet 320/500® L/B	DoD	None listed
Boeing zinc-nickel electrodeposition	Commercial	Nickel is an EPA regulated material; requires special chromate treatment
Aluminum electroplating (Alumiplate)	DoD	Complicated application process
Aluminum manganese	DoD	Relatively expensive; inadvertent water in the bath creates HCl
Geomet ® L	Commercial	None listed
Magni 511®	Commercial	None listed
Tin-nickel	DoD	Nickel is an EPA regulated material

In order to meet the current specifications for high-strength steel fasteners, our efforts will focus on using electroactive polymers as replacements for cadmium coatings. Electroactive polymers–specifically polyaniline (PANI) have been shown to provide corrosion protection of steel alloys [13,14]. The Los Alamos National Laboratory (LANL) and the John F. Kennedy Space Center (KSC) team demonstrated that doped PANI coatings inhibited corrosion in carbon steel. The LANL-KSC work was based on earlier work by Jain et al. [15], in which the corrosion protective properties of EAPs were

hypothesized. Jain's hypothesis was based upon the idea that the interfacial contact between a metal surface and a doped EAP would generate an electric field that would restrict the flow of electrons from the metal to the outside oxidizing species. This process would thereby reduce or prevent corrosion. The LANL-KSC researchers demonstrated this idea by coating 0.05-cm thick films of PANI doped with p-toluenesulfonic acid onto carbon steel and exposing these samples to 3.5 wt% NaCl/0.1M HCl solutions. The PANI coat was covered with an epoxy topcoat and compared to epoxy topcoat alone. The PANI-epoxy topcoat samples performed significantly better than the epoxy topcoat alone. These initial studies were used as the foundation to develop EAP coatings to protect the ground support equipment from the corrosive effects of acid vapor generated during shuttle launches.

The mechanism of corrosion protection by EAPs, specifically PANI has been identified as both barrier protection and passivation of the metal alloy [16,17]. Thus EAPs also can serve as passivating coatings. EAPs have been shown to perform successfully in acidic [13,14], neutral and alkaline environments [18,19]. This combination of barrier and passivation protection is a significant technical advance over the sacrificial mechanism of the older cadmium, aluminum and zinc coatings. It avoids coating dissolution, together with the problems caused by corrosion products causing component seizure, lifting paint, and causing unsightly marks. The use of EAPs is not just a Cd alternative, but provides a new mechanism that could be incorporated more broadly into the entire DoD corrosion protection arsenal, including non-chrome primers and paints. Unlike Cd plating, it might ultimately even be applied by enlisted personnel in the field.

EAPs other than PANI have also been demonstrated to protect steel alloys in harsh environments. Poly(3-methylthiophene) (P3MT) films coated onto platinum and 430 stainless steel showed effective stabilization of the steel in a passive state [20]. P3MT films coated onto a 430SS rotating disk electrode (RDE) in 1N sulfuric acid solution showed galvanic protection. This protection was described by DeBerry [21], using a mechanism in which the P3MT film stabilizes the passive layer by providing a transient current to heal small defects inside the passive film before they could expand. Recently, Naval Air Warfare Center Weapons Division (NAWCWD) researchers have shown quantitative evidence that EAPs, specifically poly(2,5-bis-N-methyl-N-hexylamino)phenylene vinylenes (BAM-PPV) can provide corrosion protection for 2024 Al alloys in simulated marine environments [18] and BAM-PPV coated onto 2024 Al panels showed similar performance to chromate conversion coated 2024 Al panels up to 336 hours of neutral salt-fog tests[22].

Section IV

Materials and Methods:

Materials and General Analytical Methods

3-(Pyrrol-1-yl) proprionitrile (3PPN), 7-bromoheptanitrile (7-BHN), 1,6-dibromohexane, 1,8-dibromooctane, 5-hexenenitrile, sodium hydroxide (NaOH), 3,4-ethylenedioxyrthiophene (EDOT) and 3-aminopropyltrimethoxysilane were purchased from Aldrich and used as received. Iron (III) chloride ($FeCl_3$), iron(III) chloride hexahydrate ($FeCl_3*6H_2O$), ferric citrate (FC) ($FeC_6H_5O_7$), iron(III) acetylacetonate (FA) $(Fe(C_5H_7)_2)_3$, iron(III)oxalate hexahydrate (FO) $(Fe(C_2O_4)_3*6H_2O$, sodium thiosulfate ($Na_2S_2O_3*5H_2O$) and ammonium thiosulfate $(NH_4)_2S_2O_3$, were purchased from Aldrich and used as received. Ferric nitrate nonahydrate ($Fe(NO_3)_3*9H_20$) obtained from Baker Chemical and used as received.

^1H and ^{13}NMR spectra were acquired using a Bruker Avance 400 MHz NMR spectrometer. Mass spectra data were obtained using a JEOL thermal desorption mass spectrometer (TD-MS). Thermal analysis data on selected polymers were obtained via Differential scanning calorimetry (DSC) using a TA Instrument 2910 DSC and Thermogravimetric analysis (TGA) was conducted using a TA Instruments 2950 TGA. Melting points (m.p) were measured with a Melt-Temp and are uncorrected.

The FTIR measurements were made using a Nicolet Nexus 870 FTIR spectrometer with a liquid nitrogen cooled MCT detector. Each spectra is an average of 128-256 scans with 4 cm^{-1} resolution. The monomer and polymer bulk samples were analyzed using a "Thunderdome" attenuated total reflectance (ATR-FTIR) accessory with a germanium crystal. The samples adsorbed on a surface were analyzed using specular reflectance. The incoming radiation was at 80° with respect to the surface normal.

The particles used in the particle coating operation included 1) Monarch 900 carbon black (an organic pigment containing ~50% graphite, dispersed as ~1 μm particles), 2) molybdenum sulfide (99%, supplied from Aldrich Chemical as particles of less than 2 μm size) 3) fumed silica, supplied Aldrich as particles significantly less than 1 μm in average size, and 4) boron carbide, supplied from Aldrich as particles approximately 10 μm in average size.

Galling testing was performed in accordance with specification ASTM G98, which required galling testing performed with button and block specimens. These specimens were manufactured from AISI 4340 steel hardened to 50 – 55 HRC (representing high-strength steel). A group of button specimens were plated with cadmium (in accordance with SAE-AMS-QQ-P-416, Type II, Class 2), while others were coated with IVD aluminum (in accordance with MIL-DTL-83488, Type II, Class 2) for comparison to the polymer samples. In addition, fixtures were required that conformed to the dimensions listed in ASTM G98 for galling testing. These fixtures included a support cylinder and a plate support fixture. These were also fabricated from high-strength steel.

To evaluate the resistance of different polymer film coatings as a replacement for cadmium, Cd-plated specimens per Federal Specification QQP-416, Type II, Class 1 were used as a baseline. Bare metal (uncoated) specimens were first tested in air per

ASTM F519/F1624 to measure any residual hydrogen due to manufacturing of the specimens.

Testing at ASTM E8 (fast fracture) loading rates provided the limiting value in that insufficient time is not allotted for hydrogen diffusion to occur and cause any damage. The average value of the Notched Fracture Strength in bending, NFS(B), of the specimens obtained from certification testing of the specimens was designated as 100% NFS.

Testing in air at ASTM F1624/G129 slow loading rates provided sufficient time for hydrogen diffusion to occur to provide a quantitative measure of residual hydrogen in the as-manufactured steel specimens. RSL™ testing was used to measure the *threshold* for the onset of hydrogen embrittlement in accordance with ASTM F519 for Type 1e specimens. The average value of NFS(B) that was the limiting value of the hydrogen embrittlement *threshold* in the certification tests was 91.6 % NFS.

EAP deposited onto 4340 and 4130 high strength steels coupons were measured for film thickness using DeFelsko Model Positector 6000 and SEM/EDS measurements were done with Zeiss SEM Model EVO-50 and EDS Model LEO-EVO-50EP.

Methods:
Synthesis Section

Small-scale preparation of 3-(pyrrol-1-yl) propanoic acid (3PPA)(Figure 1)[23]

A 250 mL round bottom flask was equipped with a reflux condenser and nitrogen inlet/outlet valve. The round bottom flask was charged with 50 mL deionized water (DI water) and 13.3 g NaOH pellets. After addition of the NaOH pellets the solution became turbid. After 5 minutes, the solution was clear and homogenous. The 3-(pyrrol-1-yl) proprionitrile (10.0 g, 83.2 mmol) was added to the reaction flask and the solution refluxed for 12 hours under a positive nitrogen pressure. After 12 hours the solution was homogenous and orange colored. There was no ammonia evolution from the top of the condenser by pH paper. Cold DI water (25 mL) was added and the solution cooled to ambient temperature. The reaction flask was cooled in and ice/water bath and 14 mL of a 50% aqueous sulfuric acid solution (1:1, v/v) was added slowly. The solution was stirred and a semi-solid formed immediately. The contents of the reaction flask were extracted 3X with ether and the ether layer separated from the aqueous phase. The ether layer was dried over magnesium sulfate and the solution filtered. The filtrate was rotovapped to a semi-solid residue and dried in a vacuum dessicator (0.05 Torr, 25^{o}C) for 12 hours. An off-white tan product was obtained in 35% yield (4.0 g), m.p = 45-47^{o}C (uncorrected, literature value = 59-60^{o}C). ^{1}H NMR (DMSO-d_6): 2.67 (t, 2H); 4.09 (t, 2H); 5.95 (t, 2H) and 6.73 (t, 2H), ^{13}C NMR (DMSO-d6): 36.05, 44.40, 107.5, 120.4 and 172.3. FTIR: 3000 cm^{-1}broad (OH stretch), 1710 cm^{-1}(C=O stretch). Identified with thermal desorption-MS: molecular peak at 138.9 amu.

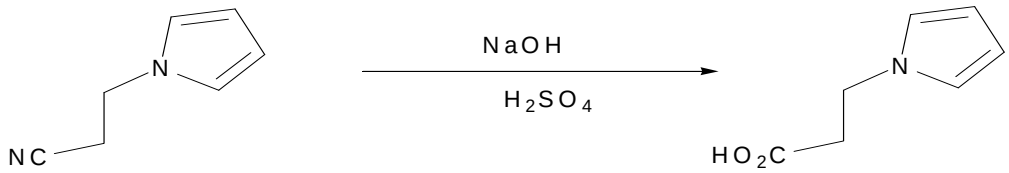

3PPN **3PPA**

Figure 1: Synthesis of 3-(pyrrol-1-yl) propanoic acid (3PPA)

Scale-up of 3-(pyrrol-1-yl) propanoic acid (3PPA): A 500 mL 3-neck round bottom flask was equipped with a reflux condenser and nitrogen inlet/outlet valve. The round bottom flask was charged with 200 mL DI water and 40 .0g NaOH pellets were added slowly with stirring to the reaction flask. After 10 minutes the solution was homogenous, and 3PPN (30.0 g, 249.7 mmol) was added to the reaction flask and the solution refluxed for 12 hours under a positive nitrogen pressure. After 12 hours, the solution became homogenous and orange colored. There was no ammonia evolution from the top of the condenser by pH paper. Cold DI water (100 mL) was added and the solution cooled to ambient temperature. The reaction flask was cooled in an ice/water bath and 100 mL of a 50% aqueous HCl acid solution (1:1, v/v) was added slowly to acidify the reaction mixture (pH =2). The solution was stirred and a semi-solid formed immediately. The solid was removed via filtration and the filtrate was extracted 3X with ether and the ether layer separated from the aqueous phase. The ether layer was dried over magnesium sulfate and the solution filtered. The filtrate was rotovapped to a semi-solid residue and both solid materials were dried in a vacuum dessicator (0.05 Torr, 25^{o}C) for 12 hours. Each solid was obtained as an off-white/tan product and the combined weight gave nearly quantitative yield (33.4g, 98%). Both products were each identified as the monomer (3PAA) via ^{1}H and ^{13}C NMR.

Synthesis of 6-pyrrol-1-yl-hexanitrile (Figure 2): [24,25]

A modification of the procedure to prepare 3-pyrrol-1-yl-proprionitrile was attempted for the above compound. A 50 mL round bottom flask was equipped with a reflux condenser, nitrogen inlet/outlet and 25 mL constant pressure addition funnel. The round bottom flask was charged with 0.7094 grams pyrrole (10.5 mmol), 0.2 mL Triton B and 1.0 g 5-hexenitrile (10.5 mmol) was added to the constant pressure addition funnel. The addition of the 5-hexenitrile to the reaction flask proceeded dropwise for several minutes at ambient temperature under a constant positive nitrogen pressure. After the addition was complete the contents were stirred at ambient temperature for two days. After two days, the solution was homogenous and deep red in color. The solution was diluted with 3 mL DI water and extracted 2 x with ether (10 mL). The ether layers were combined, dried with $MgSO_4$, filtered and the filtrate rotovapped to a brown oil. The brown oil was dried in a vacuum dessicator (0.5 Torr, 25^{o}C) overnight to give a brown oil in 0.04 grams. The NMR analysis of this product only showed starting material no reaction took place.

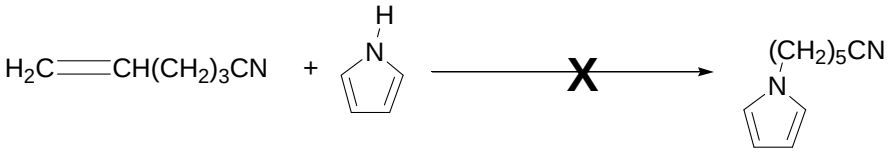

Figure 2: Synthesis of 6-pyrrol-1-yl-hexanitrile

Synthesis of 1-(6-Bromo-hexyl)-1H-pyrrole (Figure 3): [23,26-29]
The above synthesis did not produce a viable pyrrol compound an alternative method was employed to obtain long chain alkyl substituted pyrrols. A 3-neck 1 L round bottom flask was equipped with a reflux condenser, nitrogen inlet/outlet and rubber septum. The reaction flask was charged with 230 mL of dry N,N- dimethylformamide, 153.2 g of 1-6-dibromohexane (628 mmol, 97 mL), 15.0 grams of prrole (223.5 mmol) and 14.3 grams of KOH. After all reagents had dissolved in the reactin flask the contents were stirred at ambient temperature under a positive nitrogen blanket. After overnight reaction, a solid white precipitate was present in the flask. The suspension was diluted with 230 mL DI water and the aqueous phase was extracted 4x with ether (100 mL). The ether layers were combined, dried over $MgSO_4$, filtered and the filtrate rotovapped to a dark red liquid. The crude material was filtered through a Silica gel plug using hexanes as the eluting solvent. The crude product was further eluted with hexanes:ethyl acetate (99:1, v/v) through silica gel to give a yellow oil in 0.14 g (<1% yield). The purified product was confirmed by ^{1}H and ^{13}C NMR and FTIR. The low yield was due to loss on the column and further work using this literature procedure was not continued.

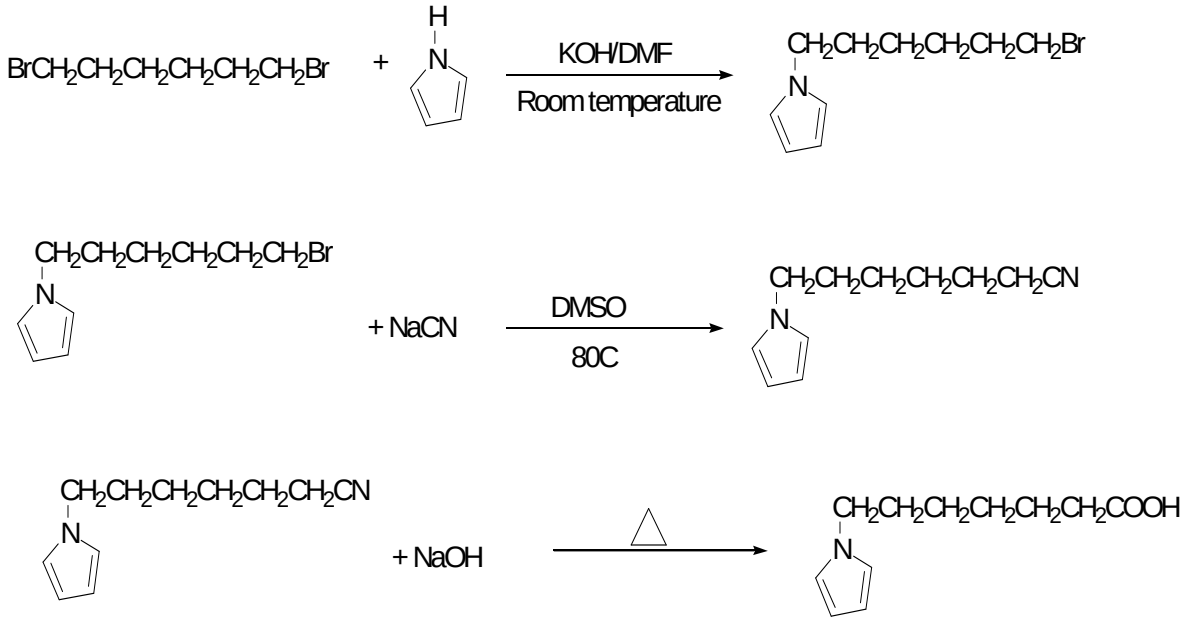

Figure 3: Synthesis of 1-(6-Bromohexyl)-1H-pyrrole, 1-(6-Cyanohexyl)-1H-pyrrole and 1(-6-Heptanoic)-1H-pyrrole

Synthesis of 7-pyrrol-1-yl-heptanitrile (Figure 4):

An alternative approach was attempted using potassium *tert*-butoxide as a strong base with 7-BHN and pyrrole.
A 250 mL 3-neck round bottom flask was equipped with a reflux condenser, nitrogen inlet/outlet and 50 mL constant pressure addition funnel. The reaction flask was flushed with nitrogen and 50 mL dry THF, 2.0 grams pyrrole (29 .8 mmol) and 3.34 g potassium *tert*-butoxide (29.8 mmol) were added to the reaction flask. The addition funnel was charged with 6.80 grams 7-BHN (35.8 mmol, 5.4 mL). After addition complete, the contents were refluxed at 80^{o}C overnight under a positive nitrogen blanket. The reaction was cooled to ambient temperature and quenched with 50 mL DI water. The aqueous solution was extracted 3 x with chloroform (3 x 35 mL), the organic layers combined and dried over $MgSO_4$. The solution was filtered and the filtrate rotovapped to an orange oil which was dried under vacuum (0.05Torr, 25^{o}C) overnight in a vacuum dessicator. The orange oil was obtained in 5.70 g (91%). ^{1}H, ^{13}C NMR (Figures 5 and 6) and FTIR (Figure 7) were used to identify the product. The proton and carbon NMR assignments are: (δ, DMSO-d_6, 400 MHz, 300K): 6.72 (t, *J* = 2.1 Hz, 2H, *pyrrole*), 5.99 (t, *J* = 2.1 Hz, 2H, *pyrrole*), 3.85 (t, *J* = 7.1 Hz, 2H, CH_2), 2.44 (t, *J* = 7.1 Hz, 2H, CH_2), 1.68 (p, *J* = 7.3 Hz, 2H, CH_2), 1.53 (p, *J* = 7.3 Hz, 2H, CH_2), 1.39 (m, 2H, *CH2*), 1.22 (m, 2H, *CH2*) and ^{13}C NMR (δ, DMSO-d_6, 400MHz, 300K): 120.42 (*CN*), 120.25 (*pyrrole*), 107.30 (*pyrrole*), 48.41 (NCH_2), 30.78 (CH_2), 27.56 (CH_2), 24.63 (CH_2), 24.57 (CH_2), 16.03 (CH_2). The FTIR peak assignments are as follows: 3095 cm^{-1} sp^2 C-H stretch, 2934 and 2861 cm^{-1} C-H stretch, 2245 cm^{-1} C≡N stretch, 1550 cm^{-1} out of phase C=C stretch, 1501 cm^{-1} in phase C=C stretch, 1462 cm^{-1} CH_2 scissor, 1425 cm^{-1} pyrrole anti-symmetric ring mode, 1280 cm^{-1} N-CH_2 stretch of 1-substituted pyrrole, 1089 and 1061 cm^{-1} in plane C-H deformation of pyrrole, 725 cm^{-1} in phase out of plane cis CH wag of pyrrole HC=CH.

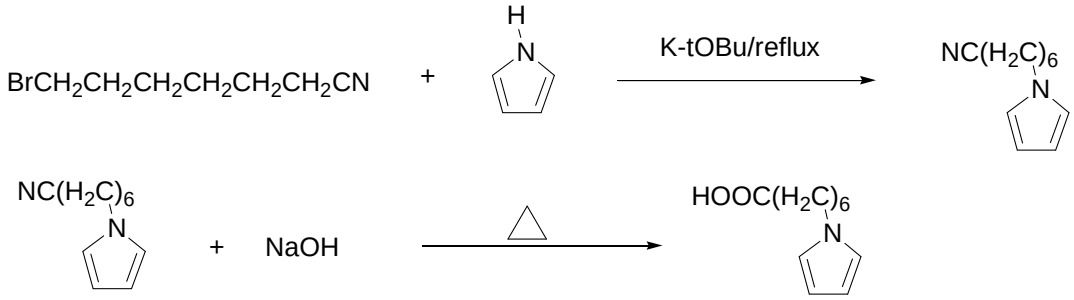

Figure 4: Synthesis of 7-PHN and 7-PHA

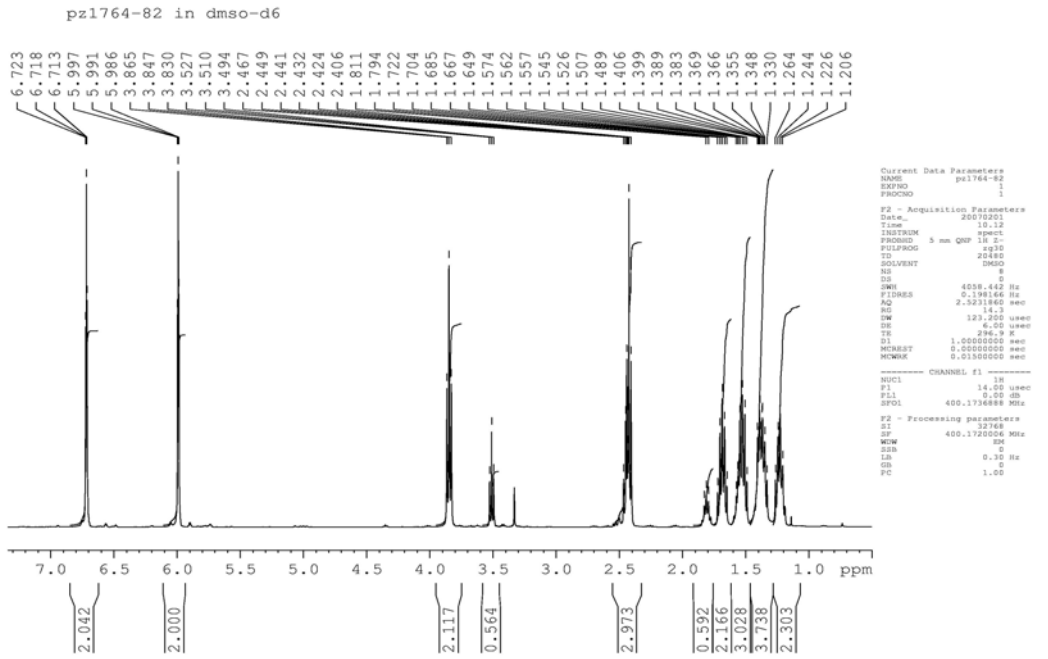

Figure 5: ^{1}H NMR of 7-PHN

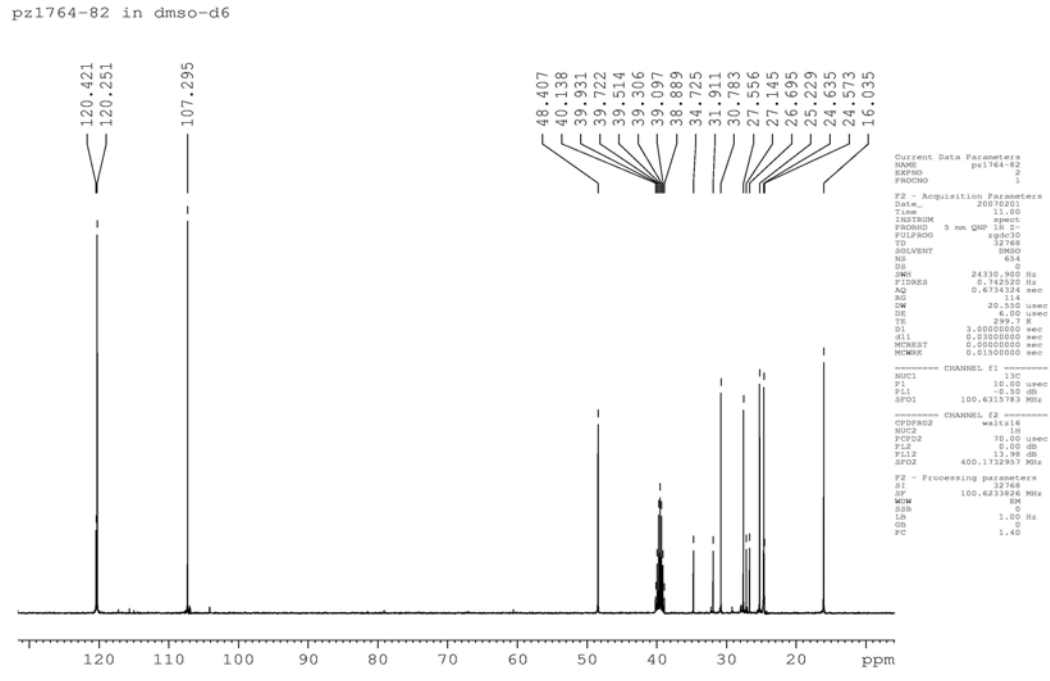

Figure 6: ^{13}C NMR of 7-PHN

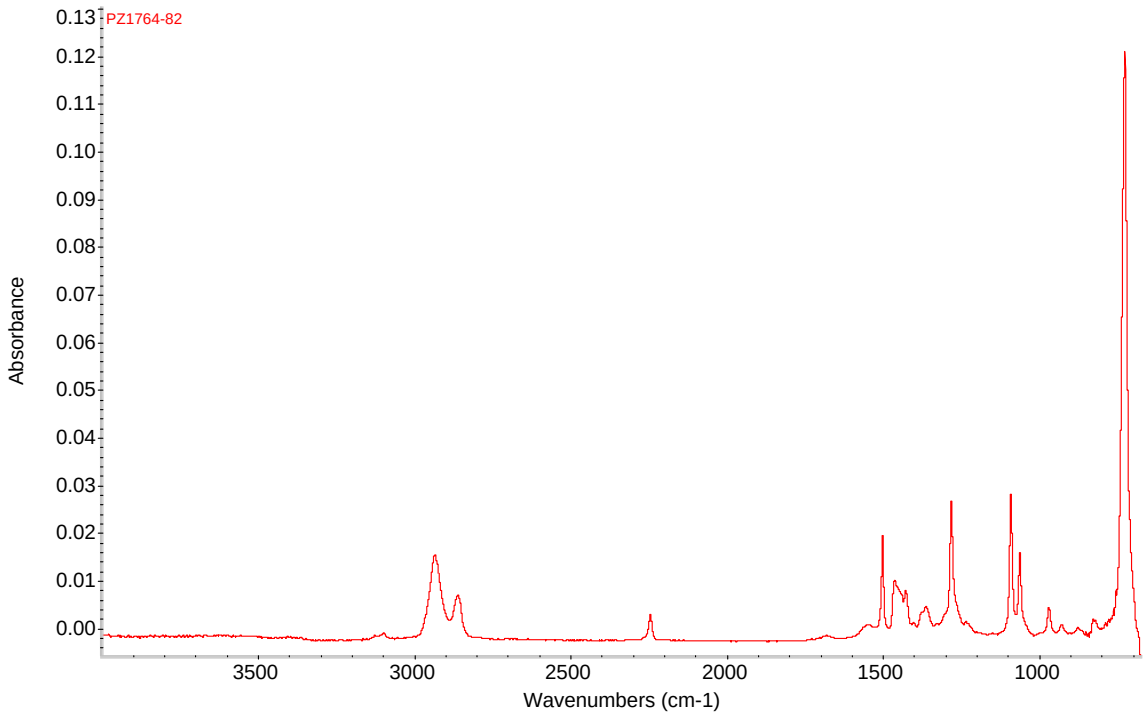

Figure 7: FTIR Spectrum of 7-PHN

Hydrolysis of 7-PHN (see Figure 4):[23] A 100 mL 3-neck round bottom flask was equipped with a reflux condenser, nitrogen inlet/outlet. The reaction flask was charged with 20 ml DI water and 2.72 grams of NaOH pellets (68.1 mmol). After 5 minutes the pellets had dissolved forming a homogenous solution and 3.0 g 7-PHN (17.0 mmol) were added to the reaction flask. The solution was refluxed for 9 hours under a positive nitrogen blanket and completion of the reaction was determined with moist pH paper until no evolution of ammonia was evident. The reaction flask was quenched with 7 mL cold DI water poured down the condenser and the solution was acidified with a 50 wt % concentrated HCl: DI water (1:1, v/v). The pH was monitored during the addition changing from pH = 12 to pH = 2. After acidification, the solution was extracted with ethyl ether (3 x 25 mL). The ether layers were combined, and dried with $MgSO_4$, filtered and the filtrate rotovapped to a red-brown oil. The oil was dried for 6 hours in a vacuum dessicator (0.05 Torr, 25°C) to give in quantitative yield a deep-red oil in 3.35 grams. ^{1}H, ^{13}C NMR (Figures 8 and 9) and FTIR (Figure 10) were used to identify the product. The proton and carbon NMR assignments are: ^{1}H NMR (δ, $CDCl_3$, 400 MHz, 300K): 10.42 (bs, -OH), 6.69 (t, J = 2.1 Hz, 2H, *pyrrole*), 6.19 (t, J = 2.1 Hz, 2H, *pyrrole*), 3.91 (t, J = 7.2 Hz, 2H, CH_2), 2.39 (t, J = 7.2 Hz, 2H, CH_2), 1.81 (m, 2H, CH_2), 1.68 (m, 2H, CH_2), 1.39 (bm, 4H, *CH2*) and ^{13}C NMR (δ, $CDCl_3$, 400MHz, 300K): 179.98 (*C*=*O*), 120.47 (*pyrrole*), 107.88 (*pyrrole*), 49.47 (NCH_2), 33.98 (CH_2), 31.36 (CH_2), 28.60 (CH_2), 26.40 (CH_2), 24.52 (CH_2). The FTIR peak assignments are as follows: 3096 sp^2 hybridized C-H stretch, 2933 and 2862 sp3 hybridized C-H stretch, 1702 C=O stretch, 1502 C=C stretch, 1467, 1411, 1335 C-H deformation modes, 1279 N-C(H_2) stretch of 1-substituted pyrrole,

1200 C-O stretch, 1090 and 1060 in plane C-H deformation of pyrrole ring carbons, 727 in phase out of plane cis C-H wag of pyrrole.

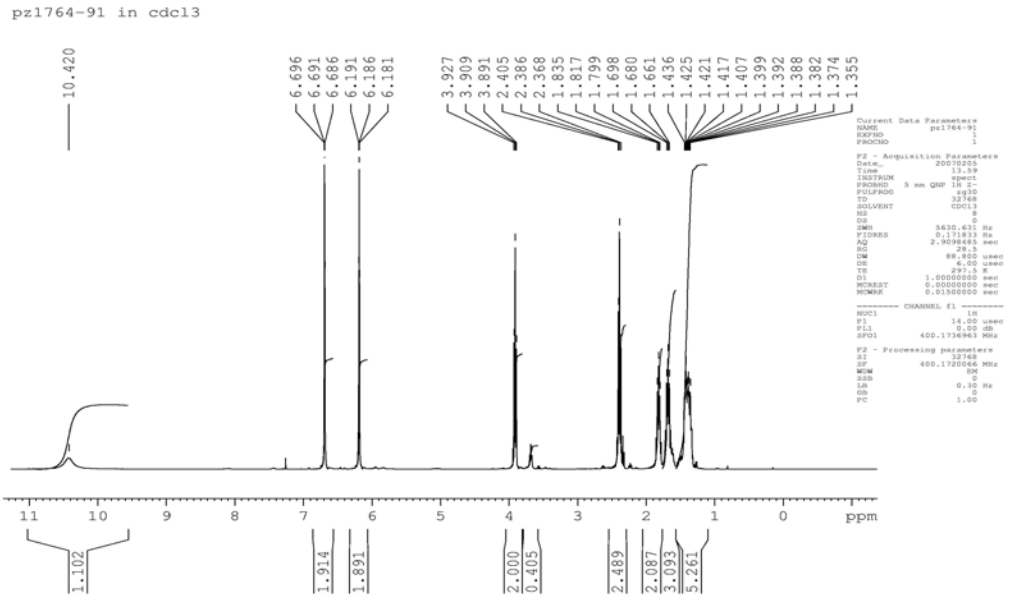

Figure 8: ^{1}H NMR Spectrum of 7-PHA

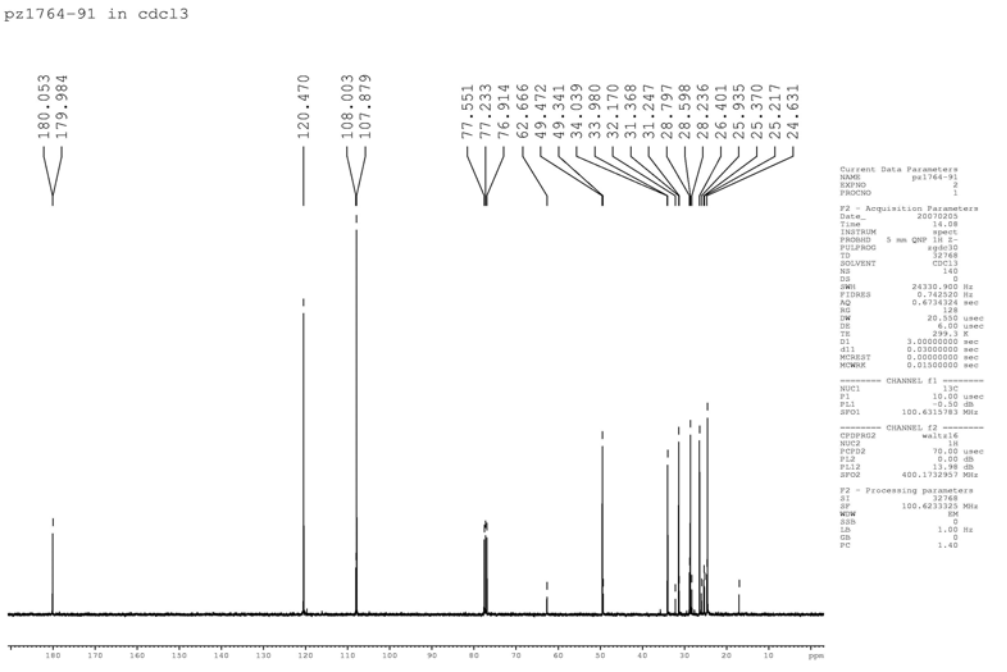

Figure 9: ^{13}C NMR Spectrum of 7-PHA

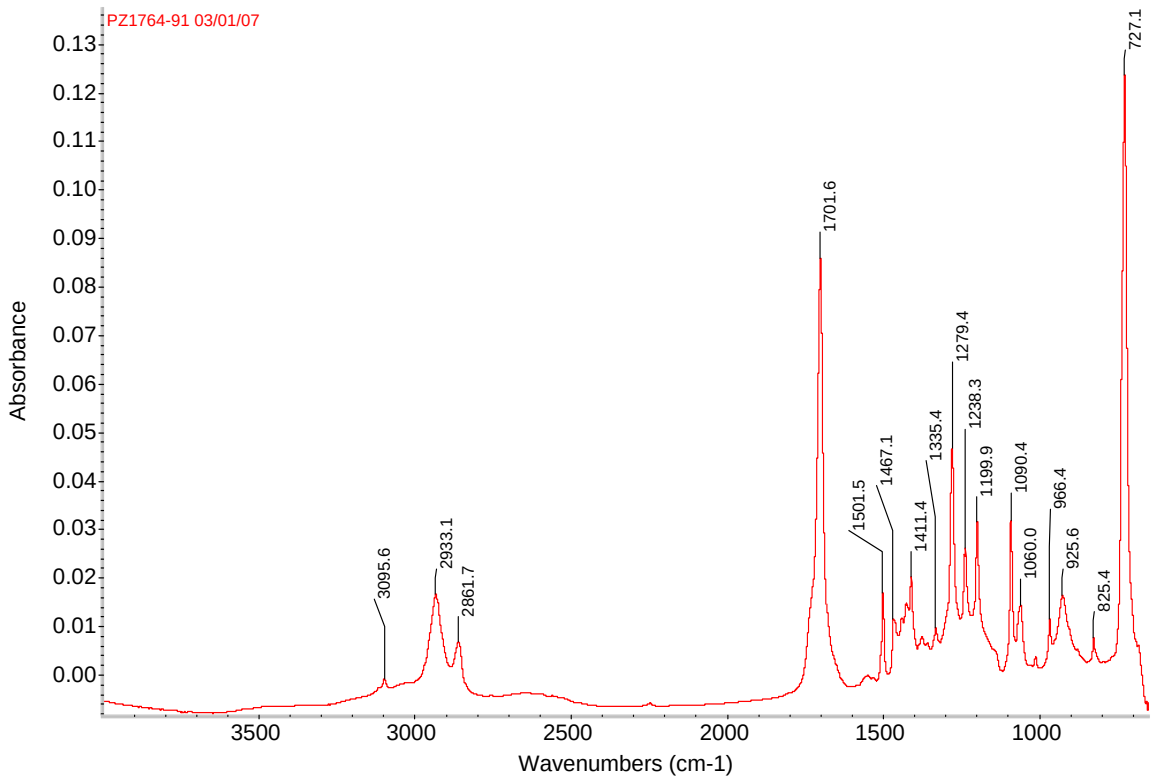

Figure 10: FTIR Spectrum of 7-PHA

The above synthesis for 7-PHN and PHA were scaled-up to the 20 gram level. The yields on average for the scale-up were less than quantitative. Yields between 65-70% were obtained on average. All spectroscopic data showed the products were obtained in high purity.

Chemical Polymerization of Thiophene Based Monomers (Figure 11): Because some of the chemical oxidants are not commonly used as such, several monomers (EDOT, 3MT, and 3MOT) known to readily undergo chemical oxidative polymerization were used for comparison with the lesser-known monomers (TC and TP; PyC was not available at the time the chemical polymerizations wee attempted.) Oxidants used were ferric chloride ($FeCl_3$, as a control), ferric citrate (FC), ferric oxalate (FO), and ferric acetylacetonate (FA). All the monomers were soluble or miscible in propylene carbonate as well as in methanol, but the same was not true for the oxidants. $FeCl_3$ and FA are both readily soluble in both propylene carbonate and methanol, but FC and FO are insoluble in both solvents. FO is fully soluble in water, but FC is only partially soluble in water. Reactions are summarized in Table 2, where NR indicates no reaction, and P indicates polymerization occurred; numbers in parentheses are reaction identification numbers. The only definitive case of polymerization was of EDOT polymerizing with $FeCl_3$ in propylene carbonate (as expected); EDOT may have polymerized in aqueous FO, but further analysis is needed to be sure. In two cases, reactions 4 and 10, no reaction was immediately evident, but upon stirring overnight, changes occurred that might be

indicative of polymerization; further analysis is needed to be sure. None of the new oxidants appears particularly successful; FC didn't induce polymerization in any case, and FA and FO results are mediocre at best. Neither of the new monomers appears to polymerize via chemical oxidative polymerization (with the possible exception of TC in $FeCl_3$).

Synthesis of Thiophene Derivatives: One of the target materials is a random copolymer of thiophene acetic acid with hexylthiophene to produce a soluble polymer with good adhesion properties. While thiophene acetic acid (TC) is commercially available, it had to be esterified to be incorporated into the random co-polymer. The esterification was readily performed with methanol and an acid catalyst. The ester and hexylthiophene were chemically polymerized with iron chloride to yield the polymer in good yields. By NMR analysis, the ester was incorporated into the polymer at between 10 and 15%. The polymer was then treated with base followed by acid to obtain the polymer with free carboxylic acid groups to promote adhesion. This polymer was then spray-cast from toluene onto clean steel 1008 panels. After flash drying at 200° C for 10 min, the polymer passed the dry tape test for adhesion.

The next target material is a random copolymer of thiophene methyl phosphonate (TP) with hexylthiophene to produce a soluble polymer with good adhesion properties. The synthesis began with the available thiophene methanol, which was converted to thiophene methyl chloride with concentrated hydrochloric acid. The thiophene methyl chloride was treated with triethyl phosphite to yield the diethyl thiophene methyl phosphonate. The material was purified by distillation and polymerized as above. By NMR analysis, the ester was incorporated into the polymer in about 10%. This polymer was then spray-cast from toluene onto clean steel 1008 panels. After flash drying at 200° C for 10 min, the polymer passed the dry tape test for adhesion.

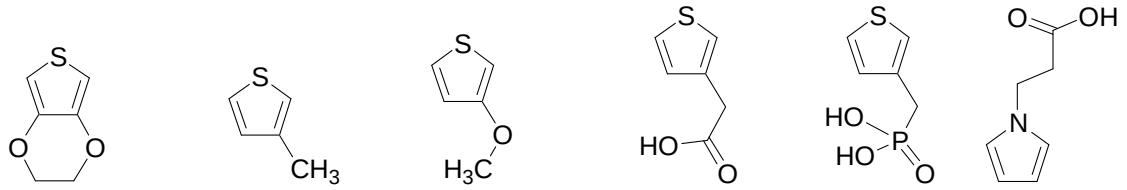

EDOT **3MT** **3MOT** **TC** **TP** **3PPA**

Figure 11: Monomers for electroless and electropolymerization

Table 2: Attempts at chemical polymerization

Monomer	Methanol				Propylene Carbonate				Water	
	FC_{insol}	FO_{colors}	FA_{sol}	$FeCl_{3sol}$	FC_{insol}	FO_{insol}	FA_{sol}	$FeCl_{3sol}$	FC_{sol}	FO_{sol}
EDOT			NR (1)					P (2)	NR (11)	P? (12)
3MT	NR (7)						NR (8)			
3MOT			NR (9)				NR? (10)			
TC		NR (3)						NR? (4)	NR (13)	
TP			NR (5)					NR (6)		

Electrochemical Polymerization of Monomers: All six monomers were polymerized electrochemically (10mM monomer in 100mM $TBABF_4/CH_3CN$.) Results are tabulated below (Table 3). Electrochemistry of EDOT, 3MT, and 3MOT has been previously reported; all polymerize nicely in the electrolyte solution used here. 3MT polymerization occurs exactly as expected. 3MOT polymerization (Figure 12) is also perfectly normal. Notice the onset of monomer oxidation is somewhat lower than for 3MT (1.02 vs. 1.32V vs. Ag/Ag+); this is due to electron donation from the ether group. TC and TP do not polymerize in the stability window of acetonitrile; see Figure 13 for an attempt to electropolymerize TP. The constant current response seen in Figure 13 over multiple redox cycles is characteristic of acetonitrile. 3PPA, on the other hand, polymerizes quite well electrochemically, as can be seen in Figure 14. 3PPA undergoes a very well-behaved, reproducible electropolymerization. A linear increase in peak current as a function of scan rate is observed for P3PPA, indicating that the film is electrode supported and electroactive.

Table 3: Results of electrochemical polymerization attempts

Monomer	$E_{on,m}$ (V vs. Ag/Ag^+)	$E_{p,m}$ (V vs. Ag/Ag^+)
EDOT	0.78	-
3MT	1.32	ca. 2.0
3MOT	1.02	1.44
3PPA	0.84	1.25
TC	no polymerization evident	
TP	no polymerization evident	

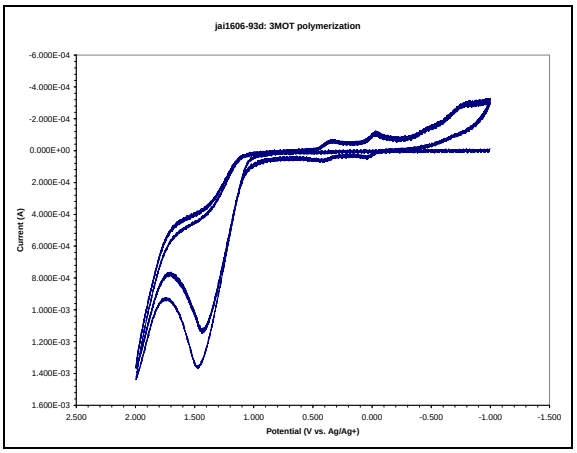

Figure 12: Electropolymerization of 3MOT

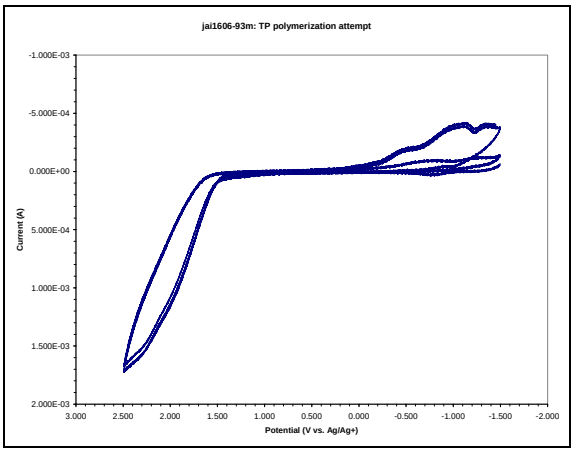

Figure 13: Attempt to polymerize TP

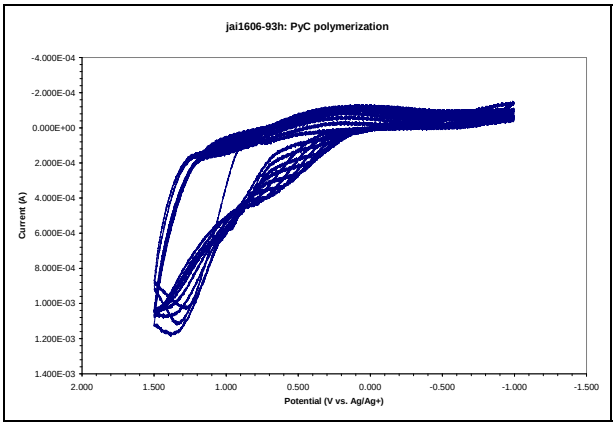

Figure 14: Electropolymerization of 3PPA

Synthesis of Poly (thiophene acetic acid methyl ester):

Thiophene acetic acid was converted to the methyl ester by reaction with methanol and an acid catalyst according to a literature procedure. 60 g of the methyl ester of thiophene acetic acid was prepared. Polymerization of the ester in chloroform with $FeCl_3$ followed by precipitation in methanol gave the polythiophene but only in relatively low yield. Several runs produced yields in the range 25 - 35%. The ^1H NMR in $CDCl_3$ was identical with the spectrum reported in the literature.[30] The weight average (M_w) molecular weight was determined by gel permeation chromatography (GPC) to be ~10,000 g/mol (see Figure 15).

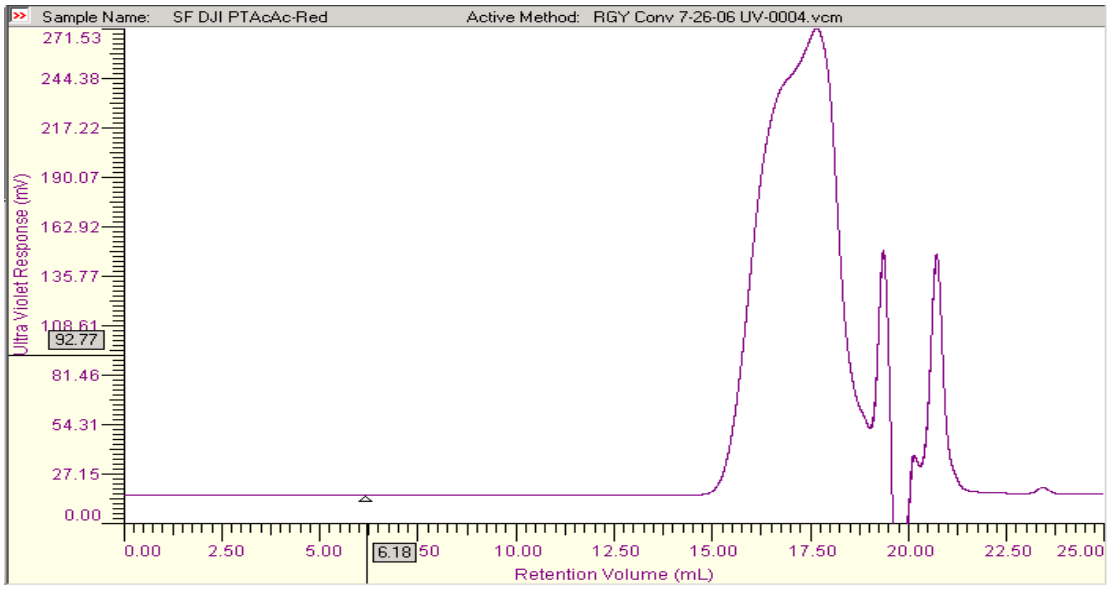

Figure 15: GPC of Poly (thiophene acetic acid methyl ester) in THF vs. polystyrene standards (Mn: 4,000; Mw: 11,000; Mz: 25,000 g/mol)

This material is of interest due to the funtionalization of the ester group (see Figure 16). By simple hydrolysis, the polymer becomes a water soluble polyanion. Following the promising results with the incorporation of amino silane, we attempted to displace the methyl group directly to yield strongly adhering films. The first experiments involved conversion and isolation of the substituted polymer.

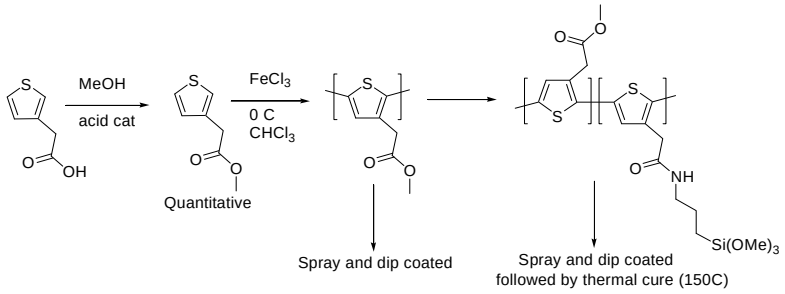

Figure 16: Synthesis and functionalization of Polythiophene Acetic Acid

Various reaction conditions for the attachment of a trimethoxysilyl-anchoring group (via reaction with 3-aminopropyl-trimethoxysilane) were explored. A suspension (~2.5 w/v) of polythiophene acetic acid methyl ester was treated with a slight excess of 3-aminopropyl-trimethoxysilane in THF. Almost immediately the suspended solids coagulated to form an intractable solid that settled rapidly when stirring was stopped.

Functionalization of polythiophene acetic acid methyl ester with 3-aminopropyl-trimethoxysilane:

Polythiophene acetic acid methyl ester (0.260 g, 1.7 meq. ester) was suspended in 10 mL anhydrous THF. 3-aminopropyl-trimethoxysilane (320 μL, 1.8 mmol) was added via syringe. Within a few seconds the suspended solids coagulated into clumps that settled out immediately when stirring was stopped. The dark colored solid was collected on a medium frit and dried under vacuum (280 mg). The solid was insoluble in $CDCl_3$ and DMSO-d_6. A repeat reaction using polythiophene acetic acid methyl ester (0.220 g, 1.45 meq. ester) was dissolved in 10 mL anhydrous THF. 3-aminopropyl-trimethoxysilane (265 μL, 1.5 mmol) was added via syringe. The solution remained homogeneous initially but after stirring overnight solid clumps had formed. The dark colored solid was collected on a medium frit and dried under vacuum (240 mg). The solid was insoluble in $CDCl_3$ and DMSO-d_6. The material was insoluble in chloroform dimethylsulfoxide, tetrahydrofuran and dimethylformamide. The ^{1}H NMR spectrum could not be obtained due to the insoluble nature of the material. Reaction of the ester with 0.5 equivalents of the amine produced a similar result, the material essentially insoluble in the above mentioned solvents. The methyl ester polymer is more soluble in DMF. When the reaction is carried out in DMF the reaction mixture is homogeneous with no precipitates formed initially. However, on stirring for several hours an intractable solid formed. Similar results were note for the reaction of the methyl ester polymer with 0.75, 0.5 and 0.25 equivalents of 3-aminopropyl-trimethoxysilane. Analysis of these materials was difficult. The formation of intractable/insoluble solids suggests that a crosslinking reaction is taking place. Reaction of the trimethoxy terminus with adventitious water could be responsible for this crosslinking. Using this to our advantage, we decided to treat the polymer just before spray casting with the amino silane.

Pre-Spray Cast Method of polythiophene acetic acid methyl ester with 3-aminopropyl-trimethoxysilane:

Polythiophene acetic acid methyl ester (1g) was dissolved in 10 mL anhydrous DMF. 3-aminopropyl-trimethoxysilane (0.2 mL) was added via syringe. The solution was heated at 80°C for one hour. The resulting dark solution was filtered into an airbrush reservoir and sprayed onto steel panels. The panels were dried at 150° C for one hour. These materials formed hard well adhered films on steel (both 1010 and 4340). Analysis of these films by FTIR, determined the approximately half of the esters were converted to amides by the amino silane and a strong O-Si-O peak is present (Figure 17).

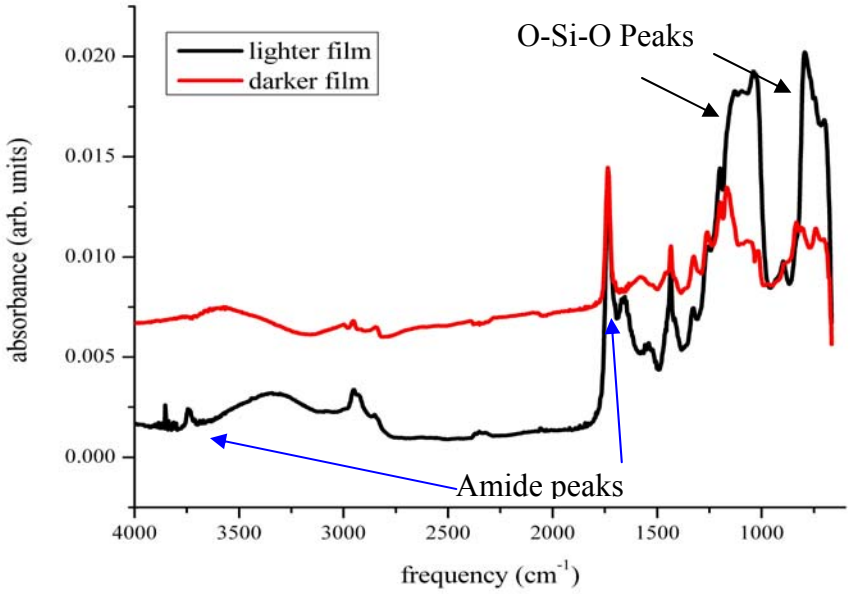

Figure 17: FTIR Analysis of Amino Silane Functionalized Polythiophene Acetic Acid Spray-cast on Steel

Electroless Deposition of 3PPA:[31] The electroless deposition (NLS) of the monomers utilized in this study was based on a prescreening process using the electropolymerization results described previously, based on the principle that the monomers with the lowest oxidation potential would undergo facile electroless polymerization. Since 3PPA does undergo electropolymerization at a low potential, it is a candidate for the electroless deposition. The electroless deposition consisted of 3 steps using the 3PPA and 7-PHA monomers.

Step I: The high strength steel substrate (4340 or 4130) [3x3x0.25"; 3x6x0.25", galling specimens and defect tolerance specimens] were cleaned using toluene, acetone, methanol and isopropanol to remove grease, dirt and any other debris that may be present on the sample. The samples were then air dried for 15 minutes prior to deposition. No evidence of corrosion was visible during this stage of the electroless deposition process.

Step II: The cleaned sample was placed in a Pyrex glass dish (size depended on sample dimensions) and a 0.5 wt %/vol. of 3-aminopropyltrimethoxy silane solution was added to the samples. The samples were allowed to stand in the silane solution for 5 minutes after which time the samples were removed and dried in a vacuum oven (28 in Hg, 100^{o}C). After one hour, the samples were removed from the oven and allowed to cool in a dessicator for one hour. The steel samples were measured with FTIR to determine if the silane had reacted with the substrate. A very thin layer of 3-aminopropyltrimethoxysilane was deposited on a high strength steel surface which is

shown in Figure 18, confirming the presence of the silane on the surface before the polymer deposition.

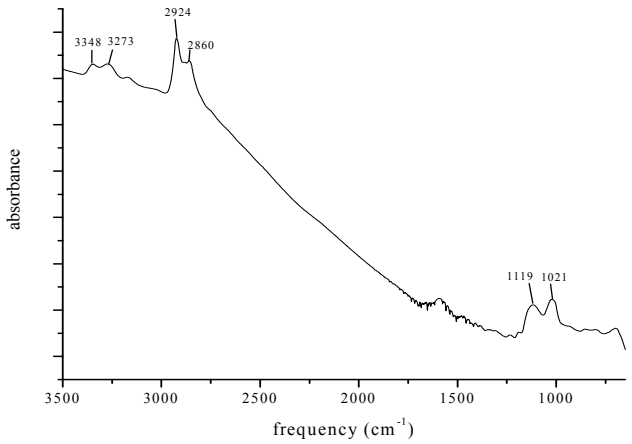

Figure 18: 3-aminopropyl trimethoxysilane on high strength steel button

Step III: The silanated sample was then placed back into the Pyrex glass dish for the polymerization deposition process. Numerous attempts using a variety of solvents, (e.g DI water, methanol) and oxidants ($FeCl_3$, $FeCl_3*6H_2O$, $FeC_6H_5O_7$, $Fe(C_5H_7)_2)_3$, $Fe(C_2O_4)_3*6H_2O$, $Na_2S_2O_3*5H_2O$ and $(NH_4)_2S_2O_3$) were tried. The oxidants $FeCl_3$ and $FeCl_3*6H_2O$ performed the best during the polymerization. Several different molar concentrations of the monomer in DI water were examined during the deposition (0.03M, 0.25M, 057M). The 0.25M solution of 3PPA and oxidant $FeCl_3$ at a concentration of 0.67M were found to be the optimum conditions for the electroless deposition process. Both the monomer solution and oxidant solution were added simultaneously to the Pyrex dish containing the steel samples. The solution was briefly agitated (<5 minutes) and covered and allowed to react at ambient temperature for 6 hours. After 6 hours a black film was present on the substrate. The substrate was dried in a vacuum oven (28 in Hg, 70^oC) for 6 hours. After 6 hours of drying time, the substrate was removed from the oven and cooled to room temperature in a dessicator. The identification that the polymer (P3PPA) had reacted with the silane coated substrate was confirmed by FTIR. The polymer deposited on a silanated surface is shown in Figure 19. It is different from the bulk polymer sample (as prepared using $FeCl_3$ in DI water and purified after polymerization) (Figure 20). Peaks at ~ 3440, 1593, and 1539 cm^{-1} are indicative of the N-H stretch, amide I and amide II bonds, respectively, of a secondary amide. The carbonyl peak of the carboxylic acid group at 1710 cm^{-1} decreased in intensity, indicating that it's concentration decreased significantly. Thus, the polymer during the electroless deposition underwent a reaction at the surface with the amino-silane that was on the surface to form the amide. The polymer is deposited on the surface as a non-uniform film, with a general thickness range from 2-30 microns. The polymer (P3PPA) does show brittleness with some flaking off of the material.

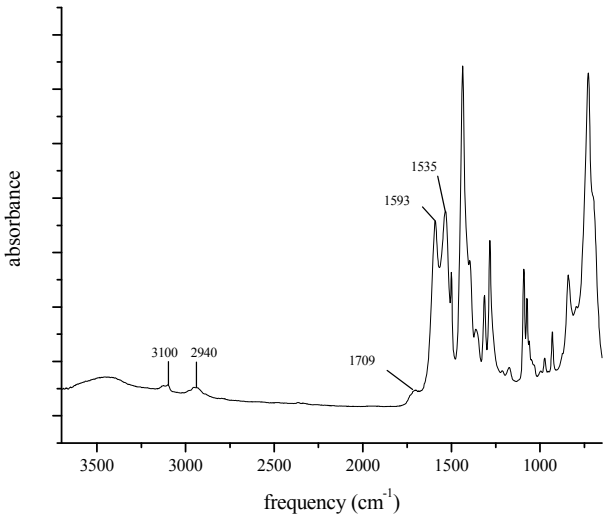

Figure 19: P3PPA deposited on high strength steel substrate

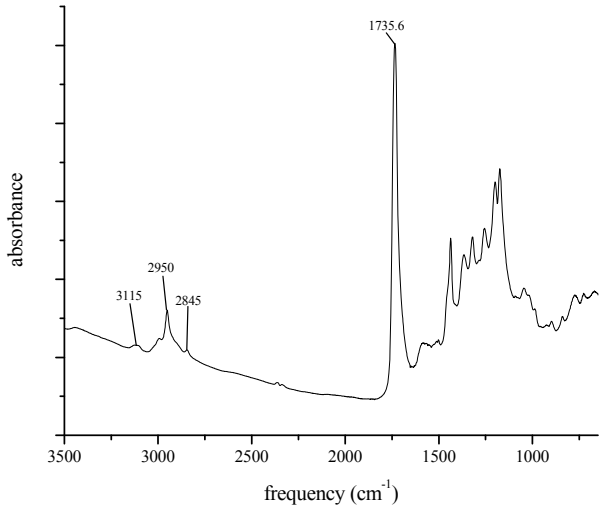

Figure 20: Bulk P3PPA

Electroless Deposition of 7-PHA:[31]

A repeat of the electroless deposition using the 7-PHA monomer in a mixture of DI water and methanol using the ferric nitrate nonahydrate ($Fe(NO_3)_3*9H_20$) as oxidant was successfully deposited onto both 4340 and 4130 high strength steel coupons. The use of the longer alkyl substituted pyrrole provided better coverage of the steel substrate without the pinhole and brittleness formation as found with the 3PPA deposition process.

Step I: The high strength steel coupons (4130 or 4340, 1x3x0.125", 3x3x0.125", 33xx0.25", 3x6x0.25") were cleaned using a toluene rinse with wire brush (1 minute), methanol rinse (1 minute), IPA rinse (1 minute) and final rinse with methanol. The samples were then allowed to dry at ambient temperature for 5 minutes.

Step II: The panels were coated with an aqueous mixture of 3-aminopropyltrimethoxy silane: Tyzor 131 (dewetting agent), (v/v, 75/25). The coating process was by doctor blading a thin film of the solution onto the surface of the substrate or dipping the substrate into the solution. The coated sample was then placed in a vacuum oven at 28 in Hg, 50°C for 30 minutes and the temperature increased to 100°C for an additional 30 minutes. After one hour of total drying time the samples are removed and allowed to cool to ambient temperature. Figure 21 shows FTIR spectrum of the deposited 3-aminopropyltrimethoxy silane: Tyzor 131 pretreatment coating on the substrate. The peak assignments are as follows: 3346 cm^{-1} N-H stretch, 2944 cm^{-1} C-H stretch, 1604 cm^{-1} 1° amine NH_2 scissor, 1496 cm^{-1} CH_3 and CH_2 deformation modes, 1393 cm^{-1} CH_3 umbrella deformation, 1178 cm^{-1} C-N stretch, 1072 cm^{-1} Si-O stretch, 826 cm^{-1} NH_2 wag.

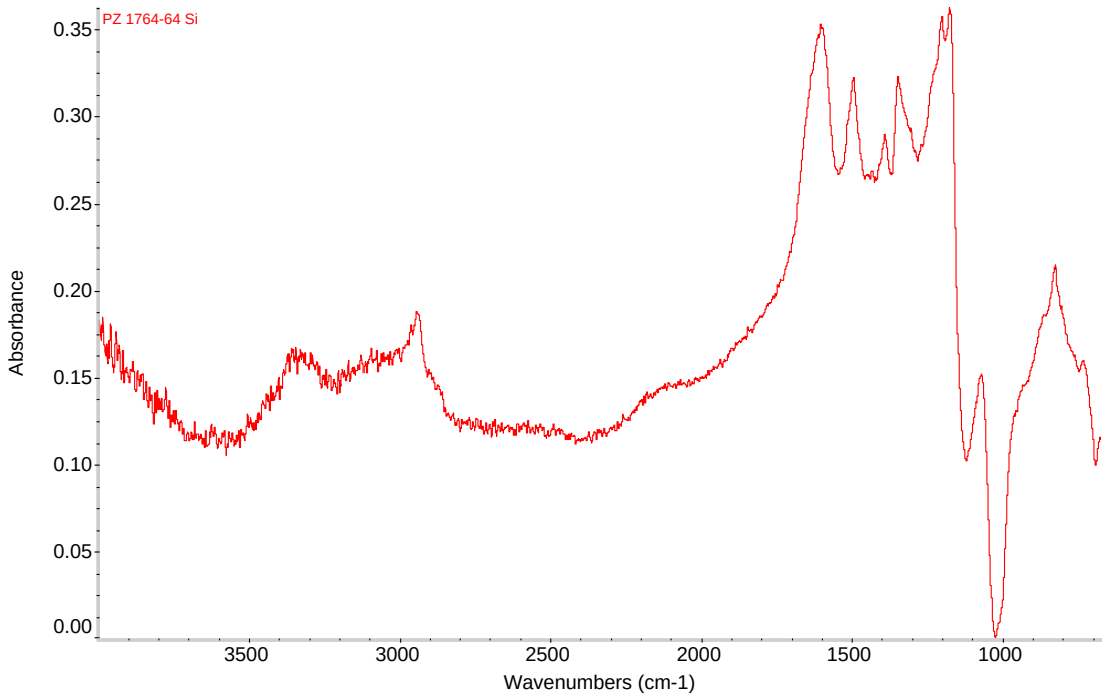

Figure 21: FTIR spectrum of pretreatment coating onto 4340 high strength steel coupon

Galling testing: Galling testing was performed in accordance with specification ASTM G98, which required galling testing performed with button and block specimens. These specimens were manufactured from AISI 4340 steel hardened to 50-55 HRC (representing high-strength steel). A group of button specimens were plated with cadmium (in accordance with SAE-AMS-QQ-P-416, Type II, Class 2), while others were

coated with IVD aluminum (in accordance with MIL-DTL-83488, Type II, Class 2) for comparison to the polymer samples. The remainder of the uncoated specimens were coated with various electroactive polymers. In addition, fixtures were required that conformed to the dimensions listed in ASTM G98 for galling testing. These fixtures included a support cylinder and a plate support fixture. These were also fabricated from high-strength steel.

Surface Roughness Testing: The surface roughness of the various buttons were measured in order to verify that they met the 10 to 45 μin guideline within the ASTM G98 specification. Table 4 displays the surface roughness averages of representative samples. The cadmium plating samples had a surface roughness outside of the desired range; however, it is believed this is the nature of the coating, and therefore unavoidable. Several different electroactive polymer coatings were compared to the IVD aluminum and cadmium plated samples. Several of the electroactive polymer samples were embedded with 2μm diameter spherical particles for increased lubricity. These embedded samples showed higher surface roughness and greater variability than the samples that were coated with the polymer only. Some of the coatings behaved like greases, resulting in damage to the coating during surface roughness measurements, and therefore could not be measured.

Table 4. Average surface roughness measurements of coated steel buttons.

Coating	Button 1 Surface Roughness μin	Button 2 Surface Roughness μin	Button 3 Surface Roughness μin	Average Surface Roughness (Ra) μin
Cadmium	75.8	75.4	79.0	76.7
IVD Aluminum	32.2	38.4	33.4	34.7
P3PPA	43.2	50.5	45.3	46.3
P3PPA with graphite	96.7	177.9	192.5	155.7
P3HT MoS_2	N/A	N/A	N/A	N/A
P3HT	126.1	100.4	N/A	113.3
P3PPA+MoS_2	161.9	294.5	N/A	228.2
P3PPA+SiO_2	125.2	99.9	75.2	100.1
P3PPA	N/A	N/A	N/A	N/A
P3PPA + boron carbide	N/A	N/A	N/A	N/A

Galling Test Procedure: The galling test was performed in accordance with ASTM G98. The previously described buttons with a 0.5-inch diameter were used for testing. The procedure utilized a 10,000-lb Instron static frame load cell. Belleville spring washers were used as part of the setup in order to keep the load constant during the turning operation (Figure 22). The first round of testing was performed using buttons and plates coated with similar coatings. As a result, both of these coatings galled on themselves, and it was determined that testing should be performed with only the button plated with the test coating and the steel plate left uncoated. The galling threshold of the bare AISI 4340 steel was determined in order to measure the increased galling resistance provided by the coatings.

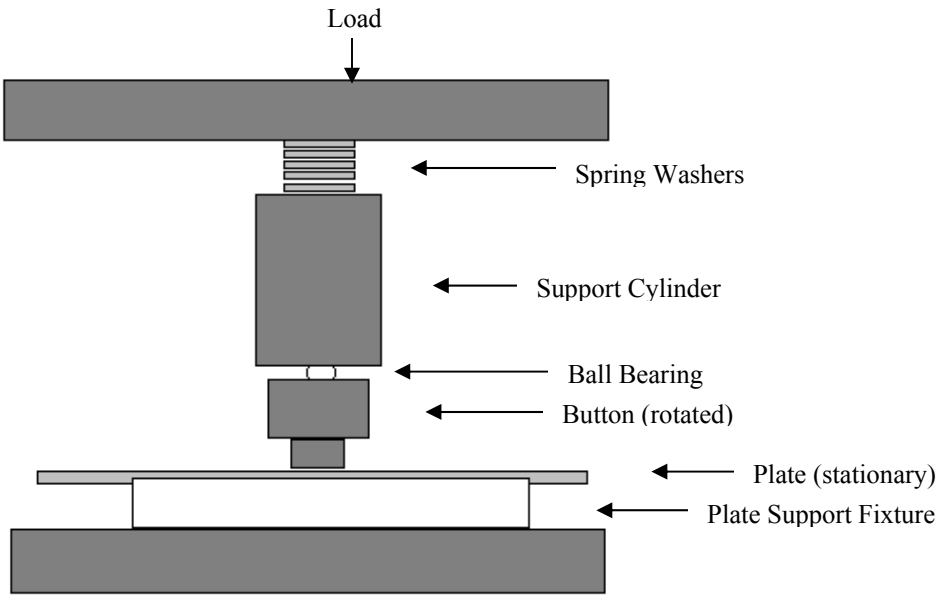

Figure 22: Schematic of galling test setup.

The test procedure consisted of the following:

i. Buttons and plates were cleaned ultrasonically with isopropyl alcohol. However, the alcohol disturbed some of the polymer coatings, so cleaning of the polymer coated buttons was omitted.
ii. The plate was placed in the support fixture so that an area free of surface defects could be used for galling testing.
iii. A button of the same coating material was loaded into the fixture with the ball bearing and support cylinder.
iv. An appropriate load was selected for testing
v. The button was rotated, using a modified tap wrench around the square bulk section, within the required 3 to 20 seconds, with an average of approximately 10 seconds.
vi. The load was released and the button and plate were examined for signs of galling.
vii. An appropriate load was chosen for further testing of the plating (if necessary) with a new button and a clean area of plate.

Hydrogen Embrittlement Studies

Baseline Evaluation Using Cd Plated Specimens: In order to evaluate the resistance of different EAP film coatings as a replacement for cadmium, Cd-plated specimens per Federal Specification QQP-416, Type II, Class 1 were used as a baseline. Bare metal (uncoated) specimens were first tested in air per ASTM F519/F1624 to measure any residual hydrogen due to manufacturing of the specimens. Testing at ASTM E8 (fast fracture) loading rates provided the limiting value in that insufficient time is not allotted for hydrogen diffusion to occur and cause any damage. The average value of the Notched Fracture Strength in bending, NFS(B), of the specimens obtained from certification testing of the specimens was designated as 100% NFS. The testing in air at ASTM F1624/G129 slow loading rates provided sufficient time for hydrogen diffusion to occur to provide a quantitative measure of residual hydrogen in the as-manufactured steel specimens. RSL™ testing was used to measure the *threshold* for the onset of hydrogen

embrittlement in accordance with ASTM F519 for Type 1e specimens. The average value of NFS(B) that was the limiting value of the hydrogen embrittlement *threshold* in the certification tests was 91.6 % NFS.

Degradation from Cd-plating: As a baseline for comparison to other coatings, specimens were Cd-plated per Federal Specification QQP-416 and tested in air at the same slow loading rate as the unplated specimens as a measure of any residual hydrogen due to the plating process. The *threshold* was found to be lowered from 91.6% to 85% NFS. This means that the bake out was inadequate in removing the hydrogen introduced into the steel during Cd-plating.

Environmentally Induced Hydrogen Stress Cracking (Hydrogen Embrittlement): The Cd-plating produces a galvanic couple with the 4340 steel specimen. The Cd-plating is anodic, sacrificially corroding relative to the steel; whereas, the steel is being cathodically protected with hydrogen being generated at its surface. Depending on the porosity of the Cd-plating, hydrogen will diffuse and be absorbed by the steel causing a degradation in strength with time. The Open Circuit corrosion Potential (OCP) of the Cd-plating in a 3.5% sodium chloride solution was measured against a Saturated Calomel Electrode to be -0.770 Vsce. By comparison, the steel specimen was -0.670 Vsce resulting in a difference in galvanic potential of 100mV. This difference in galvanic potential in salt water is the driving force for the generation of hydrogen on the surface of the Cd-plated 4340 steel specimen at 51 HRC. The RSL™ *threshold* per ASTM F519 is a measurement of the degradation due to immersion of a Cd-plated steel component in an marine salt water environment. The degradation, which is a measure of the susceptibility to hydrogen embrittlement, was found to be significant, reducing the fracture strength to 37.5% NFS(B) implying that the Cd-plating per Federal Specification QQP-416 is relatively porous even with the chromate conversion coating (The presence of chrome was verified with the SEM/EDX). A defect in the coating (holiday) causes a further reduction to 32.5% NFS(B) due to the direct exposure of the bare metal to the solution. No barrier exist due to the Cd-plating

Electrochemical Impedance Spectroscopy (EIS) Measurements: The corrosion behavior of the different samples (Cd plated and EAP coated 3x3x0.25) was evaluated in 0.5 N NaCl solution (open to air). EIS measurements were obtained at the open-circuit or corrosion potential E_{corr} in the frequency range of 100 KHz – 5mHz. The samples were exposed to the test solution for several days and measurements were taken as a function of time. A Gamry PCI4/300 potentiostat and Gamry EIS300 Software were used for the impedance measurements. The impedance spectra have been plotted as Bode plots, where the logarithm of the impedance modulus, $|Z|$, and the phase angle, Φ, are shown as functions of the logarithm of the frequency f of the applied ac signal.

Neutral Salt Fog Exposure: The Cd plated high strength steel coupons (3x6x0.25), bare metal and EAP coated coupons were placed in neutral salt fog chamber for corrosion performance evaluation on NAVAIR-AD racks (15^{o} angle) in accordance with ASTM B117. Additional testing using EAP coated steel substrates (1008/1010) were examined for corrosion protection in neutral salt fog chambers.

Sample Preparation for ICP-AES/IC Analysis: Two high strength steel (4340) panels were covered with different protective coatings. The first panel was coated with P(7-PHA)and the second with cadmium. The panels were individually rinsed with 20 ml of deionized water before being place in the salt fog chamber (T=0 hours). The panels were then removed at specific time intervals (T = 19, 72, and 96 hours), re-rinsed with a fresh 20 ml aliquot of deionized water, and placed back in the salt fog chamber. The rinsates at each time interval were collected and analyzed. The samples were analyzed as collected. Deionized water was used to rinse two coated steel panels exposed to salt fog. The panels were placed in a salt fog chamber for a period of time, removed from the chamber, rinsed, and returned to the salt fog chamber. The rinsates were collected and analyzed for cadmium, chromium, iron, and nitrate ions.

Metals Analysis of Rinsate from P(7-PHA) Coated Steel Substrates: The rinse samples were analyzed on a TJA *IRIS Advantage* inductively coupled plasma atomic emission spectrometer (ICP-AES) interfaced to a COMPAQ Deskpro computer, using ThermoSPEC software for data collection. The system was calibrated from 0 to 10 ppm using certified calibration standards. The calibration curve was verified using a certified 1 ppm check standard. Each sample was aspirated into an argon plasma using an autosampler, a peristaltic pump, and a nebulizer. All elements were analyzed simultaneously. For each element, three replicate emission intensities were measured by the charge injection detector in the spectrometer, averaged, and converted to solution concentrations using the established calibration curve. A reporting limit of 100 ppb (ug/L) was established for the analysis. This procedure is comparable to that found in EPA Method 200.7, *Determination of Metals and Trace Elements in Water and Wastes by Inductively Coupled Plasma - Atomic Emission Spectrometry*.

Ion Analysis of Rinsate from P(7-PHA) Coated Steel Substrates: The solutions were analyzed for nitrate ions by ion chromatography using a Dionex ICS-2500 ion chromatograph. The ICS-2500 consists of the following modules: an LC25 Chromatography Oven (set at 30^{o}C), a GP50 Gradient Pump, an EG50 Eluent Generator, an ED50 Electrochemical Detector, and an AS40 Autosampler. An AS18 separator column was used as the solid phase and a 23 mM potassium hydroxide solution produced by an eluent generator module was used as the mobile phase at a flow rate of 1 ml/min. An ASRS ULTRA II self-regenerating ion suppressor at a current of 193 mA was in-line after the separator column to replace counter cations with hydrogen ions, which increases the signal to noise ratio. Anion detection was realized with a conductivity detector. This procedure is comparable to that found in EPA Method 300.1, *Determination of Inorganic Anions in Drinking Water by Ion Chromatography*.

Section V

Results and Accomplishments:

Monomer Synthesis and Polymerization Processes: The preparation of the monomers proceeded according to the literature proceedures. The yields were high and reproducible. The structure determination of the monomers was accomplished via NMR, FTIR and MS analysis providing proof that the compound listed was obtained. The base polymers (thiophene and pyrrole) are inert with HMIS and NFPA rating of 0, 0 and 0 for health, flammability and reactivity.

The polymer applied onto steel substrates via air-brush and electroless deposition of the monomer does not introduce toxic materials into the bath. The process is benign and an environmentally green alternative to the current Cd plated baths for high strength steel. The process is portable, repeatable (though variation was seen in coating thickness and uniformity in the film) and a variety of substrate shapes and sizes can be coated via this non-line-of-sight electroless deposition process.

Hydrogen Embrittlement Studies/Defect Tolerance Testing: The Electroactive Polymer coating process does not introduce hydrogen into the specimens as compared to the Cd-plating. The Cd-plated specimen still had some residual hydrogen as determined by the 85.0% NFS(B) vs 91.6% NFS(B) (Table 5), where as the EAP coating of Lot #1 (P3PPA) and Lot #2 (P3PPA) was 90-95%, comparable to 91.6% for the baseline bare metal specimen.

Table 5: Resistance of Electroactive Polymer (EAP) (PPPA) coated specimens to Hydrogen Embrittlement

	Cd-Plated %NFS	**EAP Coated Lot #1 %NFS**	**EAP Coated Lot #2 %NFS**	**Baseline Bare %NFS**
NFS(B)	NA	NA	NA	100
RSL™ *threshold* in Air	85.0	95.0	90.0	91.6
RSL™ *threshold* @ -0.80Vsce	37.5	46.5	47.5	NA
RSL™ *threshold* @ -0.80Vsce with holiday	32.5	49.0	59.5	NA

Cd-OCP = -0.770 Vsce in 3.5% NaCl Solution

Fe-OCP = -0.670 Vsce in 3.5% NaCl Solution

NFS = Notched Fracture Strength

The OCP of the Electroactive Polymer coating (Figure 23) is very close to the 4340 steel and therefore does not introduce hydrogen into the steel during environmental exposure due to the galvanic couple with the 4340 steel, as with the Cd-plating. Even with patches of the coating, it did not drive the mixed potential towards the more negative

value of zinc (-1.1 Vsce), which could lead to environmentally induced hydrogen embrittlement.

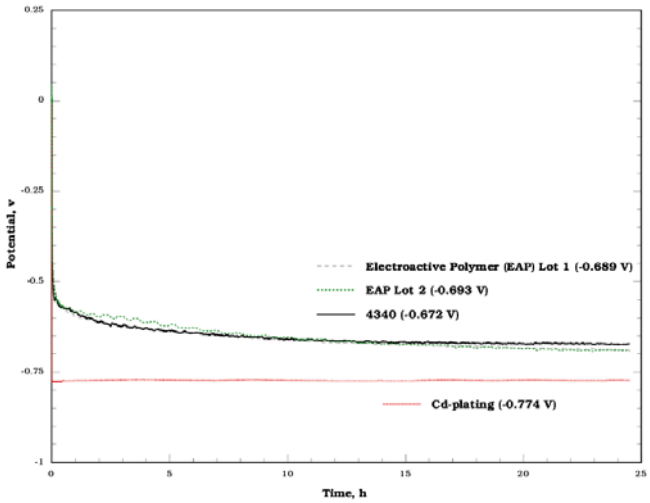

Figure 23: Overlay plot of OCP tests results

Galling Testing Results: The uncoated button and plate were tested first in order to determine an approximate threshold galling stress for uncoated AISI 4340 steel. Once the threshold was established, the various coatings were tested to see how much galling protection each provided. The load frame used for this test had a maximum load of 10,000-lbs, which equates to a stress of 51 ksi on the button. If galling did not occur at the maximum load, a value of 51+ ksi was recorded as the threshold galling stress. The uncoated AISI 4340 steel began to gall at a stress of approximately 10 ksi. Figures 24 and 25 show the results of this testing.

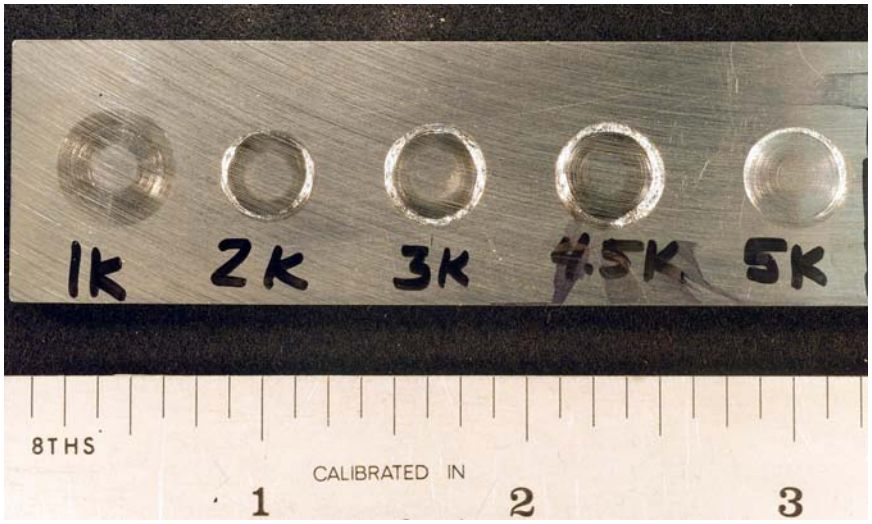

Figure 24: AISI 4340 steel plate subjected to galling testing with uncoated steel buttons, showing galling between 1000lbs and 2000lbs
(5ksi to 10ksi)

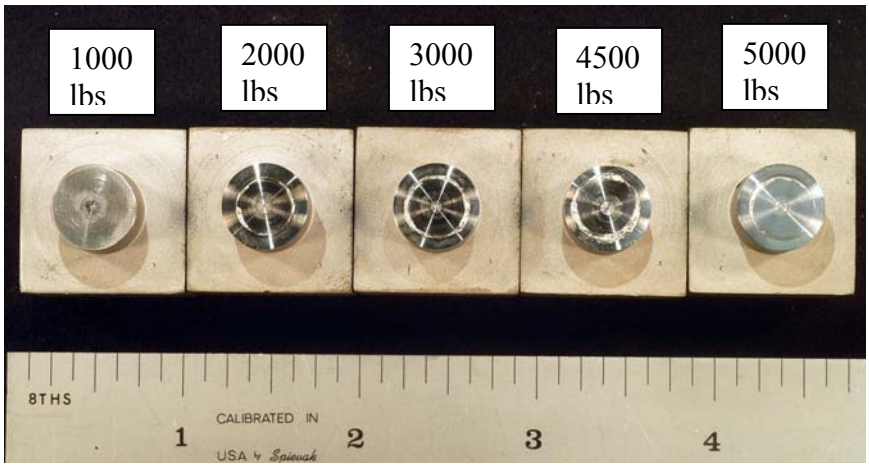

Figure 25: AISI 4340 steel buttons tested for galling on a steel plate (shown in Figure 24), displaying galling between 1000lbs and 2000lbs (5ksi to 10ksi).

The cadmium plated buttons were tested for galling resistance against the bare AISI 4340 steel plates. Cadmium is considered a gall resistant coating; therefore, cadmium on steel was tested at a starting stress of 10 ksi (2,000-lbs). After each test, the load was raised incrementally by 1,000-lbs until galling was noted. After each test, smearing and transfer of the cadmium was noted, but no galling was observed. At the maximum load of 10,000-lbs, no galling was noted and a maximum threshold galling stress of 51+ ksi was recorded. Figures 26 and 27 show the results of this testing.

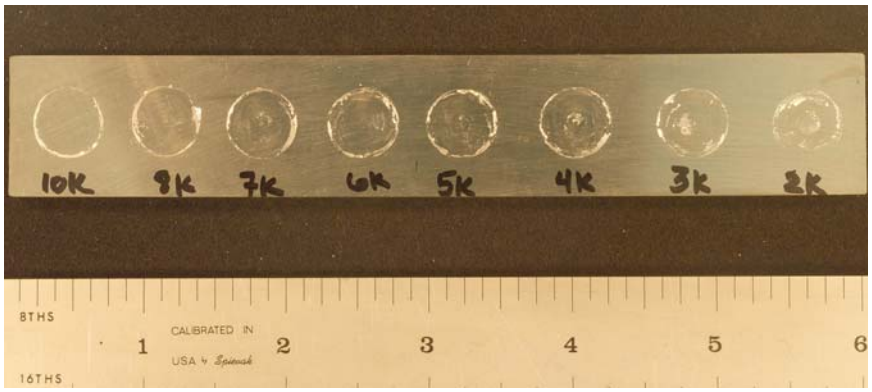

Figure 26: AISI 4340 steel plate subjected to galling testing with cadmium plated steel buttons, showing no galling at a maximum load of 10,000lbs.

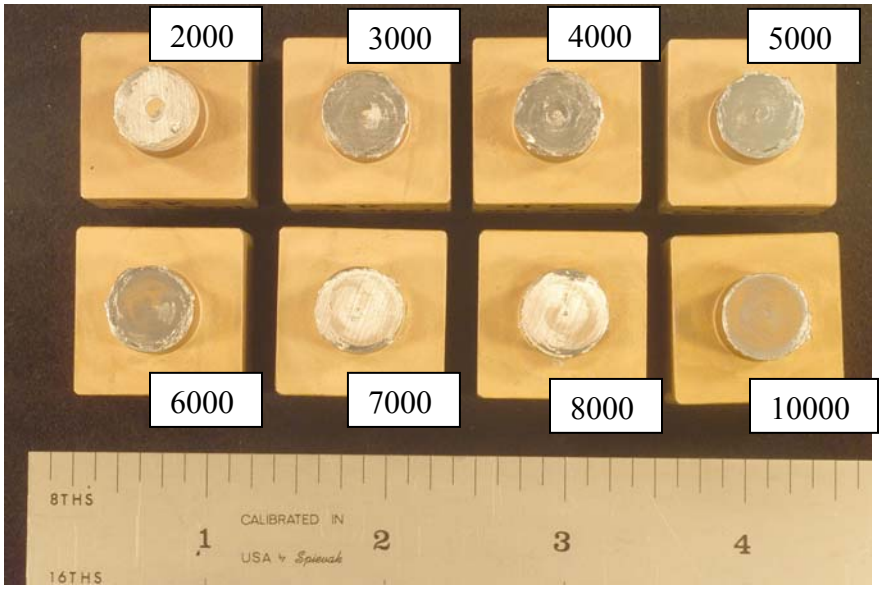

Figure 27: Cadmium plated steel buttons tested for galling on an AISI 4340 steel plate (see Figure 26), showing no galling at a maximum load of 10,000lbs.

The IVD aluminum coating was tested in the same manner as the cadmium plating. The testing was started at 2,000-lbs, and was raised by 2000-lbs until galling was noted. During testing it was noted that it was much more difficult to rotate the aluminum samples at low loads than the cadmium samples at higher loads. At 8,000-lbs, the aluminum-coated sample was unable to be rotated using two 8-inch lever arms. After approximately 1/8 (~45º) of a rotation, the test was stopped and the sample was removed and visually inspected. No galling was noted on the base metal, however it was assumed that the onset of cold welding was occurring and if the sample could have been rotated, metal would have been galled. A galling stress of 31 ksi was assumed for the IVD aluminum sample which are shown in Figures 28 and 29.

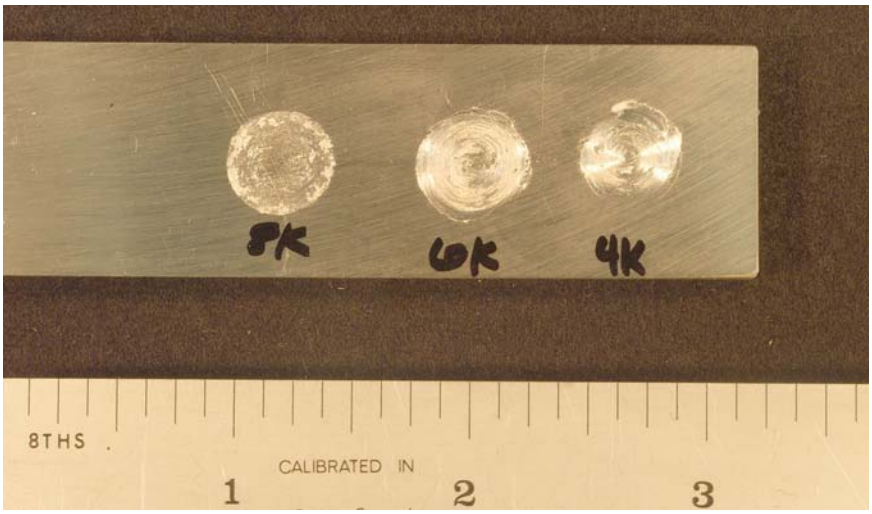

Figure 28: AISI 4340 steel plate tested for galling with IVD aluminum coated steel buttons, showing no obvious visible galling at a maximum load of 8,000-lbs.

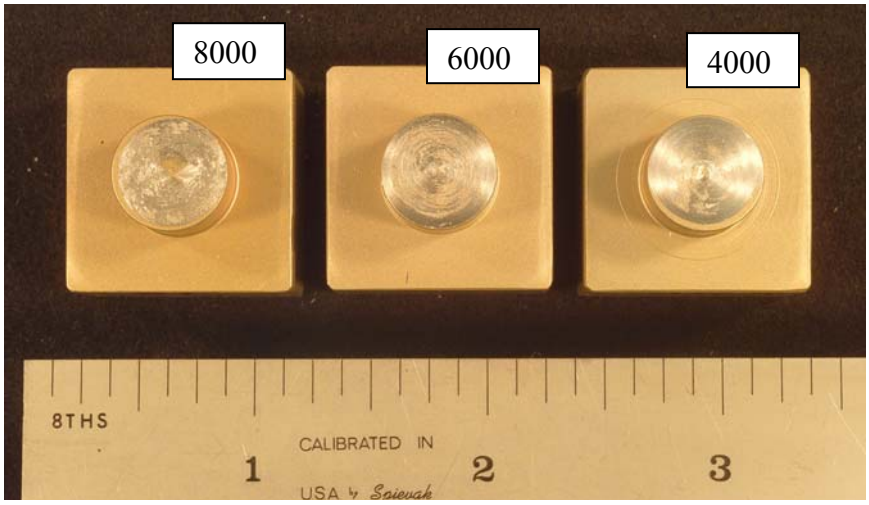

Figure 29: IVD Aluminum coated steel buttons tested for galling on the AISI 4340 steel plate (see Figure 28), showing no obvious visible galling at a maximum load of 8,000-lbs.

The P3PPA polymer coating was tested in the same manner as the cadmium plating. Separate rankings were done for the samples with and without the 2μm graphite particles. The P3PPA samples, without graphite particles, were tested first. The test started at 2,000-lbs, where slight galling was noticed. The load was lowered to 1,000-lbs, where no galling was noted. The P3PAA coating was thin and uneven, making galling determination difficult. The coating did not seem to provide much protection against steel-to-steel contact. A galling stress of 10 ksi was assumed for the P3PPA samples without the graphite particles. The P3PPA graphite embedded samples were tested starting at 2,000-lbs, where no galling was noted, but nearly all of the polymer coating

was smeared off of the button. The test operator noticed that there was not a noticeable increase in ease of rotation with the embedded graphite during testing. The load was increased to 4,000-lbs, where some slight galling of the base metal was observed. In order to determine the threshold galling stress of the sample, testing was performed at 3,000-lbs, where no galling was observed. Therefore, the threshold galling stress for P3PPA graphite embedded electroactive polymer is assumed to be approximately 20 ksi. Figures 30 and 31 show the results of the P3PPA samples with graphite embedded in the surface.

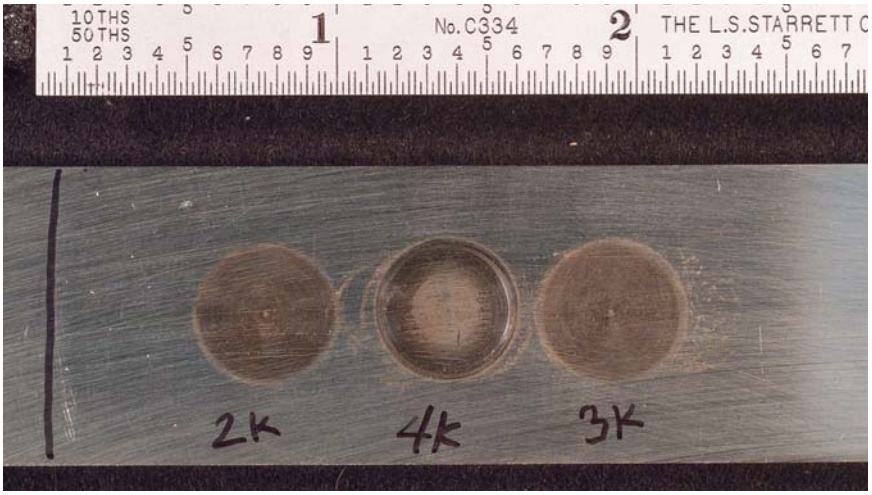

Figure 30: AISI 4340 plate tested for galling with electroactive polymer P3PPA coated buttons with embedded graphite, showing slight galling at a load of 4,000-lbs.

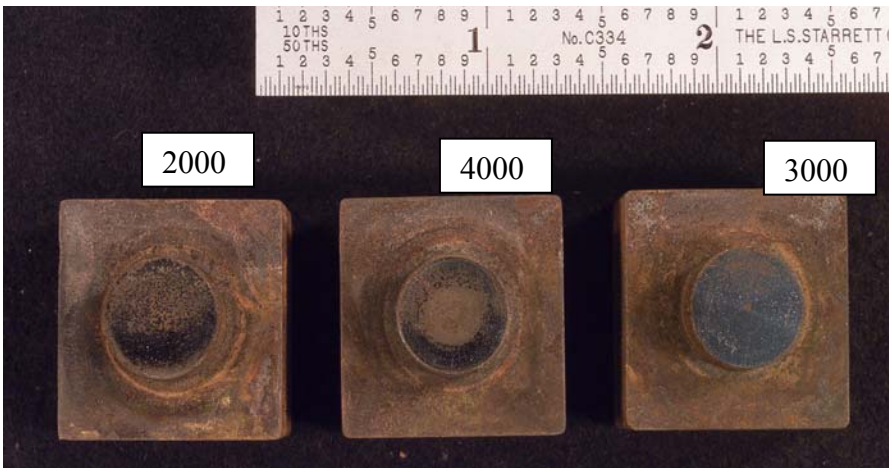

Figure 31: Electroactive polymer P3PPA coated buttons with embedded graphite tested on AISI 4340 plate (see Figure 30), showing slight galling at a load of 4,000-lbs.

The P3HT coating was tested starting at 4,000-lbs. It was noted that this coating behaved similarly to grease. The surface roughness of this coating could not be measured

due to the poor adhesion of the coating. When the buttons were cleaned in isopropyl alcohol, the coating began to flake off, therefore the cleaning step was omitted for the remaining P3HT samples. The three remaining samples were tested at 4,000-lbs, 6,000-lbs, and 8,000-lbs, where no galling was noted on any of the samples.

Polymer sample P3PPAwas tested with both embedded MoS_2 and SiO_2 particles. The P3PPA MoS_2 samples were tested at 2,000 and 4,000-lbs. At 4,000-lbs galling of the coating was observed. The button and plate were fused together after testing and when they were broken apart, torn coating was seen. The P3PPA SiO2 samples were tested in a similar manner, starting at 2,000-lbs. These samples were difficult to turn, showing poor lubricity, but no visible galling was noted. At 8,000-lbs the samples were unable to turn, and a galling stress of 41 ksi was assumed. The results can be seen in Figures 32 and 33 show the samples with MoS_2 while Figures 34 and 35 show the samples with SiO_2.

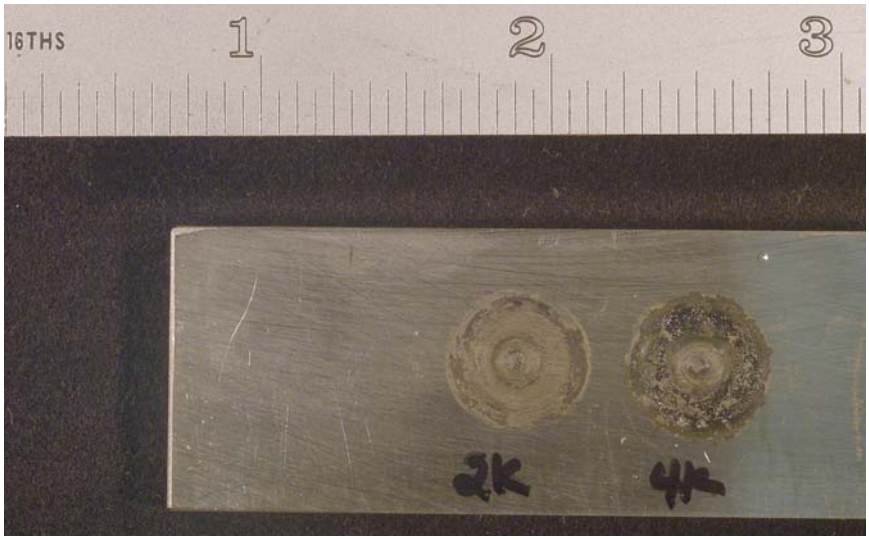

Figure 32: AISI 4340 plate tested for galling with electroactive polymer P3PPA with MoS_2 coated buttons, galling of the coating was noted at a load of 4,000-lbs.

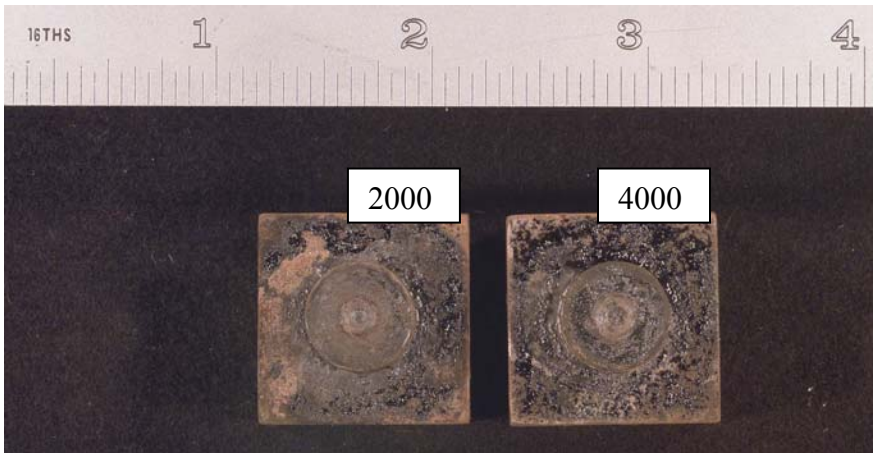

Figure 33: Electroactive polymer P3PPA with MoS_2 coated buttons tested on AISI 4340 plate (see Figure 32), galling of the coating was noted at a load of 4,000-lbs.

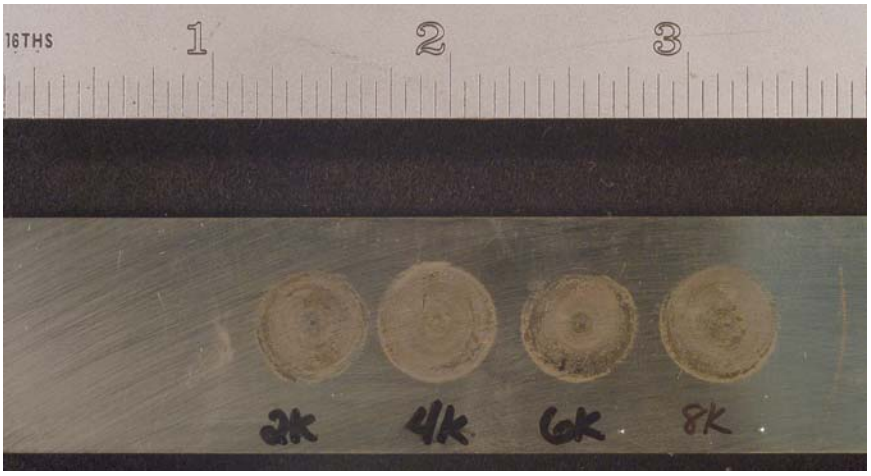

Figure 34: AISI 4340 plate tested for galling with electroactive polymer P3PPA + SiO_2 coated buttons, galling was assumed at 8,000-lbs when the button could no longer be rotated.

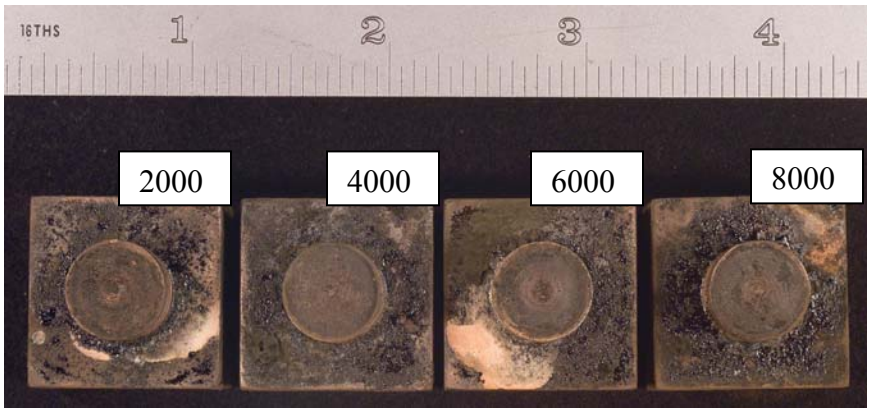

Figure 35: Electroactive polymer P3PPA with SiO_2 coated buttons tested on AISI 4340 plate (see Figure 34), galling was assumed at 8,000-lbs when the button could no longer be rotated.

Final samples of P3PPA with boron carbide were also tested for their galling resistance properties. The P3PPA was a very thin layer of coating, and showed little galling resistance over direct steel on steel contact. P3PPA showed some initial signs of galling at a load of 2,000-lbs.and with the addition of boron carbide to the P3PPA resulted in only a minimal increase in galling resistance. The coating flaked off during rotation and galling was noticed at a load of 4,000-lbs.

Scanning Electron Microscopy: ASTM G98 states that only the unaided eye shall be used to determine whether or not a system exhibited signs of galling. However, for the purpose of more thoroughly ranking coating galling resistance, an SEM was used to identify signs of galling at high magnification. Cadmium is a traditionally gall resistant coating, and exhibited coating smearing accounting for its lubricity when examined under the SEM. Figure 36 shows the cadmium coating tested at 10,000-lbs at a magnification of 500x. IVD aluminum was also examined with the SEM for comparison purposes. Figure 37 shows the plate tested at 6,000-lbs, showing metal transfer and tearing of the aluminum coating. The various polymer coatings were examined with the SEM to see if the same desired metal smearing could be observed. Figure 38 shows a SEM image of coating P3PPA with SiO_2 on a button tested at 6,000-lbs. This samples shows metal smearing and some tearing, but the tearing seems to be less than IVD aluminum tearing at 6,000-lbs.

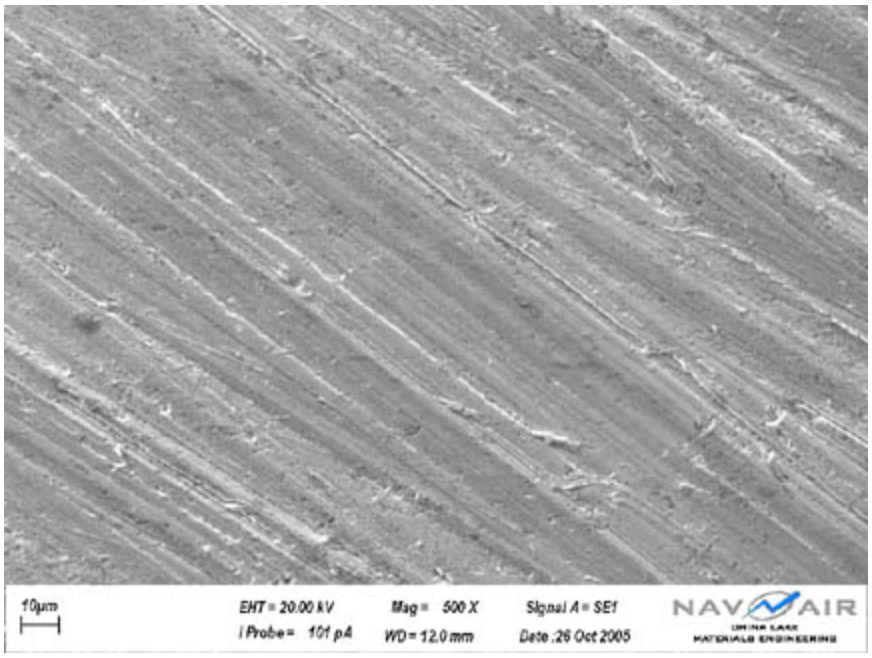

Figure 36: Cadmium coated buttons tested on AISI 4340 plate at 10,000-lbs (51ksi). Coating smearing was noticed, but no evidence of coating or base metal galling at 500X.

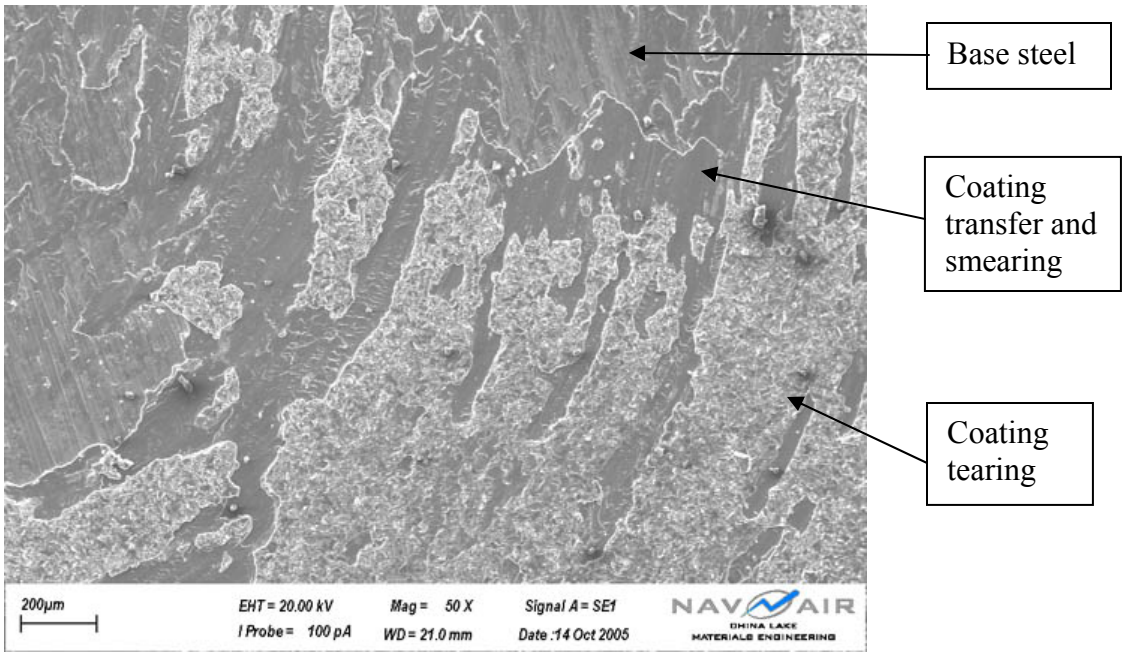

Figure 37: AISI 4340 plate galling tested for galling with IVD Aluminum coated button at 6,000-lbs. Coating transfer and tearing was noticed at 50X.

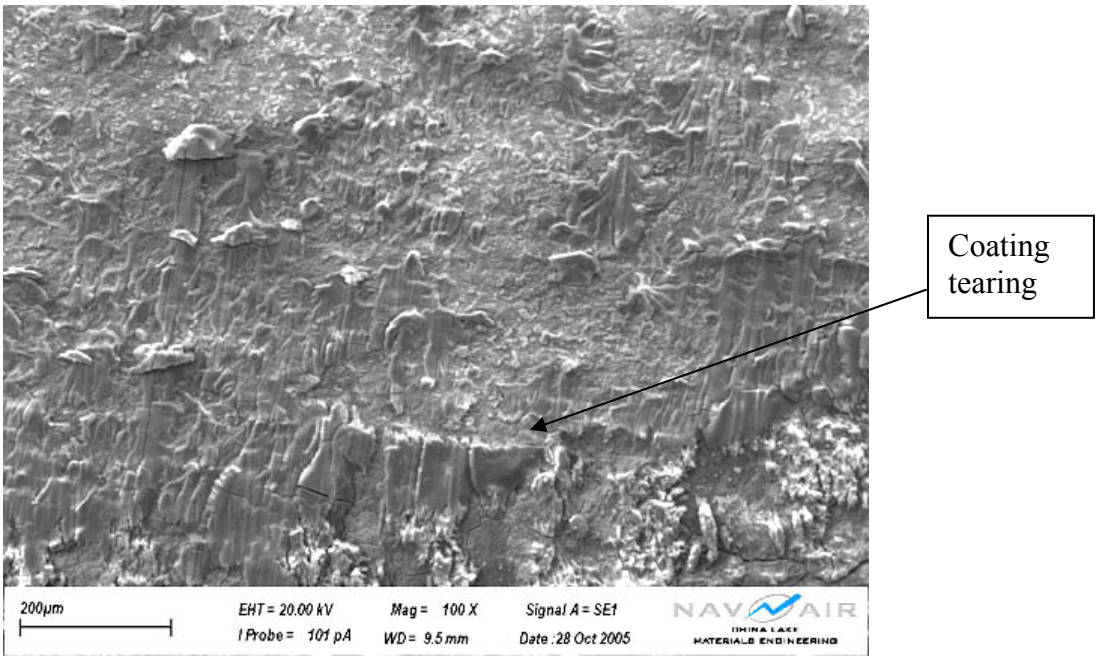

Figure 38: P3PPA with SiO_2 button galling tested at 6,000-lbs, showing significant metal transfer, but less tearing that observed with the IVD aluminum at100X.

The results of the galling studies using the EAPs and micro-and nano-particles are summarized in Table 6 which shows the threshold galling stress of each of the tested coatings. The threshold galling stress is defined by ASTM G98 as the stress where galling is first observed with the unaided eye. The stress was determined by dividing the testing load by the button area (.196 square inches). The table shows that cadmium exhibited the highest galling stress and the uncoated steel exhibited the lowest stress. Several of the polymer coatings provided little, if any, protection to steel on steel galling. Some of the other coating behaved more like a grease than a coating and did not provide an accurate galling resistance measurement. The P3PPA coating showed slight galling improvement with the addition of graphite particles. The P3PPA coating showed increased galling resistance with the addition of SiO_2, and seemed to show less galling than IVD aluminum.

Table 6: Threshold galling stress comparison of all tested coatings

Coating	Maximum Testing Load (1000-lbs)	Threshold galling stress (ksi)	Comments
AISI 4340 steel - no coating	2	10	
Cadmium	10	>51	Maximum load
IVD Aluminum	6	31	Unable to move at 8klbs
P3PPA	2	10	Little protection over unprotected steel
P3PPA + graphite	4	20	No increase in lubricity noticed by operator
P3HT + MoS_2	8	>41	Low number of samples, coating acted like a grease
P3HT	8	41	Base metal galling, coating behaved like a grease
P3PPA + MoS_2	4	20	Coating galling
P3PPA+SiO_2	6	31	Unable to move at 8klbs
P3PPA	2	10 to 15	One sample only, very slight galling noted on metal
P3PPA + boron carbide	4	20	Coating flaked off, base metal galling

EIS Measurements and Neutral Salt Fog Tests: The spectra obtained for several days of exposure for Cd plated and P3PPA coated samples on high strength steel coupons (3x3x0.25) are given in Figures 39 and 40 respectively. The EIS spectra for the Cd plated high-strength steel reflect the corrosion behavior of metallic Cd in 0.5 N NaCl and can be fit to a simple one-time constant EC. The Cd metal surface was quite stable as evidenced by the more or less constant impedance spectra for exposure periods up to 8 days. E_{corr} also remained in a very narrow range. The spectra for the P3PPA coated steel samples resembled those for bare steel indicating that the coating did not provide corrosion protection (Figure 39). The E_{corr} values were close to those for bare steel. Rusting was observed on the exposed surfaces. The rusting is due to the pore film formation in which areas of the bare metal are not completely coated with the EAP. This same problem was observed in neutral salt fog exposure tests in which visible corrosion was evident in EAP samples (Figure 41). The neutral salt fog results are summarized in Table 7.

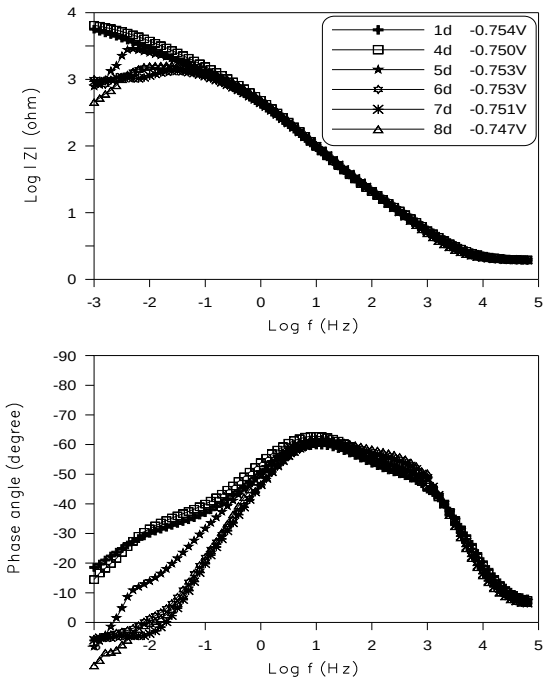

Figure 39: Impedance spectrum of Cd plated high strength steel.

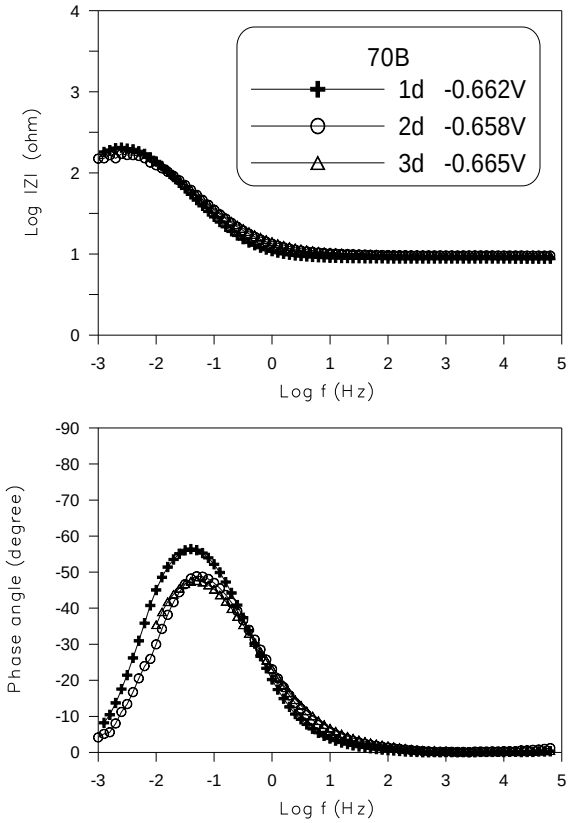

Figure 40: Impedance spectrum of P3PPA coated onto high strength steel.

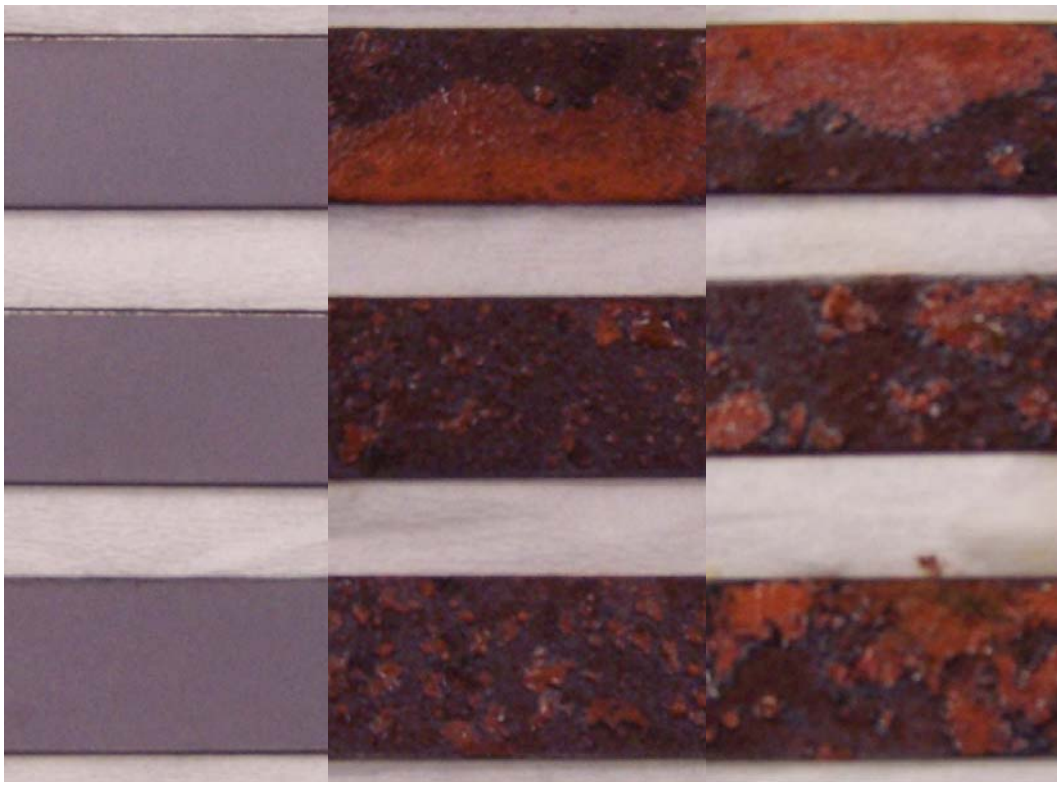

Figure 41: Time = 0hrs (left), Time = 18hrs (middle), and Time = 42 hrs (right) for Neutral Salt Fog with Spray-cast TC + MoS_2 overcoat

Table 7: Neutral Salt Fog Exposure Tests on 1008 and High Strength Steel Coupons

EAP	Substrate	Application of Coating	Time (hrs) rust	Observation
Cd plated	High strength steel 4340	immersion	>96	No rust at 96 hrs
P3HT	1008	Spray	24	Rust localized to few spot on substrate
TP + MoS_2	1008	Spray	18	Rust
TC+ MoS_2	1008	Spray	18	Rust
P3PPA	High strength steel 4340	Electroless deposition	12	Rust

Discussion of Accomplishments for FY05 and Future Work for FY06

In terms of the project goals, namely, synthesis of EAP-based materials and testing of the properties of interest, the work has shown some success. Although all of the improved properties have not been demonstrated simultaneously in a single material, the successful synthesis and testing has led to a greatly improved understanding of the key factors that influence the properties of interest. For instance, the corrosion testing clearly demonstrates that the quality of the coating film and its adhesion to the substrate are the main determinant of corrosion resistance. The highest quality films resulted from the spray techniques used with the poly-alkylthiophenes, however, the best adhesion was observed in films made from polypyrrole (which had no alkyl side groups but a much higher concentration of acid groups) with a silane pretreatment. The latter films had flaking problems, which typically result from a glass transition temperature that is above room temperature, and can be solved by the use of alkyl-substituted pyrrole monomers. Both the chain length and concentration of acid groups could be systematically varied to produce an EAP with the optimal combination of properties. In addition, a combination of spray or powder coating, with a short electroless deposition to fill in any holes or inaccessible areas, could be used to optimize film quality. Since some corrosion protection from good quality EAP films is evident in the results, and since previously optimized EAP formulations have provided acceptable levels of corrosion protection in previous materials[32, 33], there is good reason to believe that an optimized EAP, with the addition of hard particles to resist galling, would possess all the properties needed to serve as an effective replacement for cadmium-based coatings on high strength steels. In essence, the results have enabled us to identify the correct compositional elements, or pieces of the puzzle, for a successful coating system, what remains is to assemble and optimize the elements in order to produce a successful coating system.

Continued SERDP SEED Effort for FY06: Improved Corrosion Inhibition of EAP Coatings

Pre-Treatment of Steel Panels with Passivating Ions

A recent literature report showed improved adhesion of polythiophenes and polypyrroles onto steel substrates using acidic nitrate or oxalate solutions.[34] A series of panels were prepared for neutral salt fog testing. The panels were cleaned and then treated with non-acidic nitrate and oxalate solutions to displace the surface oxides. The panels were dried and spray coated with a polythiophene copolymer containing ~25% phosphonate groups as an adhesion promoter. An additional series of panels using the amino-silane adhesion promoter used previously for the polypyrroles was prepared with the spray-cast polythiophene.

While the animo silane functionized polythiophenes produced good pinhole free films, they failed in neutral salt fog. In Figure 42 below, we coated steel panels with various thickness of the functionalized thiophene polymer. In addition to spray casting, we also tried spin casting to test the effect of uniform film thicknesses. Only the thickest film gave protection in the first 24 hrs with all panels failing after 48 hrs.

0 hrs 1 coat 2 coats 3 coats

24 hrs 1 coat 2 coats 3 coats

Figure 42: Neutral Salt fog results of Amino Silane Functionalized Polythiophene Acetic Acid Spray-cast on Steel

In an effort to improve the corrosion protection, pinhole free films we prepared via electroplating of the polymer directly onto the steel. It is widely know that the polymer deposits rapidly and continues to grow to cover bare electrode surfaces. Aqueous pyrrole solutions with oxalate and nitrate electrolytes were used as per the literature.[35] After 24 hours rust spot were clearly visible on the surface of the substrates produced with KNO_3 as the electrolyte (see Figure 43). As the test continued, there were no new spots nor did they grow in size. This result suggests pinholes in the films. This was not the case in the polypyrrole electroplated from aqueous 0.1M oxalic acid (Figure 44). The films continued to degrade as exposure time increased.

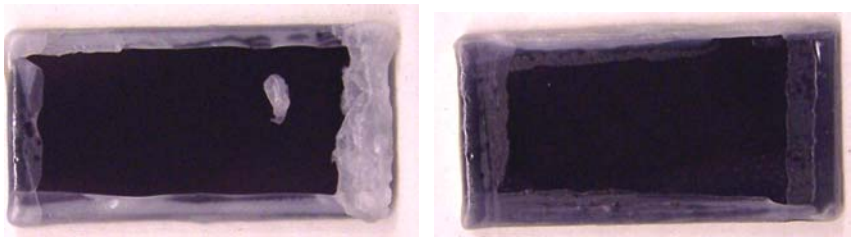

0 Hours

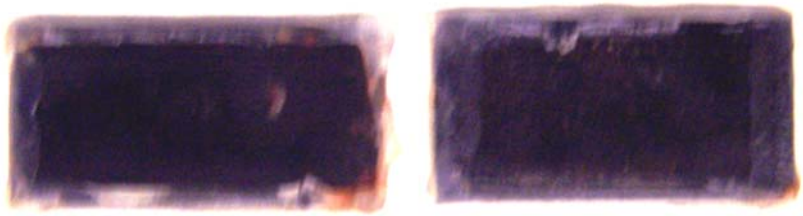

24 Hours

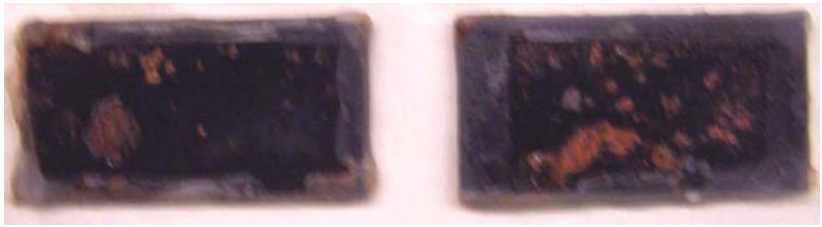

48 Hours

72 Hours

Figure 43: Neutral Salt Fog Results of Polypyrrole electroplated from aqueous 0.3M KNO_3

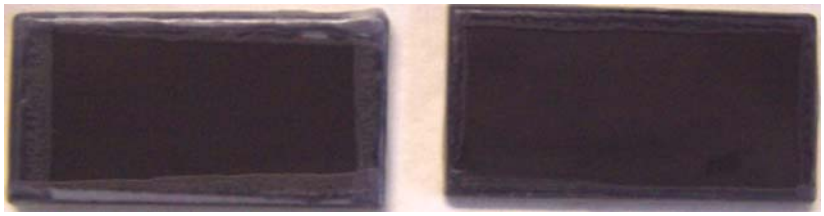

0 Hours

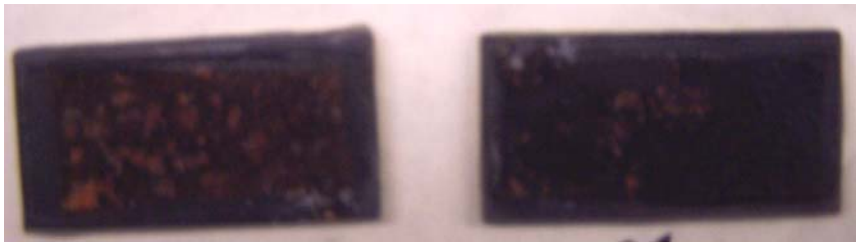

24 Hours

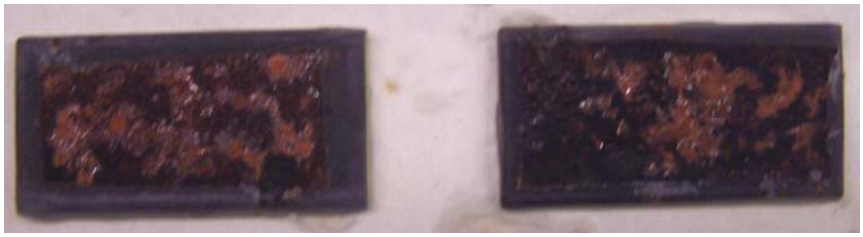

48 Hours

Figure 44: Neutral Salt Fog Results of Polypyrrole electroplated from aqueous 0.1M Oxalic Acid

In a review of an electroplating handbook, the use of "pickling" to passivate steel is common. The use of nitric acid to passivate the steel induces no marked hydrogen embrittlement.[36] Therefore, we attempted a series of experiments using a nitric acid pre-treatment. The steel samples were cleaned as per our standard protocol and then were placed in a 10w% aqueous nitric acid bath for 2 minutes. These samples were then cleaned with water and methanol. The sampled seemed rough so they were abraded with 600 grit sandpaper to smooth the surface. Polypyrrole was electrodeposited from a 0.3 M aqueous KNO_3 solution at a constant potential 1.3 V vs Ag wire (to fill all pinholes and form compacted films). Small bumps or tubes were seen on the surface of the films. These could be removed by rubbing. These samples also failed salt fog in the first 24 hrs (Figure 45).

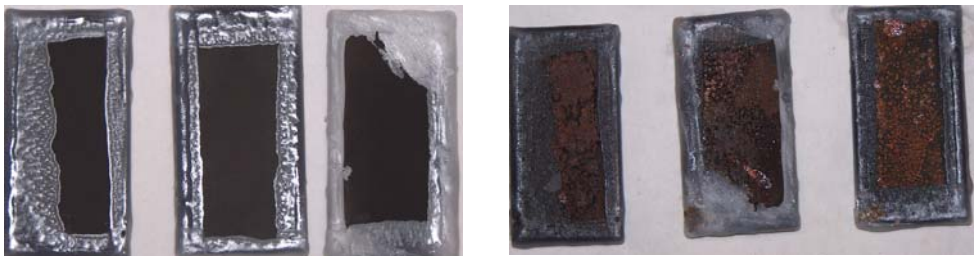

0 hrs 24 hrs

Figure 45: Neutral Salt Fog Results of Polypyrrole electroplated onto "pickled" Steel from aqueous 0.3M KNO_3 Solutions

Further analysis of the bumps to determine the cause failure in salt fog revealed some unique structures (Figures 46 and 47). While none of the structures allow a clear channel to the steel substrate, rust was evident. An explanation for the observed failure was not evident.

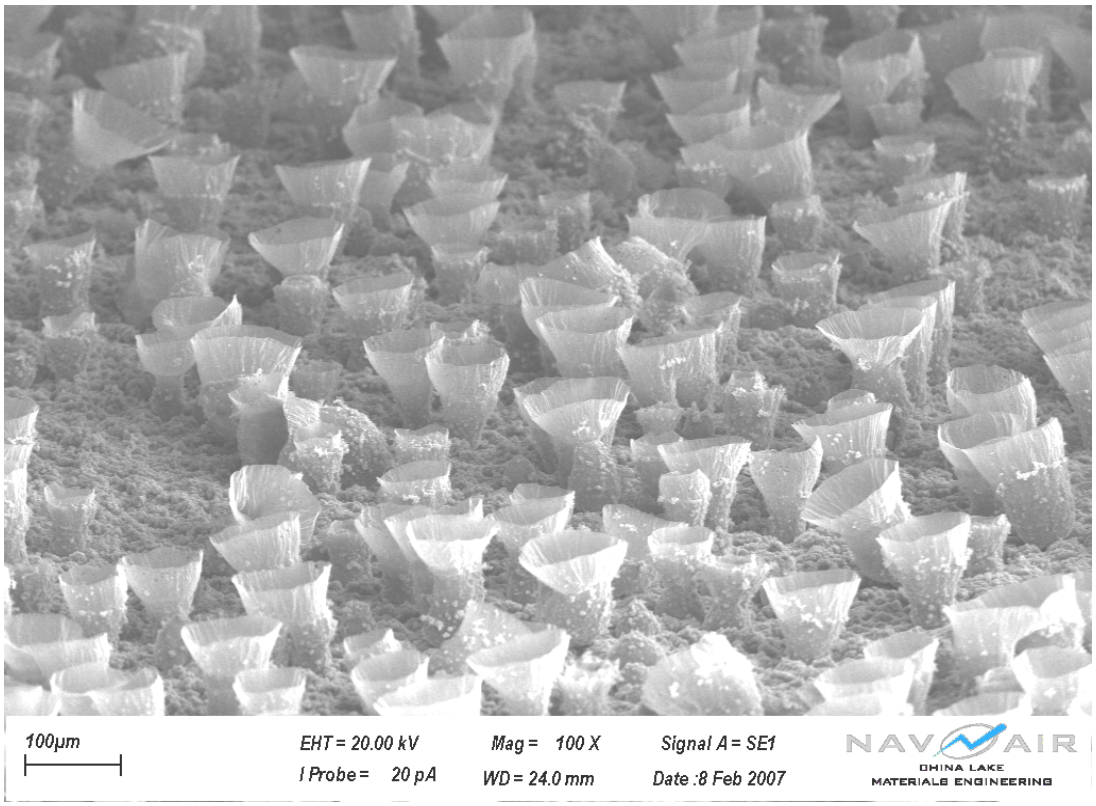

Figure 46: Polypyrrole Structures Electropolymerized on "Pickled" Steel

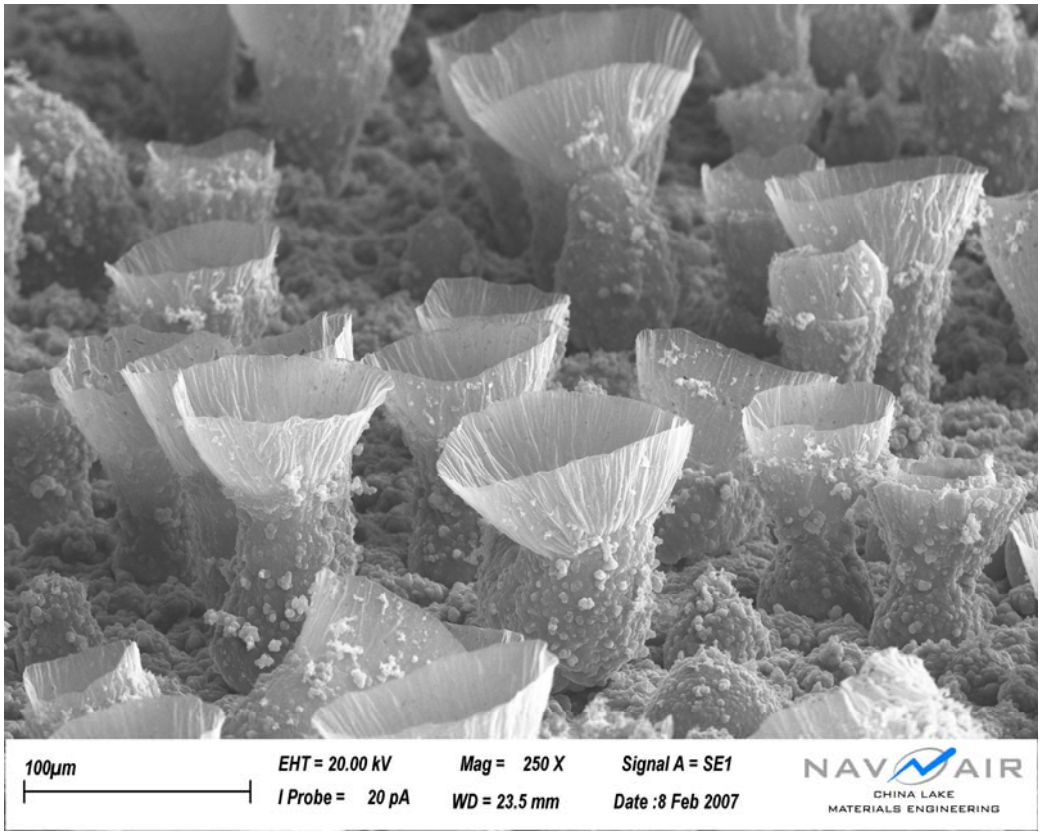

Figure 47: Close-up of Polypyrrole Structures Electropolymerized on "Pickled" Steel

Adhesion and coating thickness of polymer on 1x3" high strength steel panels (4130):

Two 1x3" panels were analyzed for coating thickness and adhesion for electroless deposited P(7-PHA). One panel was coated with only the silane-based pretreatment (adhesion promoter) on the steel substrate. The other panel had the both the adhesion promoter and the EAP.

The coating thickness was measured for both the adhesion promoter and the polymer-adhesion promoter system. Measurements were made using an eddy current coating thickness gauge. The panel with only the adhesion promoter was observed to have two very distinct zones of different thicknesses. The thicker zone averaged 0.0025" (63.5 microns) while the thinner zone averaged 0.00063" (16 microns). The coating thickness gauge used was not able to distinguish between the polymer and the adhesion promoter, thus for the panel that had the polymer on top of the adhesion promoter, the measured thickness was for the combination of the two coatings. The average thickness for this combination was 0.0033" (84 microns).

The adhesion of the coatings to the steel substrate was tested using Method B of ASTM-D 3359. For the panel with only the adhesion promoter, the zone of thicker coating was subjected to the adhesion test. Images of the panels before and after the test are shown in Figure 48. Both panels were judged to qualify between 3B and 4B on the classification chart from ASTM-D 3359 as seen in Table 8. This means the areas tested lost between 1 and 15% of their total coating. Table 8 illustrates the adhesion strength of

the silane-based adhesion promoter and the conductive polymer to the steel substrate. The samples were tested per ASTM-D 3359 Method B. Both the polymer and the adhesion promoter appear qualify between Classification 3B and 4B. Coating thickness measurements were made using an eddy current coating thickness gauge. The adhesion promoter had two distinct zones of thickness on the sample; one area averaged 0.0025" (63.5 microns) while the other area averaged 0.00063" (16 microns). The thickness of the polymer and the adhesion promoter combined averaged 0.0033" (84 microns) thick. This coating is thicker than a Class 1 IVD aluminum coating (0.001" or 25 microns).

Adhesion Testing of P-7PHA onto High Strength Steel Coupons: The adhesion strength of the silane-based adhesion promoter (3-aminopropyltrimethoxy silane) and the conductive polymer (P-7PHA) onto the high strength steel substrate (4130) were tested according to ASTM-D 3359 Method B. Both the polymer and the adhesion promoter appear to qualify between Classification 3B and 4B. The coating thickness measurements were made using an eddy current coating thickness gauge. The adhesion promoter had two distinct zones of thickness on the sample; one area averaged 0.0025" (63.5 microns) while the other area averaged 0.00063" (16 microns). The thickness of the polymer and the adhesion promoter combined had averaged 0.0033" (84 microns) thick (see Table 8). This coating is thicker than a Class 1 IVD aluminum coating (0.001" or 25 microns). In Figure 48, the upper two images are of the silane based adhesion promoter before and after the ASTM-D 3359 Method B adhesion test. The lower two images are of the polymer and adhesion promoter combined before and after the same test. The polymer and adhesion promoter showed very little loss after application of the dry tape test.

Table 8: Coating Thickness of Adhesion Promoter and Polymer on High Strength Steel

Sample	Adhesion Classification	Adhesion test	Coating Thickness
Silane based adhesion promoter	3B-4B	ASTM-D 3359 Method B	0.0025" (63.5 microns) / 0.00063" (16 microns)
Silane promoter and polymer	3B-4B	ASTM-D 3359 Method B	0.0033" (84 microns)

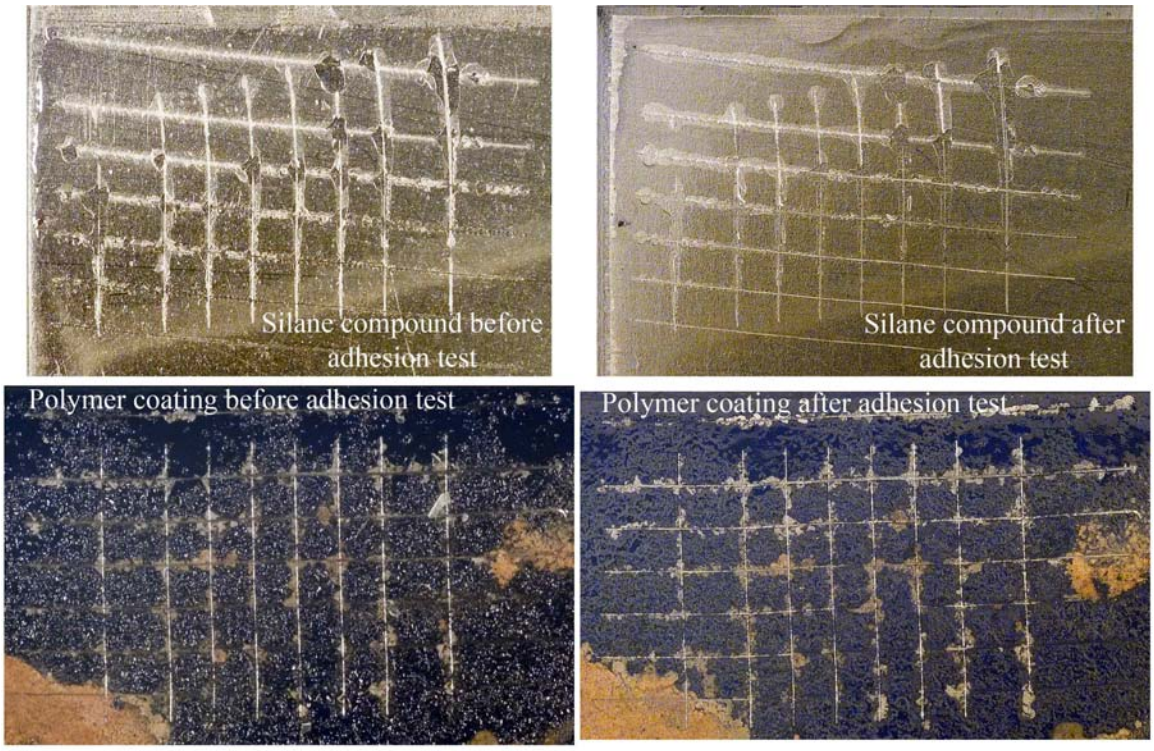

Figure 48: The upper two images are of the silane based adhesion promoter before and after the ASTM-D 3359 Method B adhesion test. The lower images are of the polymer and adhesion promoter combined before and after the same test.

Neutral Salt Fog Testing of P(7-PHA)

A steel 1x3" panel coated with only the adhesion promoter was subjected to a salt fog environment for a period of 48 hours. The panel was examined under a Scanning Electron Microscope (SEM) and Energy Dispersive Spectroscopy (EDS) for signs of corrosion at 0, 24, and 48 hours of salt fog exposure. At 0 hours of exposure, varying amounts of adhesion promoter were found, as seen in Figure 49. Figures 50, 51 and 52 illustrate the EDS spectra for the varying thicknesses. SEM analysis indicated that the thickness tended to vary the most near the panel edges and was fairly uniform nearer the center of the panel. After 24 hours of salt fog exposure, no evidence of the adhesion promoter could be found. Figures 49, 53, and 54 show the panel surface and Energy Dispersive Spectroscopy (EDS) spectra shows the lack of any silicon peak. This peak was unique to the adhesion promoter, since the alloy of the steel substrate had only 0.15-0.35 % by weight of silicon. Thus the disappearance of that peak indicated that somehow the adhesion promoter had been removed. In figure 49, the upper image illustrates a difference in coating thickness. The darker hue of the grayscale shows a thicker coating. The lightest areas barely registered an Si peak from the EDS (Figures 50-54), while the darkest area had a significant peak. The lower image shows the same test panel after 24 hours in a neutral salt fog chamber. In this picture, no Si peak was found anywhere on the panel. The adhesion promoter was washed away during the test. The darker areas of this lower SEM image (Figure 49) show iron oxide present and the lighter areas un-

corroded steel. The adhesion promoter may be soluble in water and/or saline solutions. The goal of the test was to examine the effects of 96 hours of salt fog on the adhesion promoter, but the test was cut short at 48 hours because there was no adhesion promoter left.

Steel 1x3" panel coated with P(7-PHA) over adhesion promoter:

A steel 1x3" panel coated with conductive polymer over the silane-based adhesion promoter was subjected to a salt fog environment for a period of 96 hours. The panel was examined under an SEM and EDS for signs of corrosion at 0, 24, 48, and 96 hours of salt fog exposure. Figures 55, 56 and 57 include SEM images of different parts of the coating surface at different inspection intervals. Figure 55 shows the areas farthest from the edges of the test panel. There was no catastrophic damage after exposure over time in the neutral salt fog chamber. The craters in the images are a result of the electroless deposition process, in no cases, were there any craters that were not completely filled by the polymer compound (P(7-PHA)). There was no exposed, uncovered metal found in these images. Figures 56 and 57 show multiple cracks forming during exposure of the steel substrate in the neutral salt fog chamber. The cracks may have formed during testing as the result of the silane-based adhesion promoter dissolving away. The polymer then came apart as a result of no foundation to support itself. This is supported by the Si peak in the EDS spectrum from the areas that were missing polymer coating. The coating did change physically as time progressed. The center of the panel had the most uniform layer of polymer coating. By 48 hours of salt fog, the coating was beginning to crack, and the cracks expanded through 96 hours. However, the outer edges of the panel had defects in the coating. These areas showed signs of cracking at 24 hours of salt fog. These cracks expanded through 96 hours to the point that small flakes of polymer were disappearing. The cracking and flaking is possibly due to the adhesion promoter. In the defects where the adhesion promoter was exposed, the saline solution eroded and washed it away. As the adhesion promoter disappeared, the polymer had no foundation and cracked apart. After enough adhesion promoter had eroded, the polymer had nothing to hold it to the panel and flaked away.

Figures 58 through 64 are the EDS spectra at different locations on the coating at different inspection intervals. The overall trend was that the polymer itself did not corrode or decay in any significant amount. In Figures 58 and 59, (between 0 and 24 hours of salt fog exposure), the carbon peak dropped about 10 wt. % and the oxygen peak increased by about 8 wt. %. In Figures 60-64, (24 through to 96 hours exposure to neutral salt fog spray), the relative amounts of carbon, nitrogen, silicon, iron and oxygen observed from EDS did not change significantly. The polymer may have some "limited throwing power" due to presence of nitrate ions in the film. This "throwing power" did provide protection to several areas without polymer coating.

Steel 3x6" panel coated with cadmium and chromate conversion coating:

A steel 3x6" panel coated with cadmium and chromate conversion coating was scribed and then exposed to salt fog for 96 hours. The panel was examined at 0 and 96 hours of salt fog for signs of corrosion. Figure 65 is a comparison of one location on the

scribe at both 0 and 96 hours of salt fog. The images on the right were made using the quadrapole backscatter detector (QBSD) on the SEM. The grayscale in these images is dependent on the atomic number of the target. As atomic number increases, the area will become brighter, and vice versa. Thus, areas of iron are dark compared to areas of cadmium. There was no cadmium in the scribe at 0 hours, but at 96 hours small particles were discovered in the scribe. Also, after 96 hours of salt fog, there were no signs of corrosion of the steel substrate, nor overt signs of oxidation of the cadmium. At 96 hours, there was evidence of cadmium oxidizing as seem by the small spheres in the scribe line in the lower images. There was no evidence of any iron oxide corrosion products. The scribed areas were examined under EDS, and Figures 66 through 70 show that no oxides of iron were found. Figure 66 shows the EDS spectrum of the cadmium plated steel substrate at 0 hours. The expected cadmium, chromium and oxygen peaks as well as sulfur and selenium were detected. The sulfur peak was most likely retained from the plating bath and the selenium is sometimes used as a cadmium plating brightener. The presence of nickel in Figure 67 was unexpected. The absence of an oxygen peak indicated no pre-test corrosion was present. Figures 68-70 showed that the cadmium plating changed very little over time. There was a small buildup of sodium and chlorine from the salt fog chamber. The scribe mark (Figure 69) showed no corrosion after 96 hours exposure to neutral salt fog spray. Further, the small particles discovered in the scribe after 96 hours (Figure 70) of salt fog were cadmium oxide. Oxidation of the cadmium was expected because it is anodic to the steel substrate. The cadmium appeared to have "throwing power" because it was able to prevent corrosion of the steel substrate in the unprotected scribe mark.

Steel 3x6" panel coated with P(7-PHA) over adhesion promoter:

A steel 3x6" panel coated with conductive polymer over the silane-based adhesion promoter was scribed and then exposed to salt fog for 96 hours. The panel was examined at 0 and 96 hours of salt fog. Figures 71 and 72 illustrate one location on the panel at both time intervals. The images in these figures were captured using QBSD, so lower atomic number elements, such as carbon, appear darker. Therefore the polymer coating is a dark gray while the steel exposed in the scribe is nearly white. Corrosion products appear as a medium to light gray. At 0 hours, the polymer was a uniform coating and was not in the scribe. Pieces did appear to have flaked off as a result of scribing. After 96 hours of salt fog, the polymer around the scribe line had cracked like it did in portions of the 1x3" polymer coated steel panel exposed to 96 hours of salt fog. The scribe line most likely acted as a defect by which the salt fog was able to erode the adhesion promoter out from under the polymer, as it did in the 1x3" polymer coated panel. Figures 73 through 77 are the EDS spectra of the scribe line and the polymer near the scribe line. The polymer itself did not appear to have changed because the carbon, oxygen and iron peaks were all at about the same levels at 0 and 96 hours of salt fog exposure. Some areas of the scribe mark did corrode, as evidenced in Figure 77 while other areas of the scribe did not, as in Figure 76. The small oxygen to iron to oxygen ratio showed that corrosion was inhibited in these areas. It is not known why some areas corroded while others did not, but one possible explanation is that the polymer produced some limited kind of "throwing power."

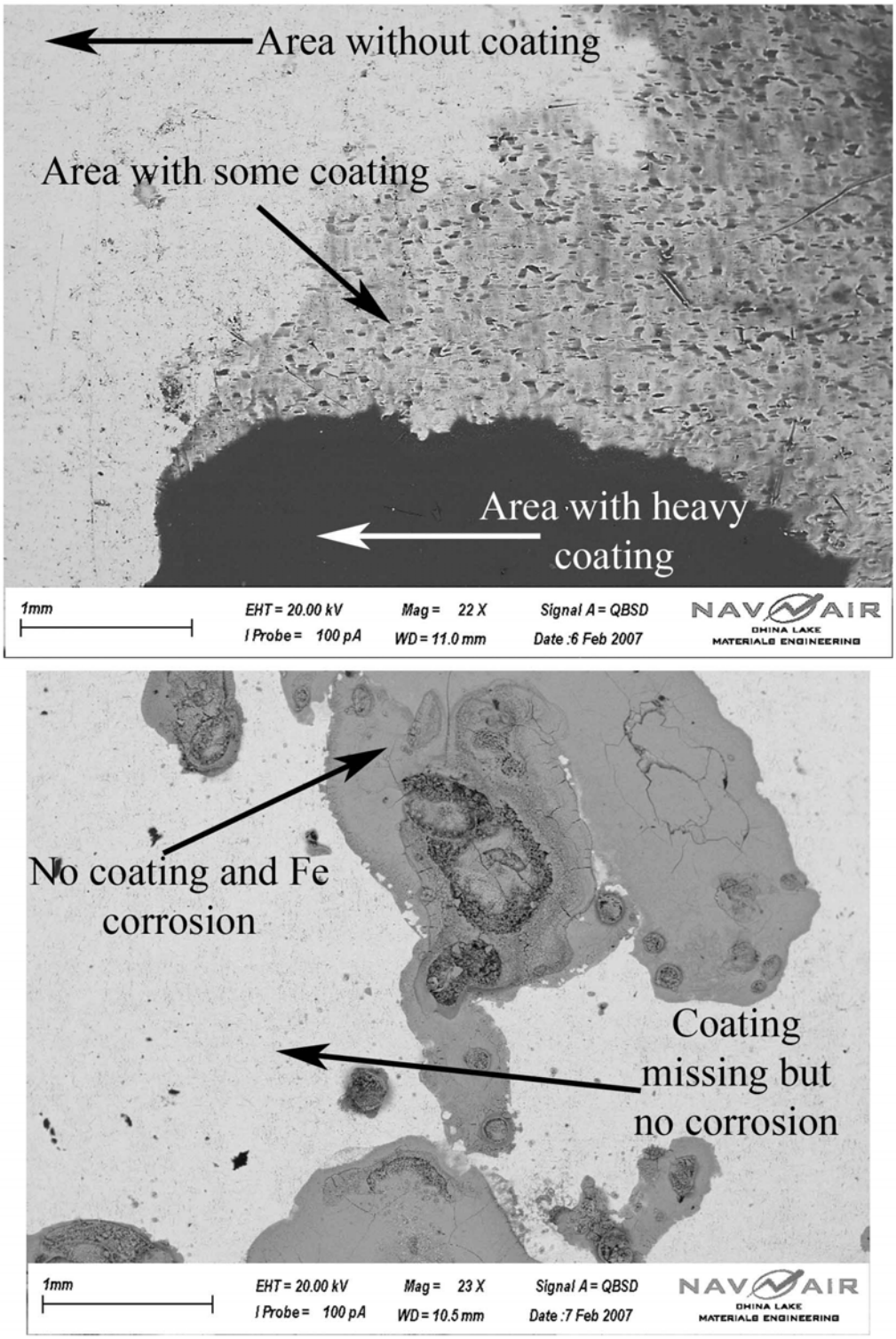

Figure 49: SEM analysis of adhesion promoter coating on steel substrate. Upper picture shows a darker hue of grayscale for a thicker coating. Lower picture shows no coating after 24 hours neutral salt fog exposure.

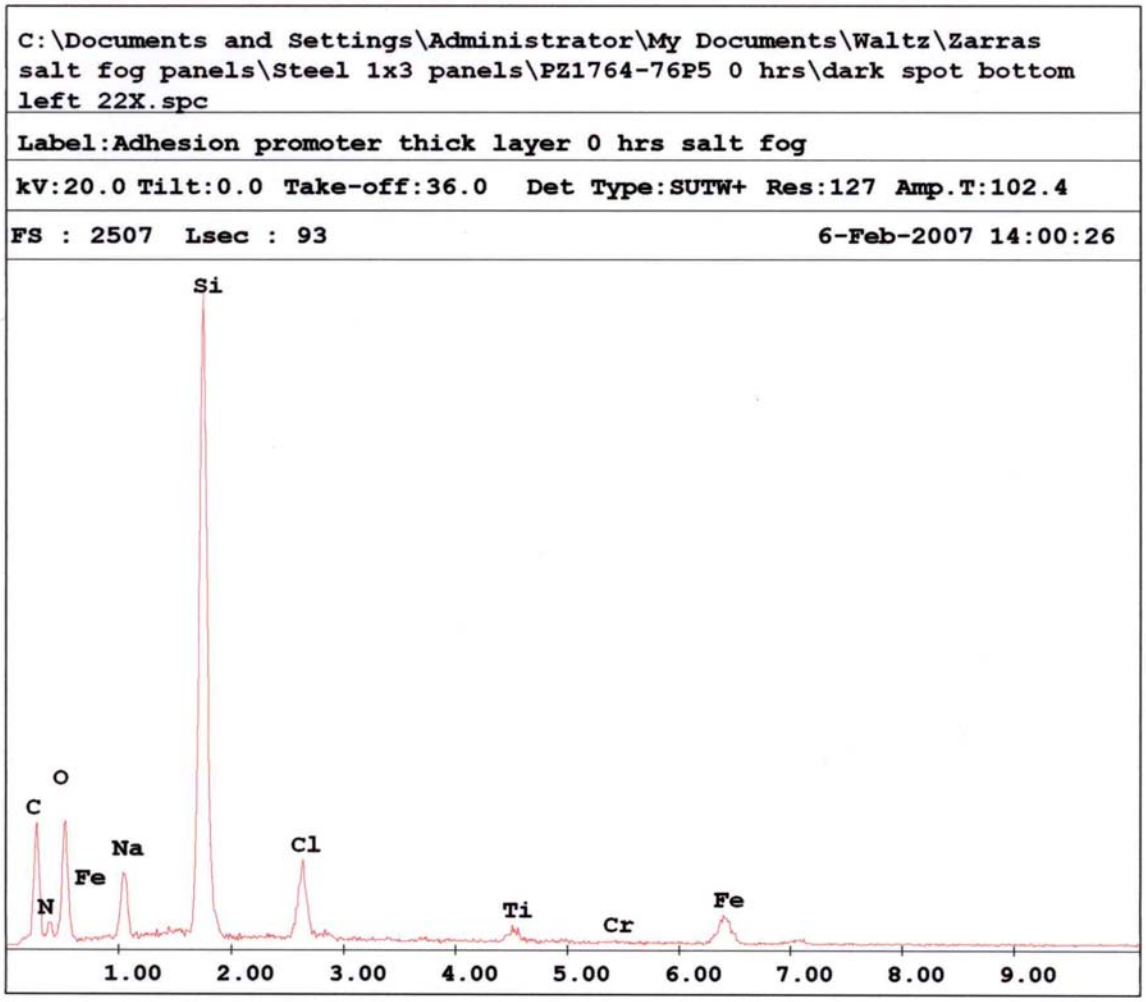

EDAX ZAF Quantification (Standardless)
Element Normalized
SEC Table : Default

Element	Wt %	At %	K-Ratio	Z	A	F
C K	41.03	55.42	0.0772	1.0308	0.1824	1.0002
N K	8.09	9.38	0.0101	1.0218	0.1225	1.0005
O K	17.04	17.28	0.0304	1.0136	0.1757	1.0004
NaK	3.23	2.28	0.0136	0.9488	0.4432	1.0027
SiK	21.31	12.31	0.1726	0.9718	0.8321	1.0013
ClK	3.45	1.58	0.0273	0.9127	0.8669	1.0010
TiK	1.00	0.34	0.0086	0.8603	0.9914	1.0088
CrK	0.11	0.03	0.0009	0.8564	1.0027	1.0206
FeK	4.73	1.38	0.0408	0.8552	1.0086	1.0000
Total	100.00	100.00				

Figure 50: EDS Spectrum of Adhesion Promoter Film Coating.

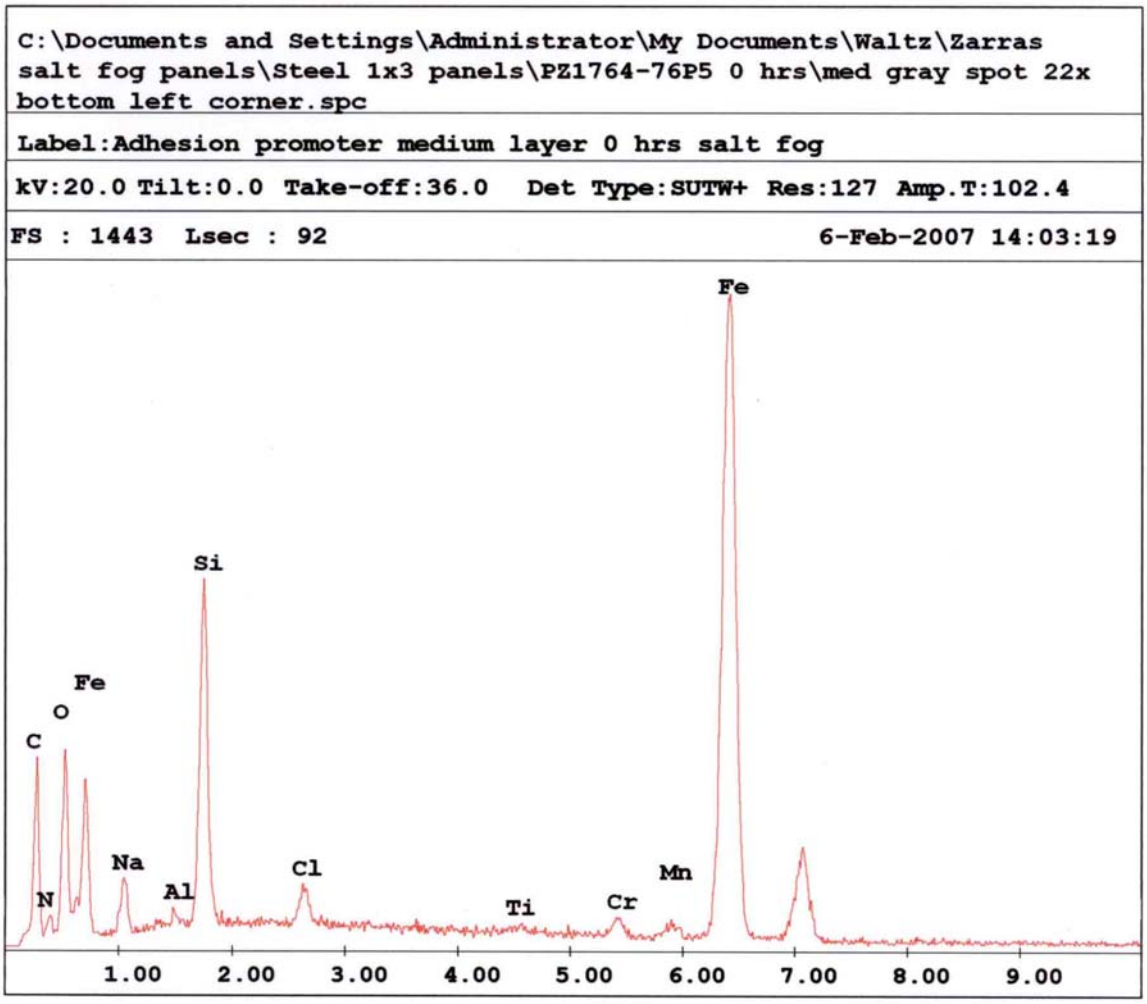

EDAX ZAF Quantification (Standardless)
Element Normalized
SEC Table : Default

Element	Wt %	At %	K-Ratio	Z	A	F
C K	23.69	48.03	0.0517	1.0977	0.1990	1.0004
N K	3.65	6.34	0.0068	1.0879	0.1700	1.0009
O K	8.24	12.54	0.0227	1.0791	0.2549	1.0020
NaK	2.34	2.48	0.0052	1.0096	0.2213	1.0005
AlK	0.25	0.23	0.0011	1.0042	0.4441	1.0025
SiK	7.32	6.35	0.0435	1.0333	0.5738	1.0012
ClK	0.89	0.61	0.0072	0.9803	0.8213	1.0062
TiK	0.14	0.07	0.0014	0.9198	0.9844	1.0876
CrK	0.67	0.32	0.0074	0.9171	1.0002	1.2075
MnK	0.68	0.30	0.0062	0.9005	1.0044	1.0000
FeK	52.12	22.73	0.4810	0.9175	1.0058	1.0000
Total	100.00	100.00				

Figure 51: EDS Spectrum of EAP Film (P(7-PHA)) at 0 hours (majority of film coated with medium thickness).

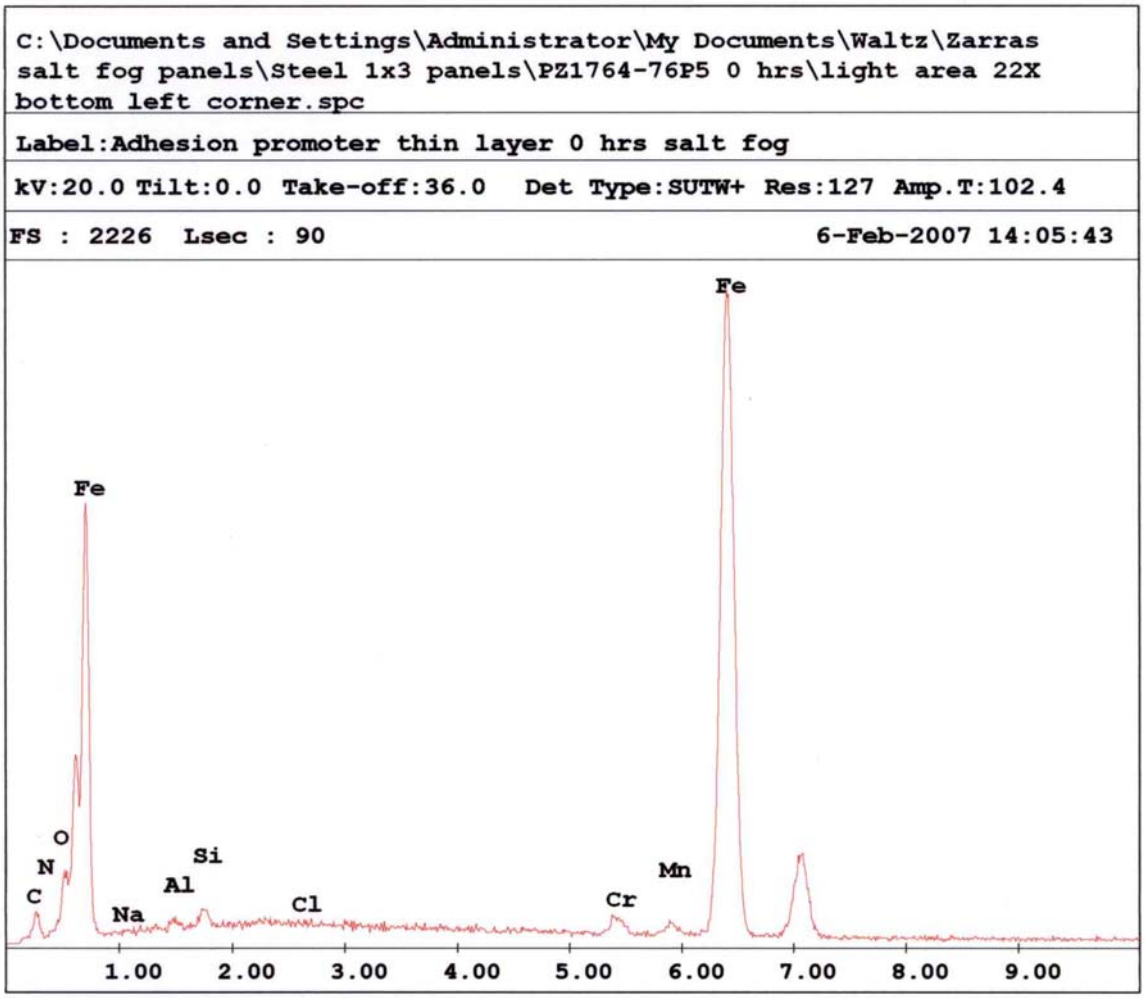

EDAX ZAF Quantification (Standardless)
Element Normalized
SEC Table : Default

Element	Wt %	At %	K-Ratio	Z	A	F
C K	7.39	24.08	0.0161	1.1558	0.1884	1.0005
N K	1.43	3.99	0.0039	1.1454	0.2359	1.0016
O K	3.89	9.53	0.0157	1.1360	0.3535	1.0041
NaK	0.12	0.20	0.0002	1.0623	0.1636	1.0001
AlK	0.48	0.70	0.0018	1.0563	0.3479	1.0008
SiK	0.83	1.16	0.0042	1.0866	0.4677	1.0013
ClK	0.16	0.18	0.0013	1.0390	0.7807	1.0088
CrK	1.09	0.82	0.0135	0.9695	0.9940	1.2895
MnK	0.81	0.58	0.0077	0.9525	0.9994	1.0000
FeK	83.80	58.76	0.8147	0.9711	1.0012	1.0000
Total	100.00	100.00				

Figure 52: EDS Spectrum of Adhesion Promoter in Thinnest Section of Film.

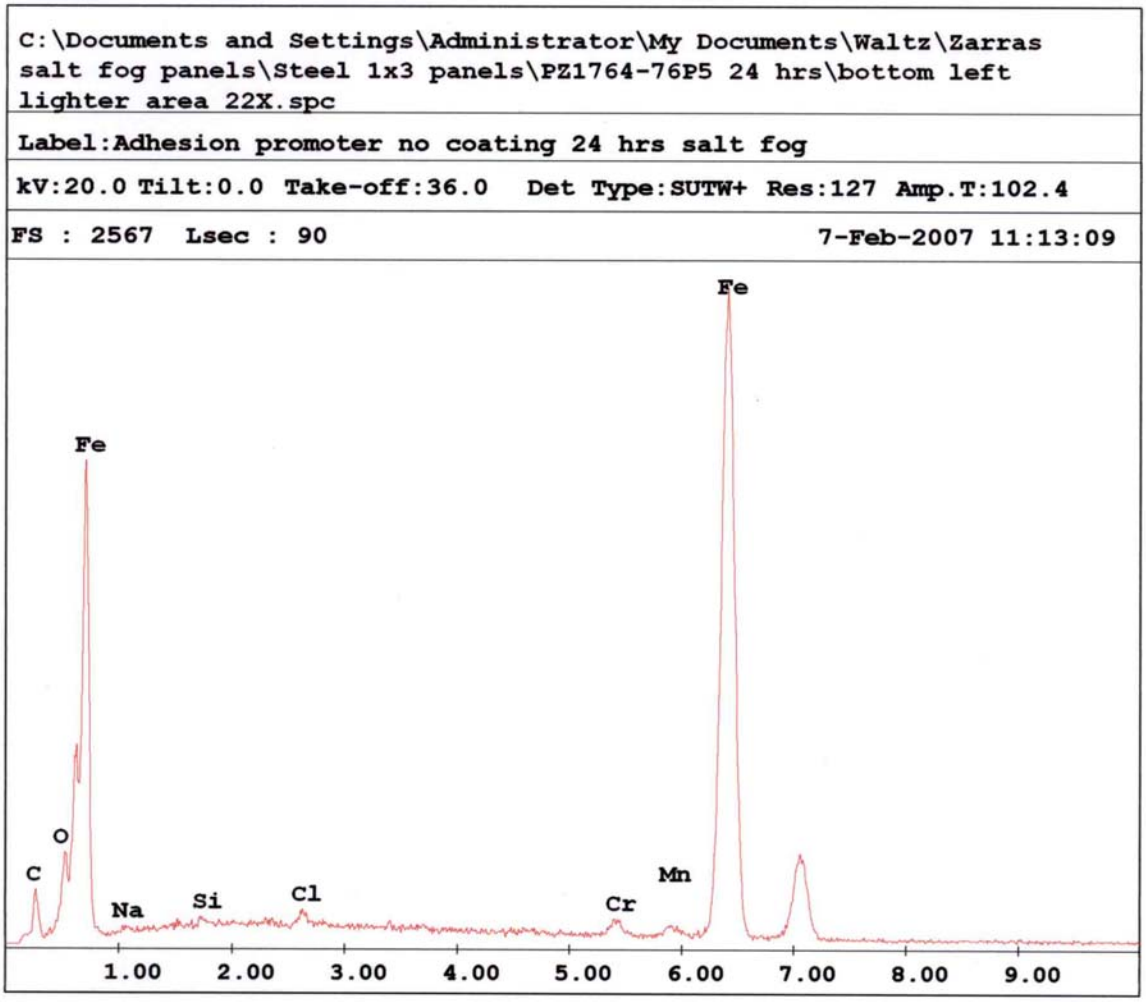

EDAX ZAF Quantification (Standardless)
Element Normalized
SEC Table : Default

Element	Wt %	At %	K-Ratio	Z	A	F
C K	11.17	33.76	0.0250	1.1492	0.1947	1.0005
O K	4.70	10.66	0.0185	1.1295	0.3480	1.0038
NaK	0.57	0.90	0.0010	1.0563	0.1677	1.0000
SiK	0.20	0.26	0.0011	1.0806	0.4778	1.0014
ClK	0.46	0.47	0.0038	1.0323	0.7913	1.0087
CrK	1.04	0.73	0.0129	0.9635	0.9955	1.2879
MnK	1.00	0.66	0.0094	0.9466	1.0006	1.0000
FeK	80.85	52.55	0.7819	0.9650	1.0022	1.0000
Total	100.00	100.00				

Figure 53: EDS Spectrum of Adhesion Promoter after 24 hrs Neutral Salt Fog Exposure.

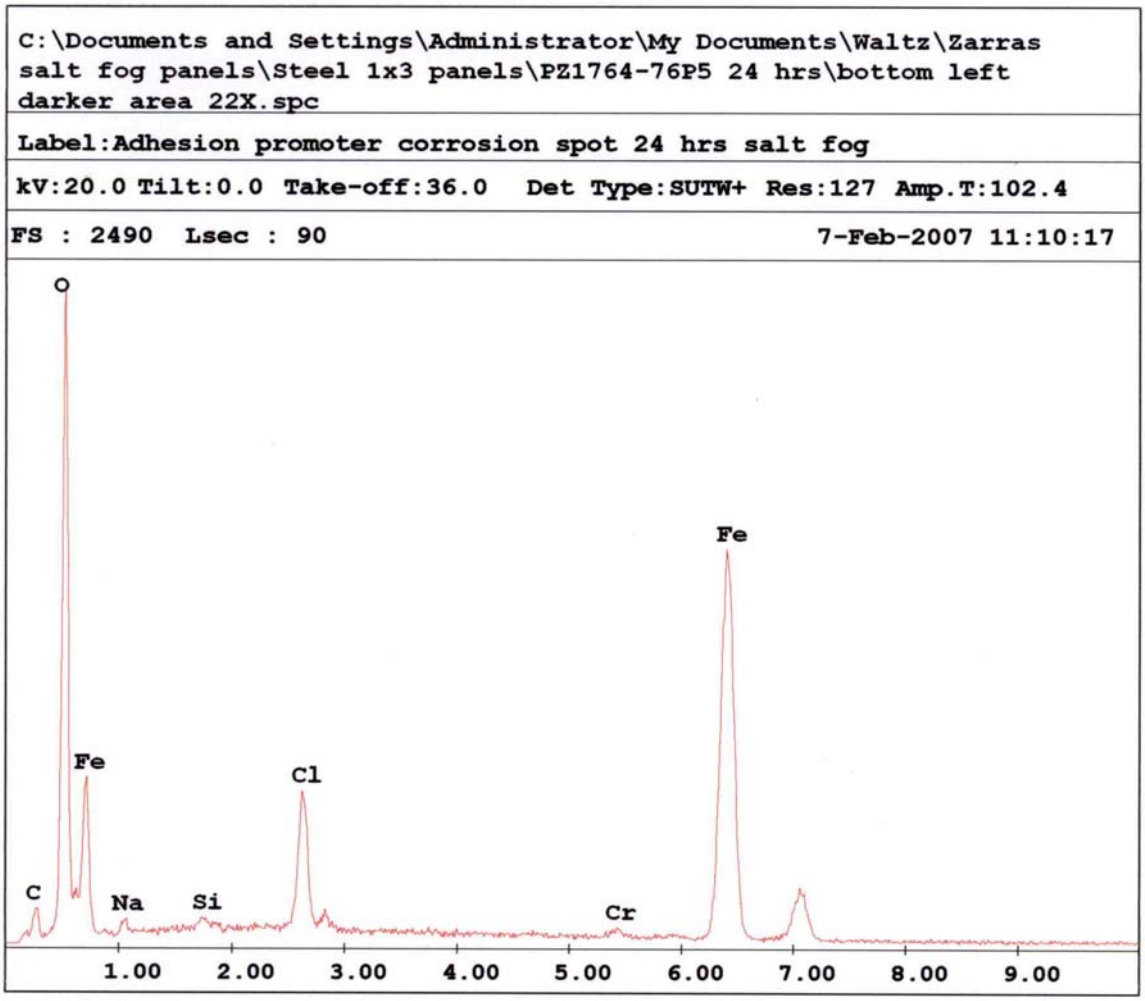

EDAX ZAF Quantification (Standardless)
Element Normalized
SEC Table : Default

Element	Wt %	At %	K-Ratio	Z	A	F
C K	8.92	19.08	0.0186	1.0991	0.1895	1.0006
O K	32.08	51.53	0.1312	1.0805	0.3778	1.0017
NaK	1.04	1.16	0.0021	1.0108	0.2033	1.0002
SiK	0.36	0.33	0.0021	1.0346	0.5525	1.0021
ClK	5.23	3.79	0.0436	0.9816	0.8448	1.0063
CrK	0.52	0.26	0.0057	0.9183	0.9990	1.2031
FeK	51.85	23.85	0.4789	0.9187	1.0054	1.0000
Total	100.00	100.00				

Figure 54: EDS Spectrum of Steel Panel After 24 hrs Neutral Salt Fog Exposure.

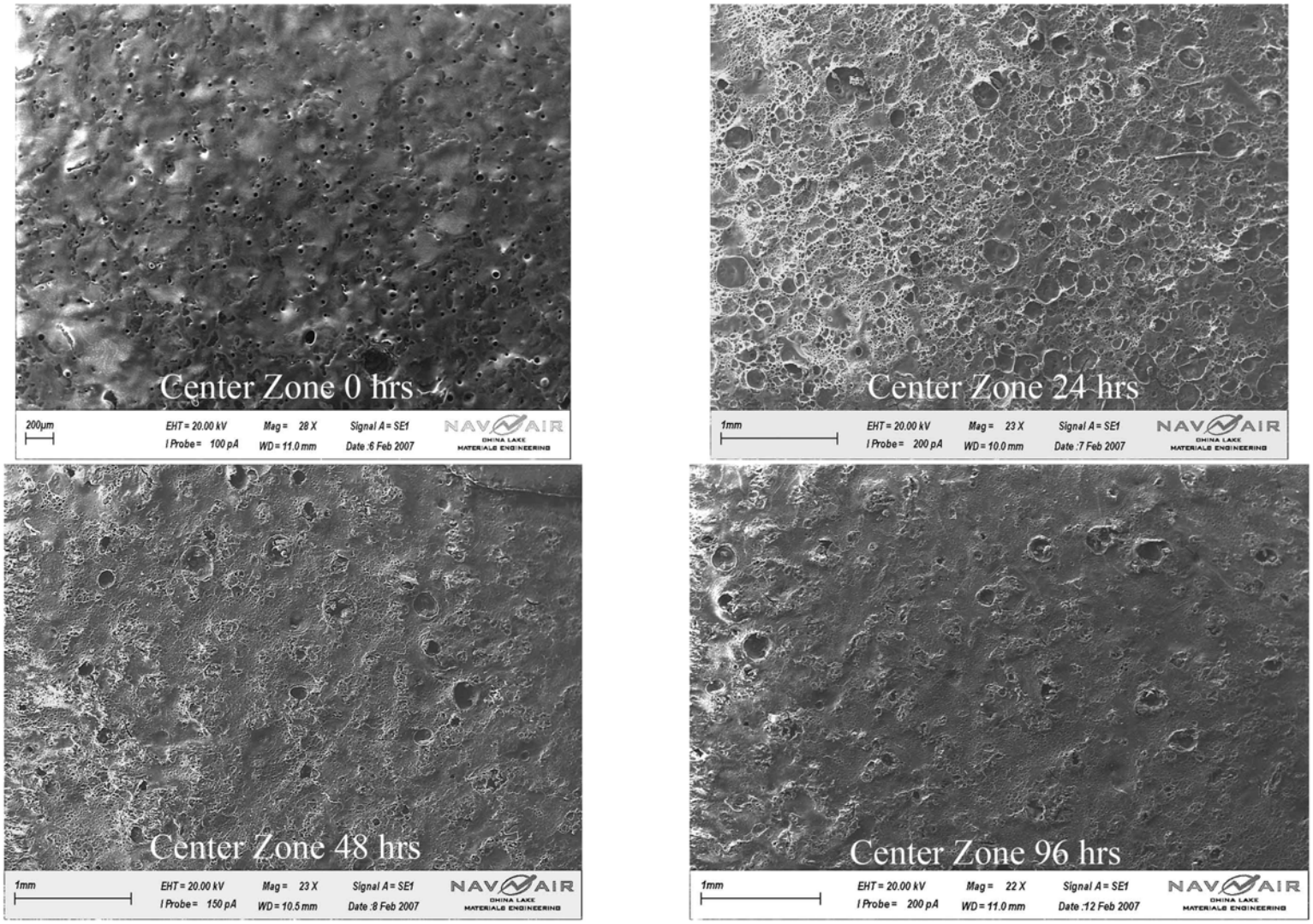

Figure 55: SEM Analysis of EAP (P(7-PHA)) onto Steel Substrate after Neutral Salt Fog Exposure.

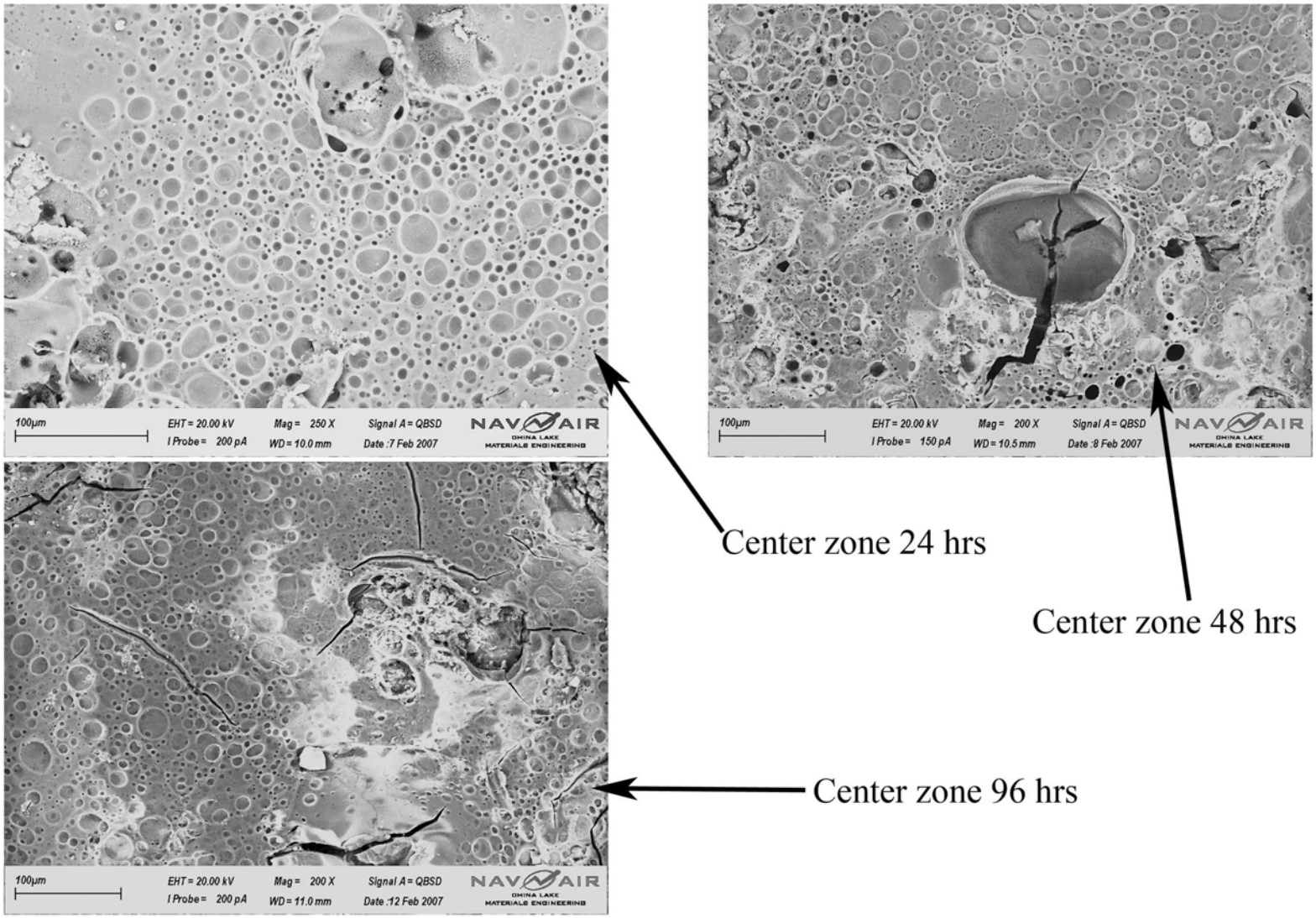

Figure 56: SEM Analysis of Coating Shows Crack Formation on Polymer Film.

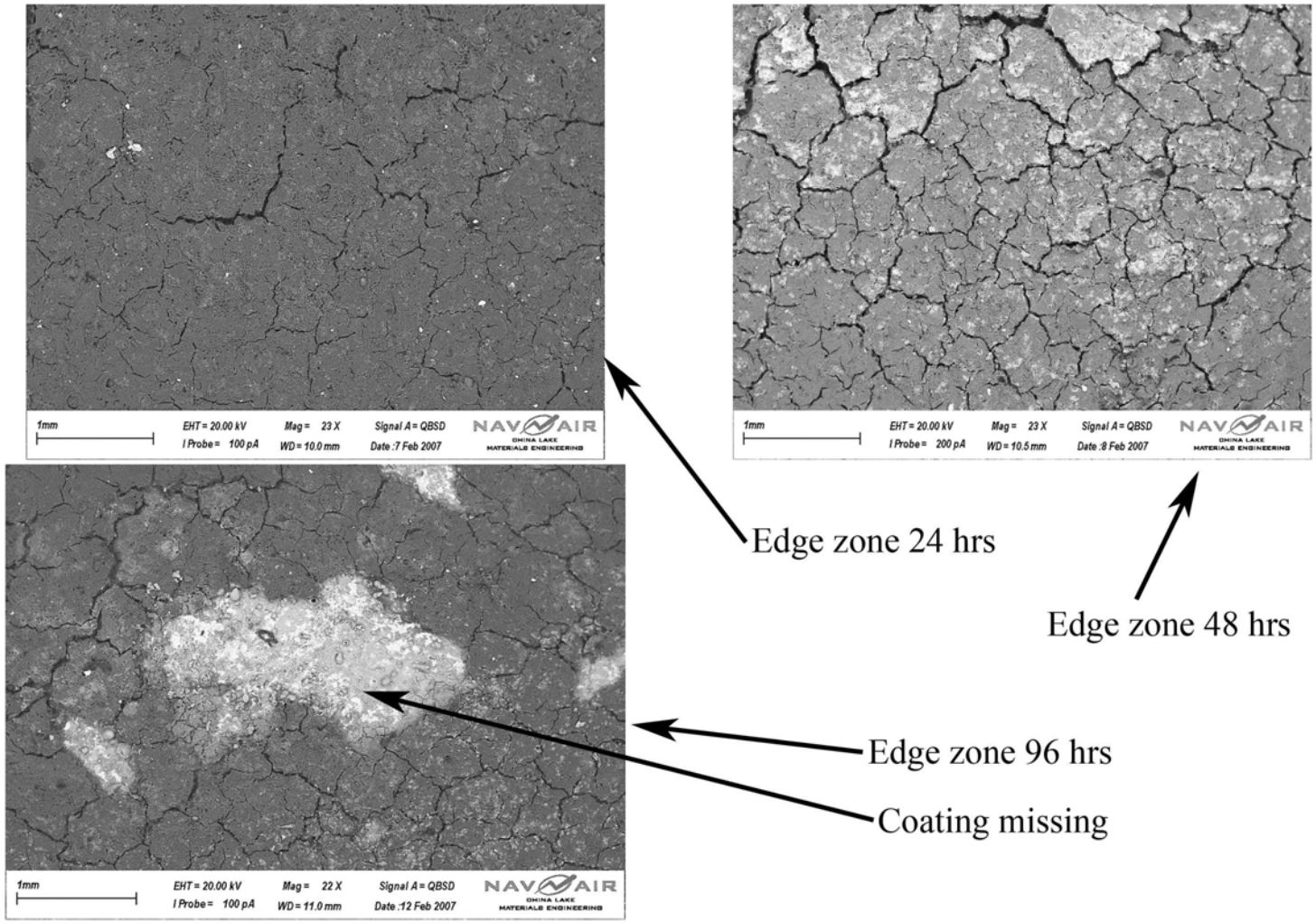

Figure 57: SEM Analysis of Outer Edges of Film After Neutral Salt Fog Exposure.

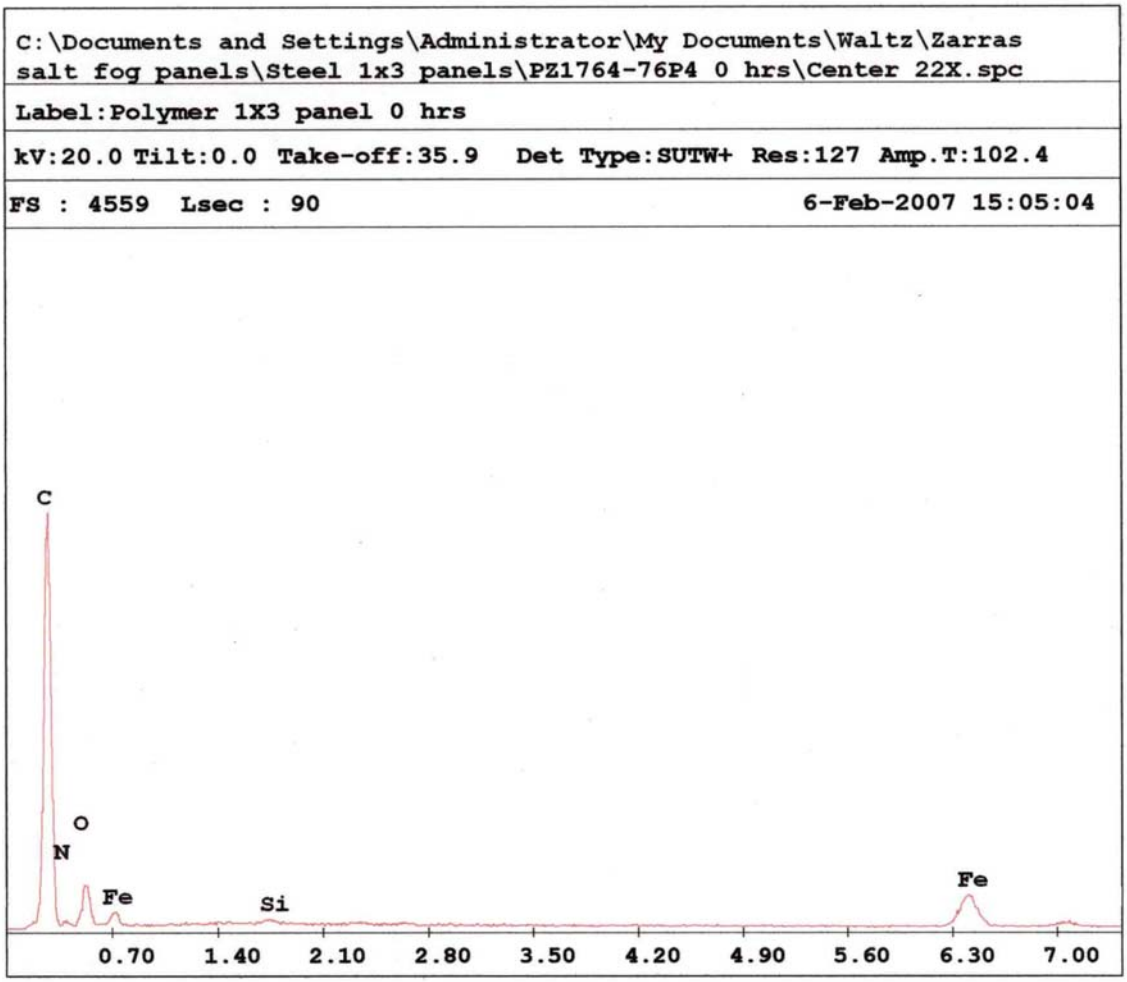

EDAX ZAF Quantification (Standardless)
Element Normalized
SEC Table : Default

Element	Wt %	At %	K-Ratio	Z	A	F
C K	73.67	82.83	0.4500	1.0156	0.6013	1.0002
N K	5.13	4.94	0.0052	1.0067	0.1008	1.0003
O K	11.70	9.88	0.0187	0.9987	0.1598	1.0002
SiK	0.23	0.11	0.0019	0.9579	0.8344	1.0003
FeK	9.27	2.24	0.0798	0.8413	1.0239	1.0000
Total	100.00	100.00				

Figure 58: EDS Spectrum of P(7-PHA) Coating at 0 Hours.

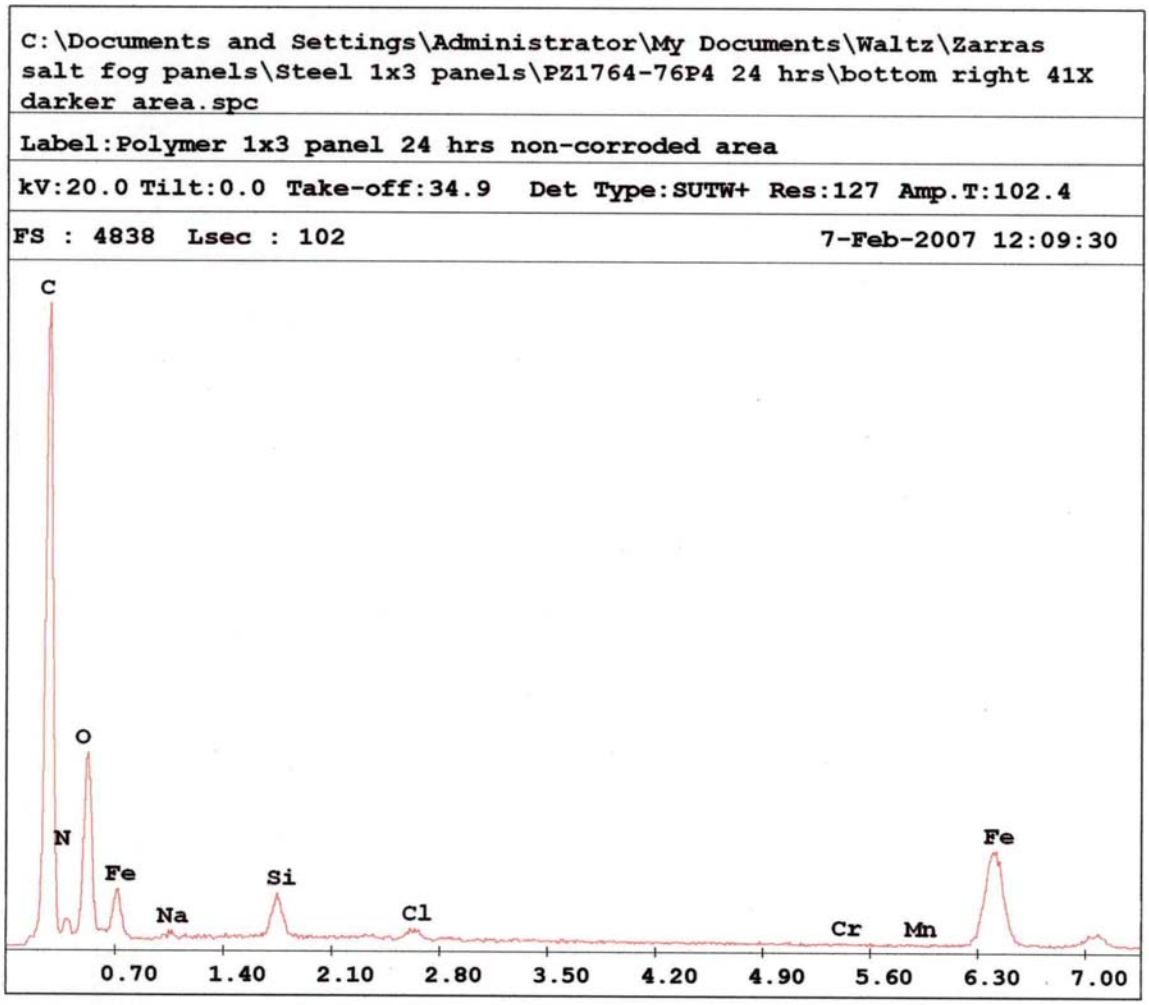

EDAX ZAF Quantification (Standardless)
Element Normalized
SEC Table : Default

Element	Wt %	At %	K-Ratio	Z	A	F
C K	59.73	71.02	0.2902	1.0216	0.4754	1.0003
N K	7.92	8.08	0.0094	1.0126	0.1171	1.0005
O K	19.23	17.17	0.0335	1.0046	0.1734	1.0003
NaK	0.23	0.14	0.0008	0.9404	0.3656	1.0001
SiK	0.99	0.50	0.0075	0.9633	0.7913	1.0004
ClK	0.27	0.11	0.0024	0.9034	0.9728	1.0027
CrK	0.04	0.01	0.0004	0.8481	1.0256	1.1137
MnK	0.00	0.00	0.0000	0.8319	1.0243	1.0000
FeK	11.59	2.97	0.1004	0.8468	1.0225	1.0000
Total	100.00	100.00				

Figure 59: EDS Spectrum of P(7-PHA) Coating After 24 Hours Neutral Salt Fog Exposure.

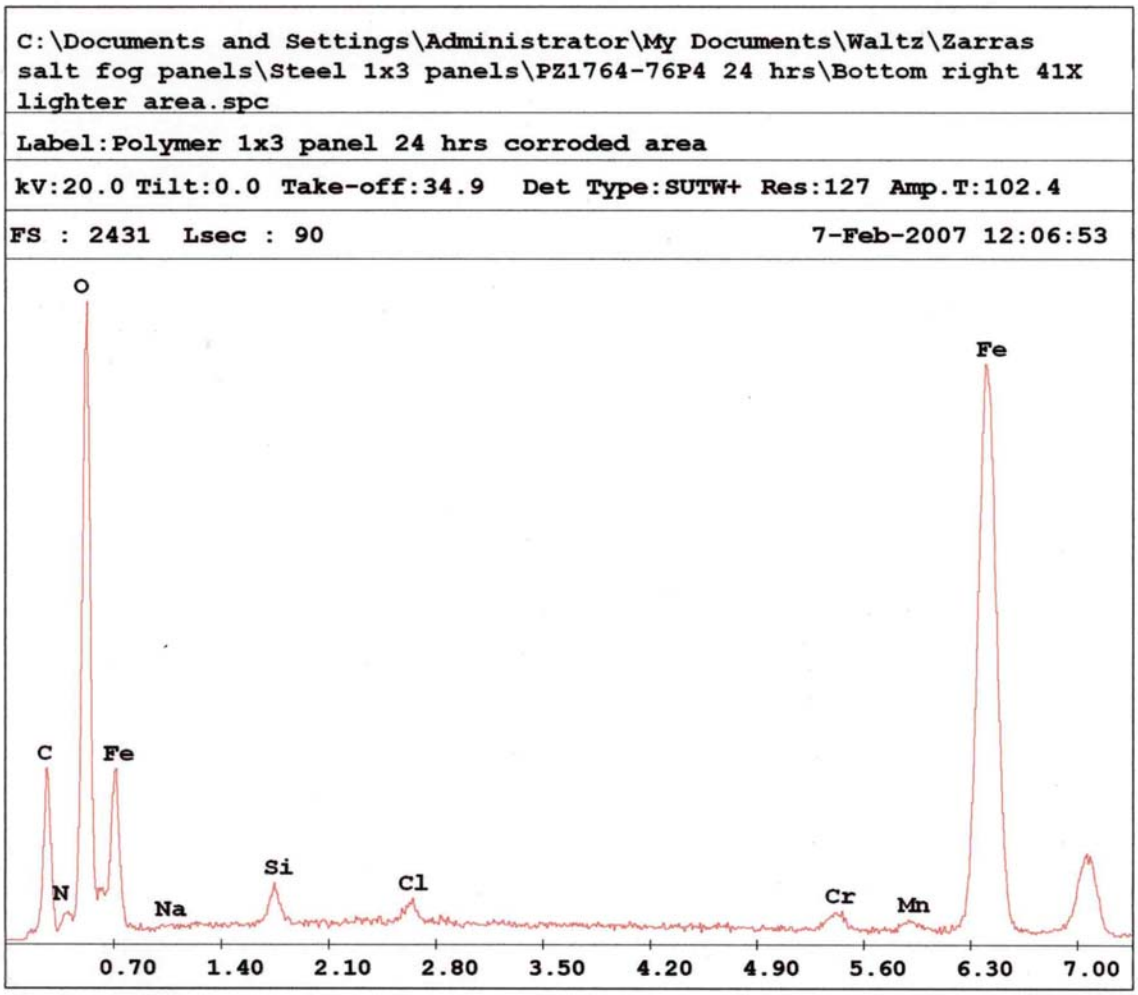

EDAX ZAF Quantification (Standardless)
Element Normalized
SEC Table : Default

Element	Wt %	At %	K-Ratio	Z	A	F
C K	20.36	38.32	0.0548	1.0867	0.2477	1.0005
N K	3.14	5.07	0.0069	1.0771	0.2030	1.0013
O K	24.86	35.13	0.0807	1.0683	0.3033	1.0016
NaK	0.14	0.14	0.0003	0.9996	0.2102	1.0001
SiK	0.86	0.69	0.0050	1.0232	0.5697	1.0011
ClK	0.53	0.34	0.0044	0.9693	0.8541	1.0065
CrK	0.92	0.40	0.0102	0.9072	1.0075	1.2244
MnK	0.70	0.29	0.0063	0.8907	1.0101	1.0000
FeK	48.49	19.63	0.4444	0.9074	1.0099	1.0000
Total	100.00	100.00				

Figure 60: EDS Spectrum of P(7-PHA) After 24 Hours Neutral Salt Fog (Outer Edges).

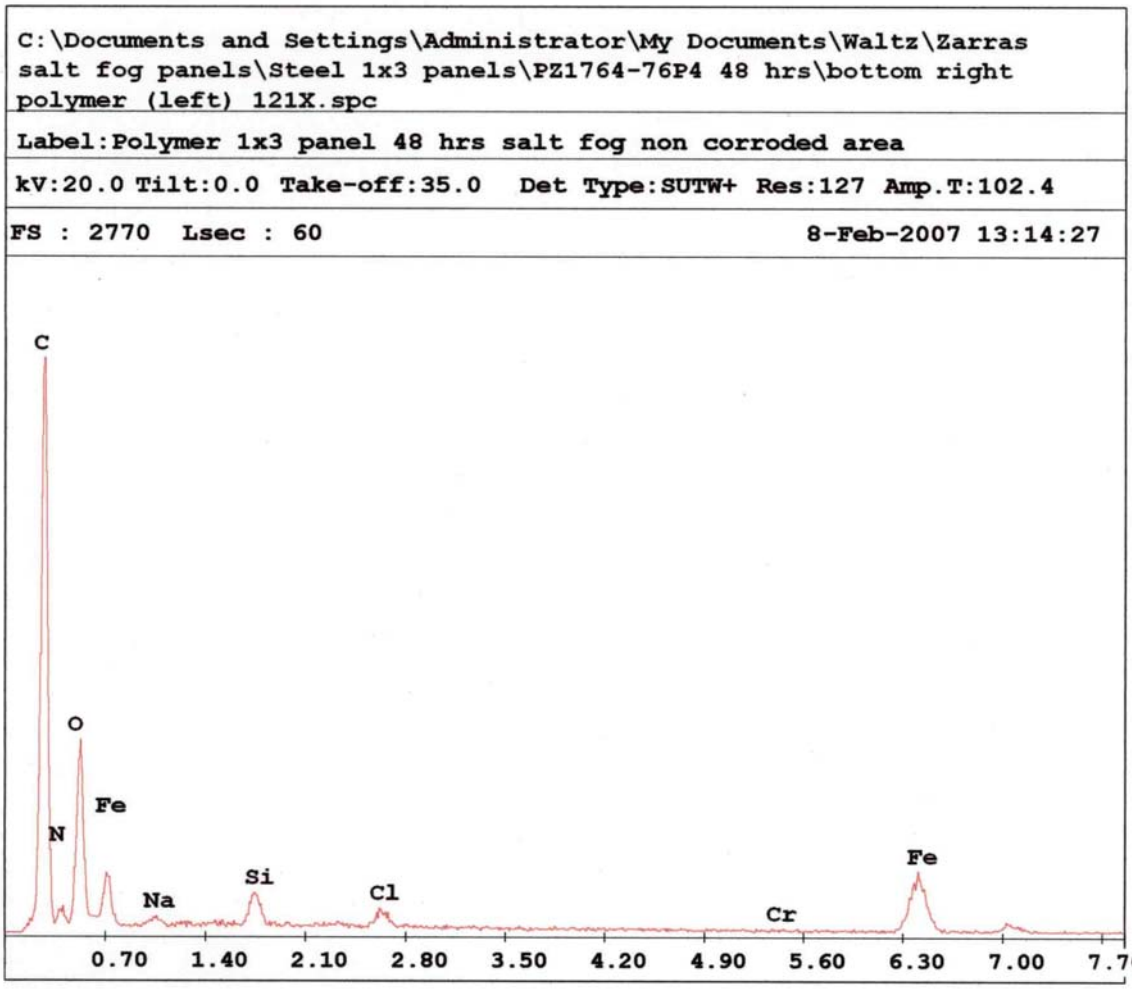

EDAX ZAF Quantification (Standardless)
Element Normalized
SEC Table : Default

Element	Wt %	At %	K-Ratio	Z	A	F
C K	60.41	69.99	0.3037	1.0166	0.4945	1.0003
N K	8.28	8.22	0.0097	1.0077	0.1166	1.0005
O K	21.82	18.98	0.0375	0.9997	0.1720	1.0002
NaK	0.32	0.20	0.0012	0.9359	0.3875	1.0001
SiK	0.95	0.47	0.0075	0.9587	0.8141	1.0005
ClK	0.57	0.22	0.0050	0.8983	0.9836	1.0019
CrK	0.00	0.00	0.0000	0.8435	1.0267	1.0809
FeK	7.65	1.91	0.0659	0.8421	1.0232	1.0000
Total	100.00	100.00				

Figure 61: EDS Spectrum of P(7-PHA) Coating After 48 Hours Neutral Salt Fog Exposure.

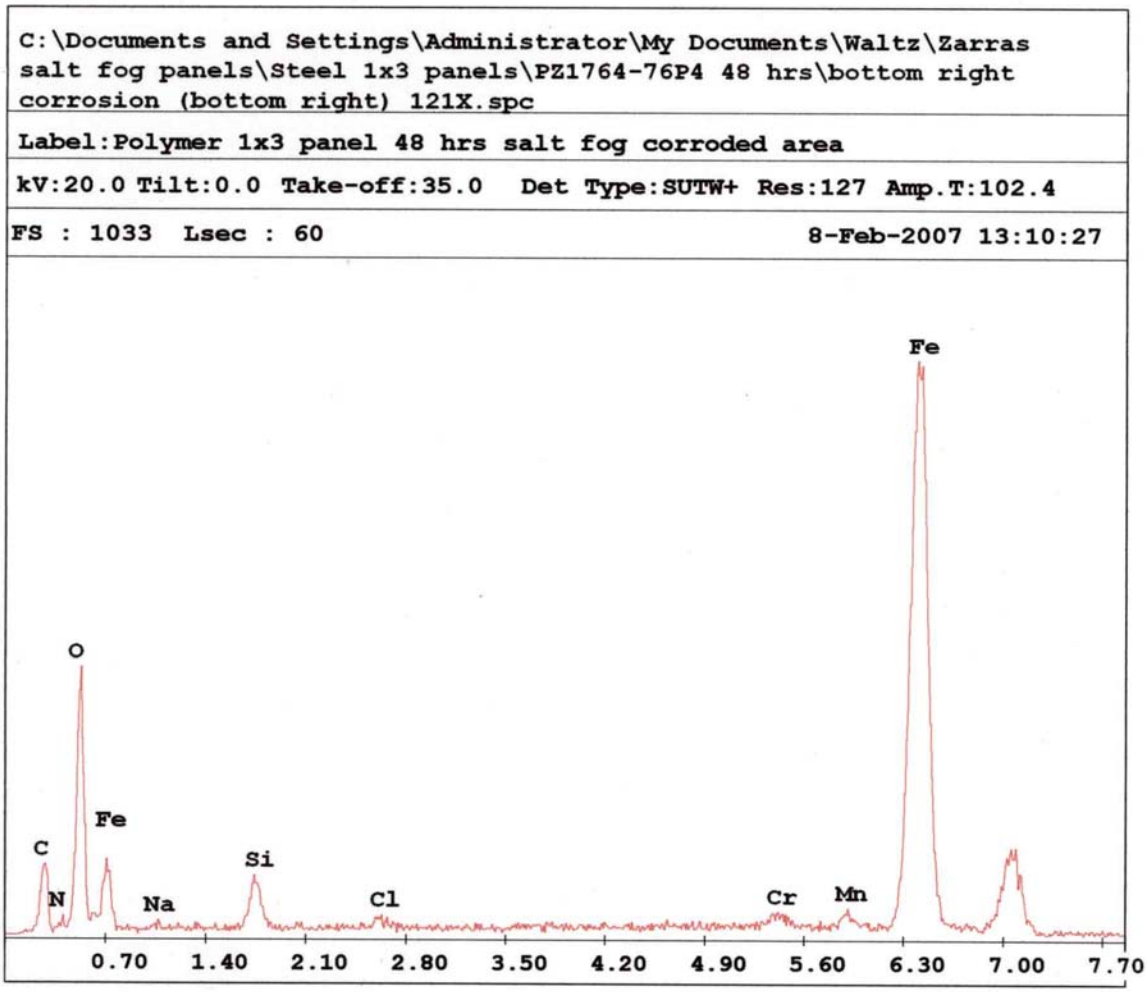

EDAX ZAF Quantification (Standardless)
Element Normalized
SEC Table : Default

Element	Wt %	At %	K-Ratio	Z	A	F
C K	14.91	35.69	0.0349	1.1200	0.2092	1.0005
N K	1.84	3.78	0.0043	1.1100	0.2097	1.0013
O K	12.64	22.72	0.0446	1.1009	0.3194	1.0026
NaK	0.51	0.64	0.0010	1.0298	0.1841	1.0001
SiK	1.81	1.85	0.0098	1.0538	0.5141	1.0012
ClK	0.36	0.29	0.0029	1.0029	0.8112	1.0076
CrK	1.01	0.56	0.0118	0.9373	1.0000	1.2546
MnK	1.30	0.68	0.0120	0.9205	1.0043	1.0000
FeK	65.62	33.78	0.6188	0.9381	1.0052	1.0000
Total	100.00	100.00				

Figure 62: EDS Spectrum of Uncoated Portions of the P(7-PHA) Panel.

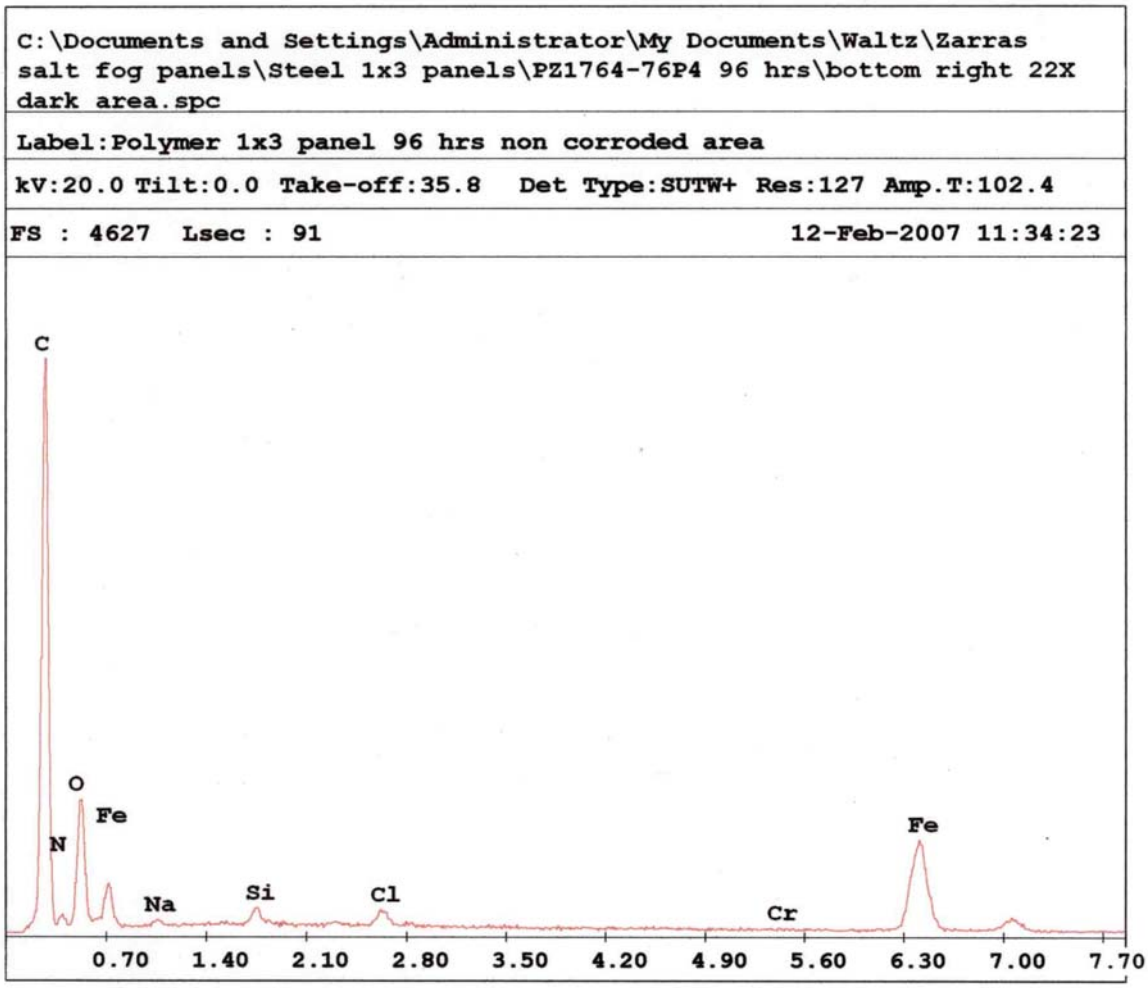

EDAX ZAF Quantification (Standardless)
Element Normalized
SEC Table : Default

Element	Wt %	At %	K-Ratio	Z	A	F
C K	62.93	74.95	0.3065	1.0231	0.4758	1.0002
N K	6.17	6.30	0.0071	1.0142	0.1128	1.0004
O K	16.51	14.76	0.0288	1.0061	0.1735	1.0004
NaK	0.31	0.19	0.0011	0.9418	0.3686	1.0001
SiK	0.45	0.23	0.0035	0.9648	0.7914	1.0006
ClK	0.54	0.22	0.0048	0.9050	0.9749	1.0031
CrK	0.06	0.02	0.0006	0.8495	1.0248	1.1265
FeK	13.03	3.34	0.1129	0.8483	1.0218	1.0000
Total	100.00	100.00				

Figure 63: EDS Spectrum of P(7-PHA) Coated Panel After 96 Hours Neutral Salt Fog Exposure.

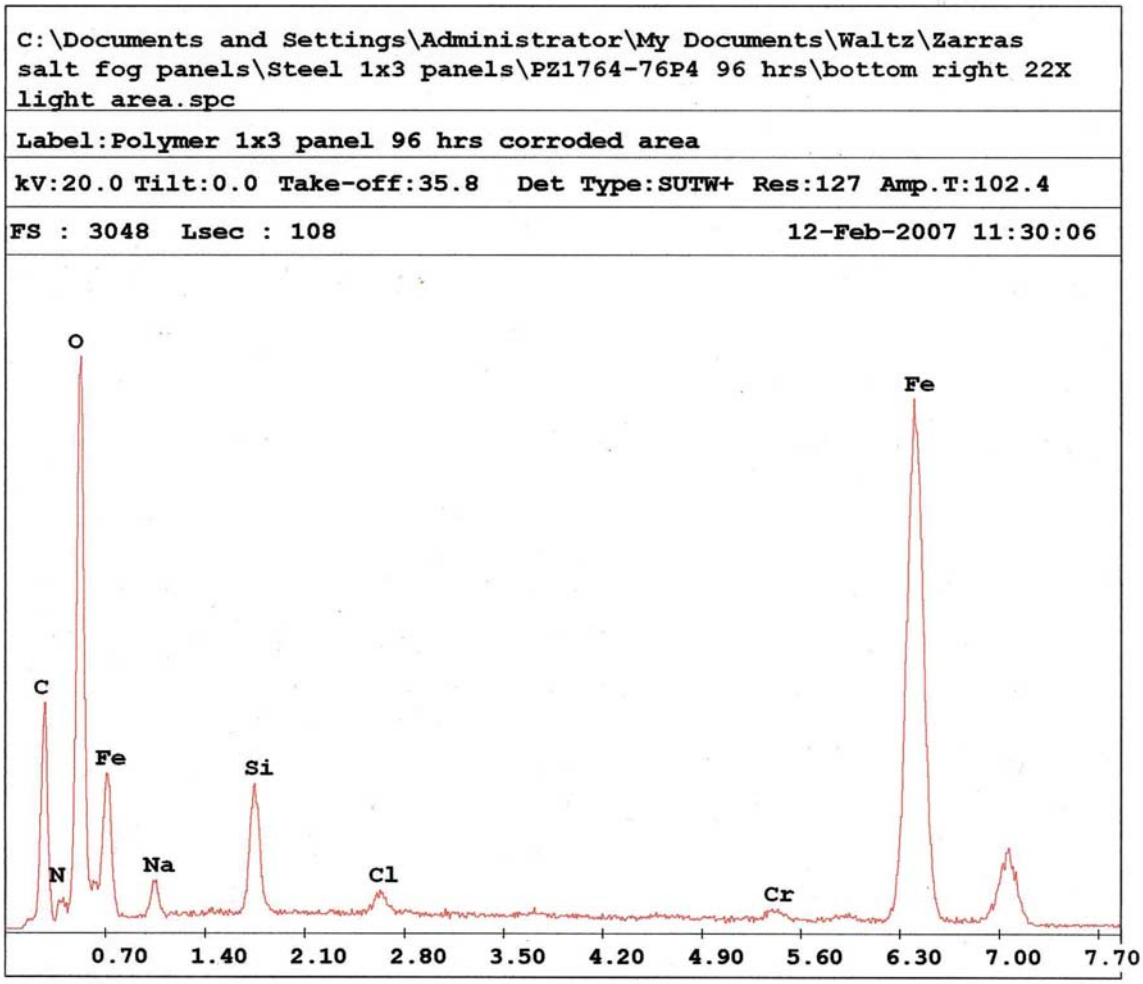

EDAX ZAF Quantification (Standardless)
Element Normalized
SEC Table : Default

Element	Wt %	At %	K-Ratio	Z	A	F
C K	24.81	43.32	0.0667	1.0758	0.2500	1.0004
N K	3.58	5.36	0.0071	1.0662	0.1856	1.0011
O K	24.02	31.49	0.0711	1.0576	0.2796	1.0014
NaK	1.49	1.36	0.0034	0.9896	0.2331	1.0002
SiK	2.79	2.08	0.0170	1.0132	0.6029	1.0010
ClK	0.47	0.28	0.0039	0.9582	0.8632	1.0058
CrK	0.56	0.23	0.0061	0.8973	1.0084	1.2073
FeK	42.29	15.88	0.3836	0.8972	1.0111	1.0000
Total	100.00	100.00				

Figure 64: EDS Spectrum of P(7-PHA) Scribe Panel at 96 hours Neutral Salt Fog Exposure.

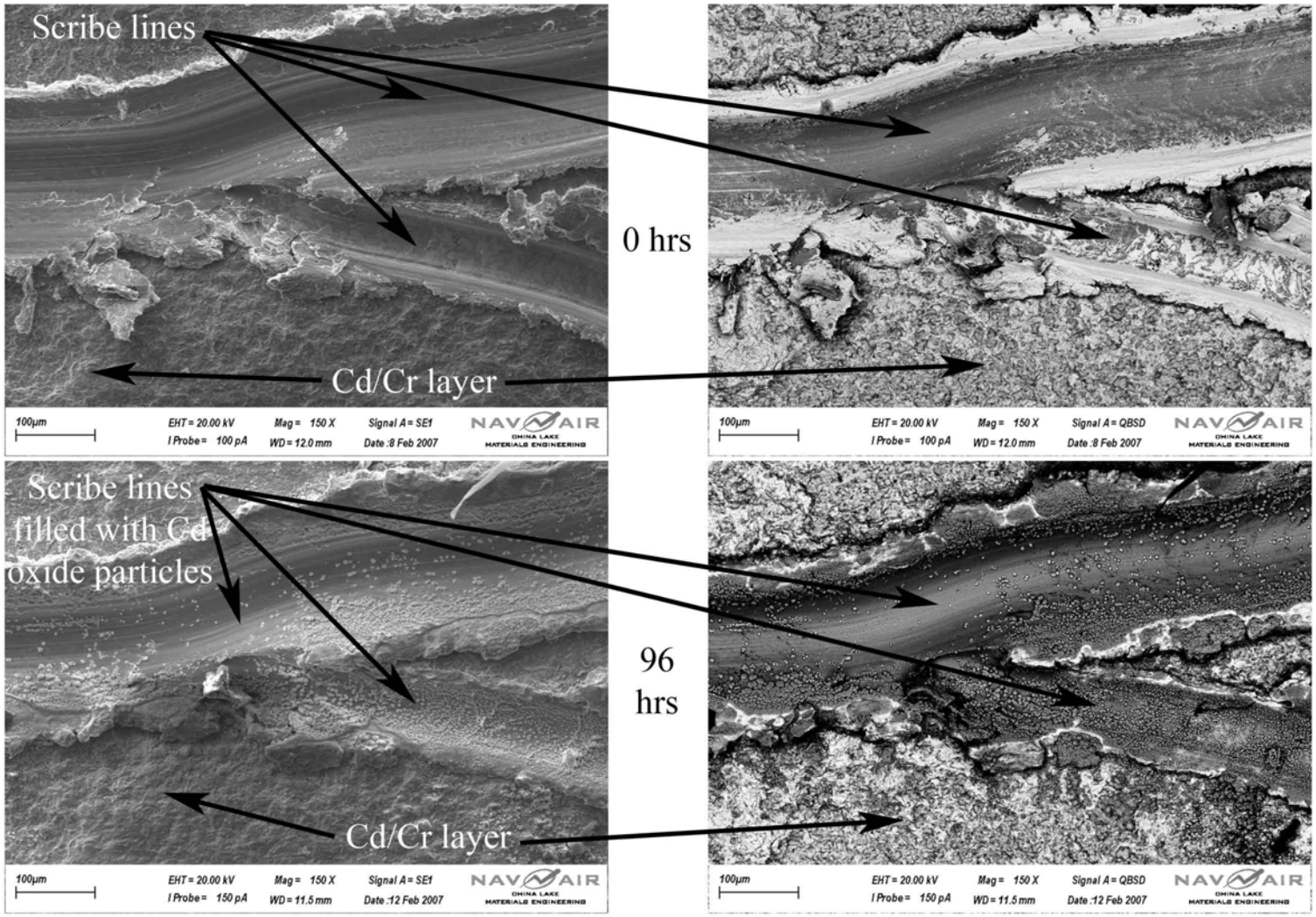

Figure 65: SEM Photograph of Cd-coated Panels at 0 and after 96 Hours Exposure to Neutral Salt Fog.

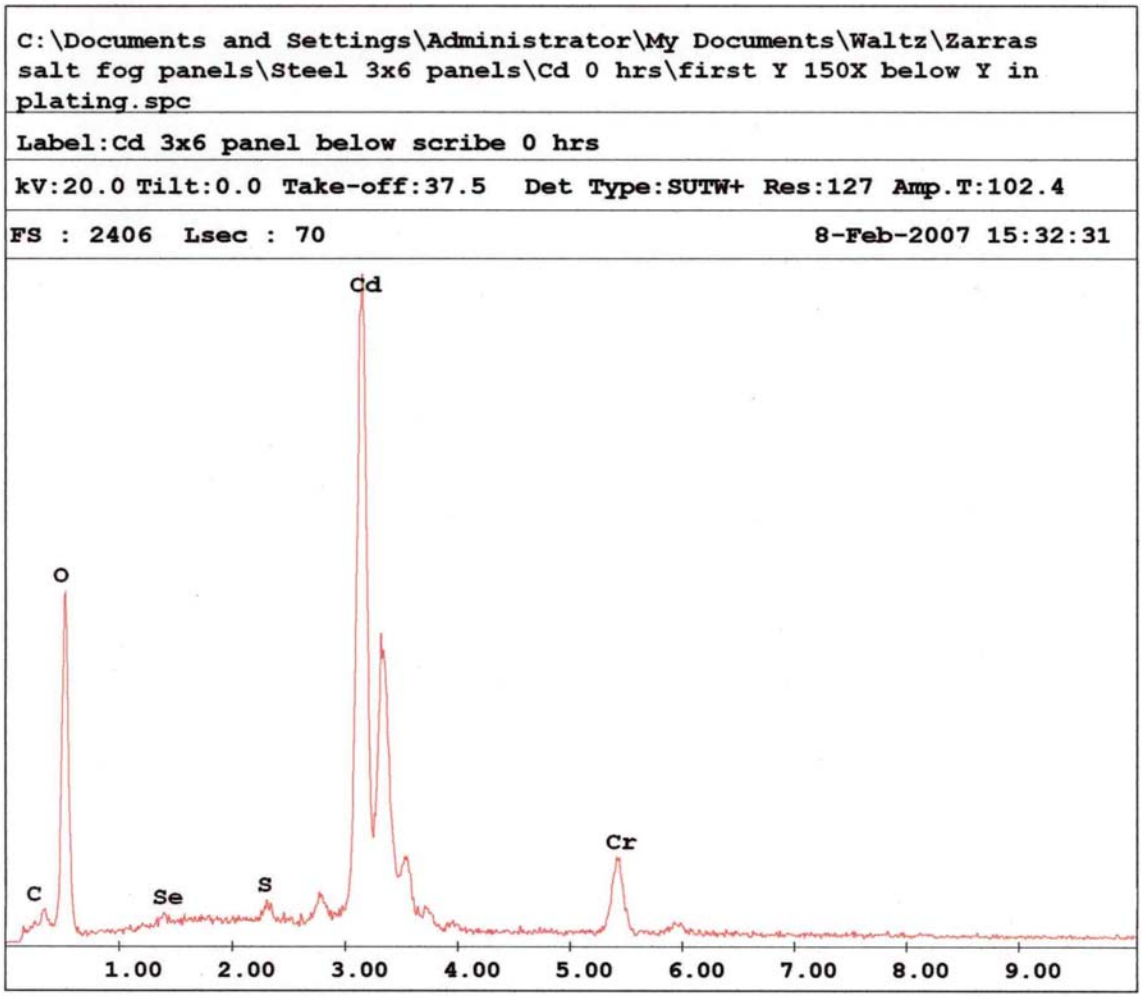

EDAX ZAF Quantification (Standardless)
Element Normalized
SEC Table : Default

Element	Wt %	At %	K-Ratio	Z	A	F
C K	1.88	5.43	0.0085	1.1719	0.3869	1.0002
O K	33.01	71.66	0.0618	1.1517	0.1625	1.0002
SeL	0.60	0.26	0.0029	0.9005	0.5342	1.0029
S K	0.54	0.59	0.0048	1.1137	0.7788	1.0248
CdL	57.57	17.79	0.5269	0.8739	1.0454	1.0017
CrK	6.40	4.27	0.0558	0.9880	0.8836	1.0000
Total	100.00	100.00				

Figure 66: EDS Spectrum of Cd-Plated Panel at 0 Hours.

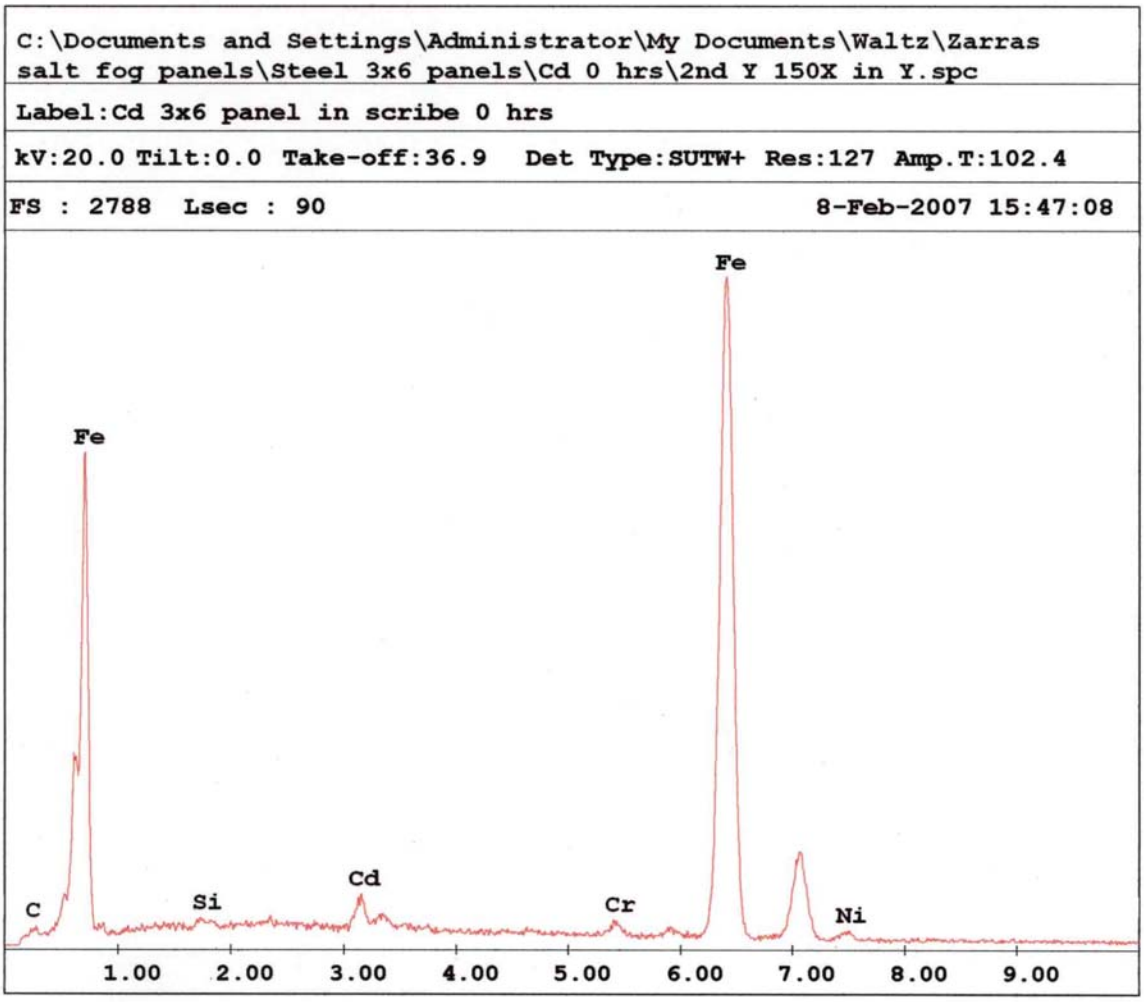

EDAX ZAF Quantification (Standardless)
Element Normalized
SEC Table : Default

Element	Wt %	At %	K-Ratio	Z	A	F
C K	4.19	16.99	0.0090	1.1784	0.1828	1.0005
SiK	0.49	0.86	0.0025	1.1072	0.4510	1.0016
CdL	2.40	1.04	0.0213	0.8769	0.9881	1.0225
CrK	0.92	0.86	0.0114	0.9899	0.9854	1.2723
FeK	90.51	79.01	0.8960	0.9920	0.9960	1.0019
NiK	1.49	1.24	0.0135	1.0093	0.8938	1.0000
Total	100.00	100.00				

Figure 67: EDS Spectrum of Scribed area of Cd-Plated Panel at 0 Hours Exposure to Neutral Salt Fog.

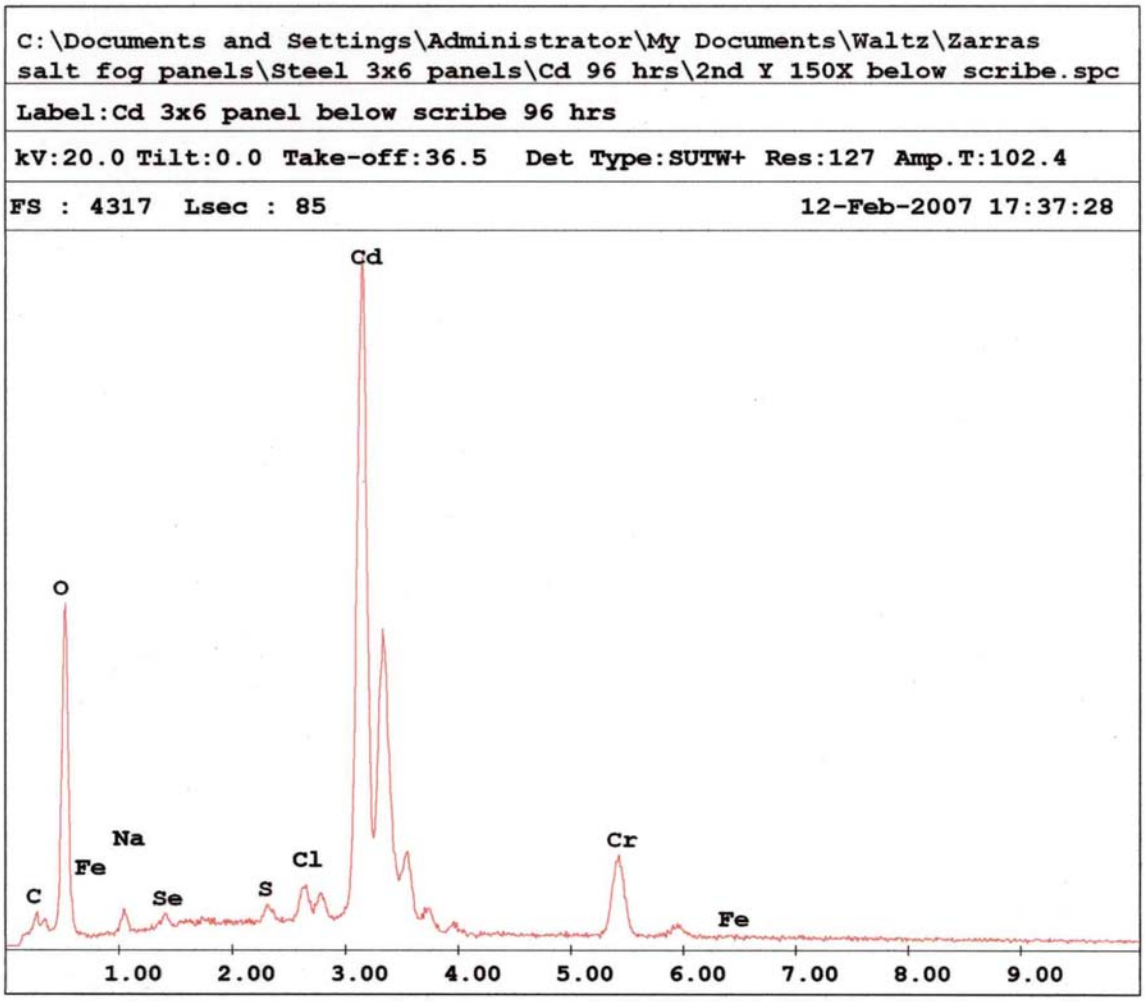

EDAX ZAF Quantification (Standardless)
Element Normalized
SEC Table : Default

Element	Wt %	At %	K-Ratio	Z	A	F
C K	3.09	8.81	0.0128	1.1695	0.3541	1.0002
O K	30.93	66.14	0.0571	1.1494	0.1607	1.0002
NaK	1.24	1.84	0.0031	1.0747	0.2352	1.0010
SeL	0.70	0.30	0.0033	0.8987	0.5304	1.0029
S K	0.38	0.41	0.0034	1.1107	0.7750	1.0243
ClK	0.95	0.92	0.0089	1.0584	0.8433	1.0400
CdL	55.63	16.94	0.5064	0.8719	1.0422	1.0018
CrK	6.75	4.44	0.0588	0.9857	0.8839	1.0004
FeK	0.33	0.20	0.0030	0.9896	0.9214	1.0002
Total	100.00	100.00				

Figure 68: EDS Spectrum of Cd-Plated Panel After 96 Hours Exposure to Neutral Salt Fog.

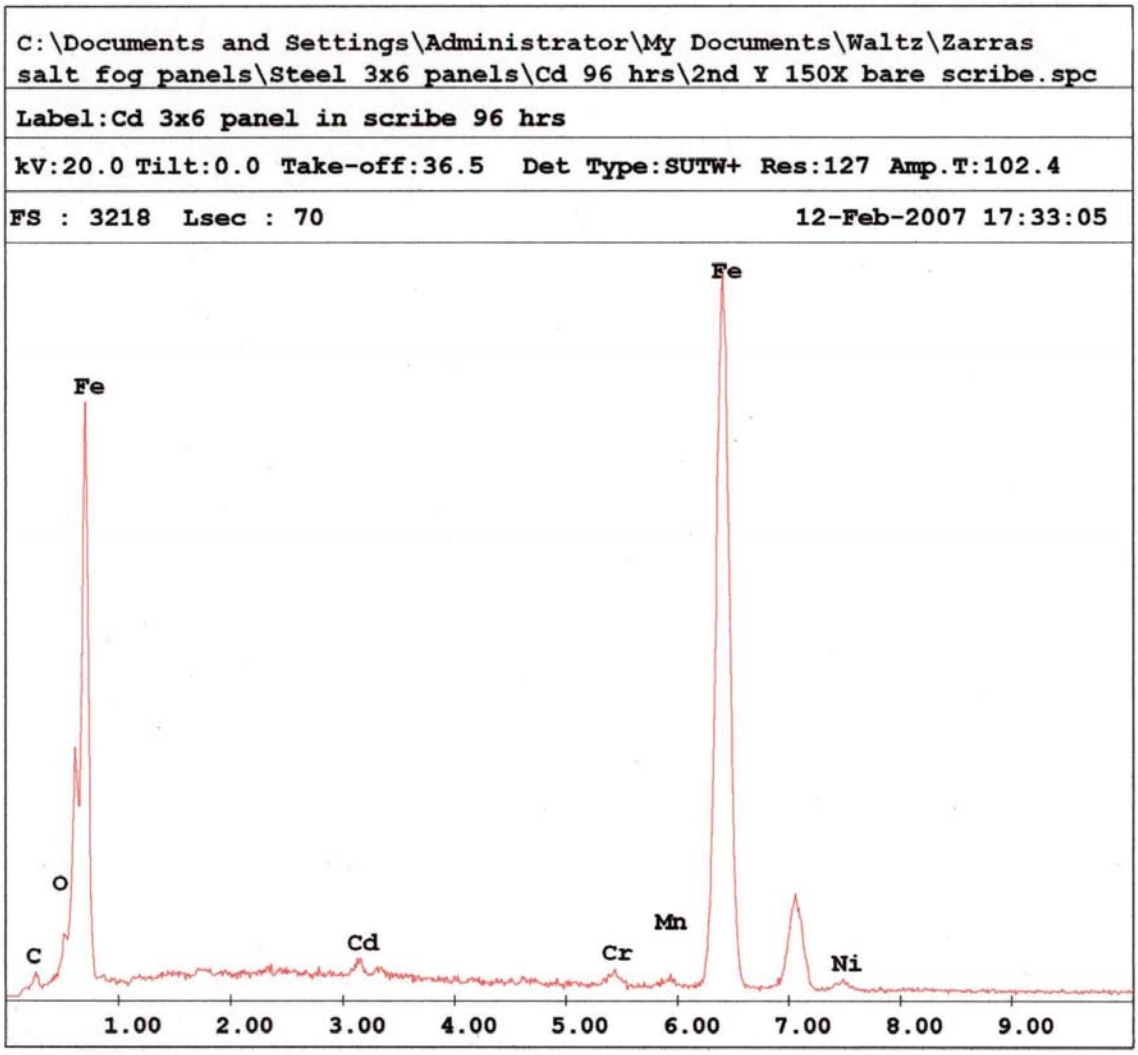

EDAX ZAF Quantification (Standardless)
Element Normalized
SEC Table : Default

Element	Wt %	At %	K-Ratio	Z	A	F
C K	4.57	17.29	0.0100	1.1710	0.1862	1.0005
O K	2.78	7.89	0.0121	1.1508	0.3748	1.0045
CdL	1.29	0.52	0.0115	0.8710	0.9934	1.0229
CrK	0.76	0.67	0.0095	0.9832	0.9892	1.2847
MnK	0.55	0.45	0.0053	0.9662	0.9956	1.0014
FeK	88.57	72.03	0.8731	0.9852	0.9986	1.0019
NiK	1.47	1.14	0.0132	1.0022	0.8961	1.0000
Total	100.00	100.00				

Figure 69: EDS Spectrum of Scribed Mark on Cd-Plated Panel After 96 Hours Exposure to Neutral Salt Fog.

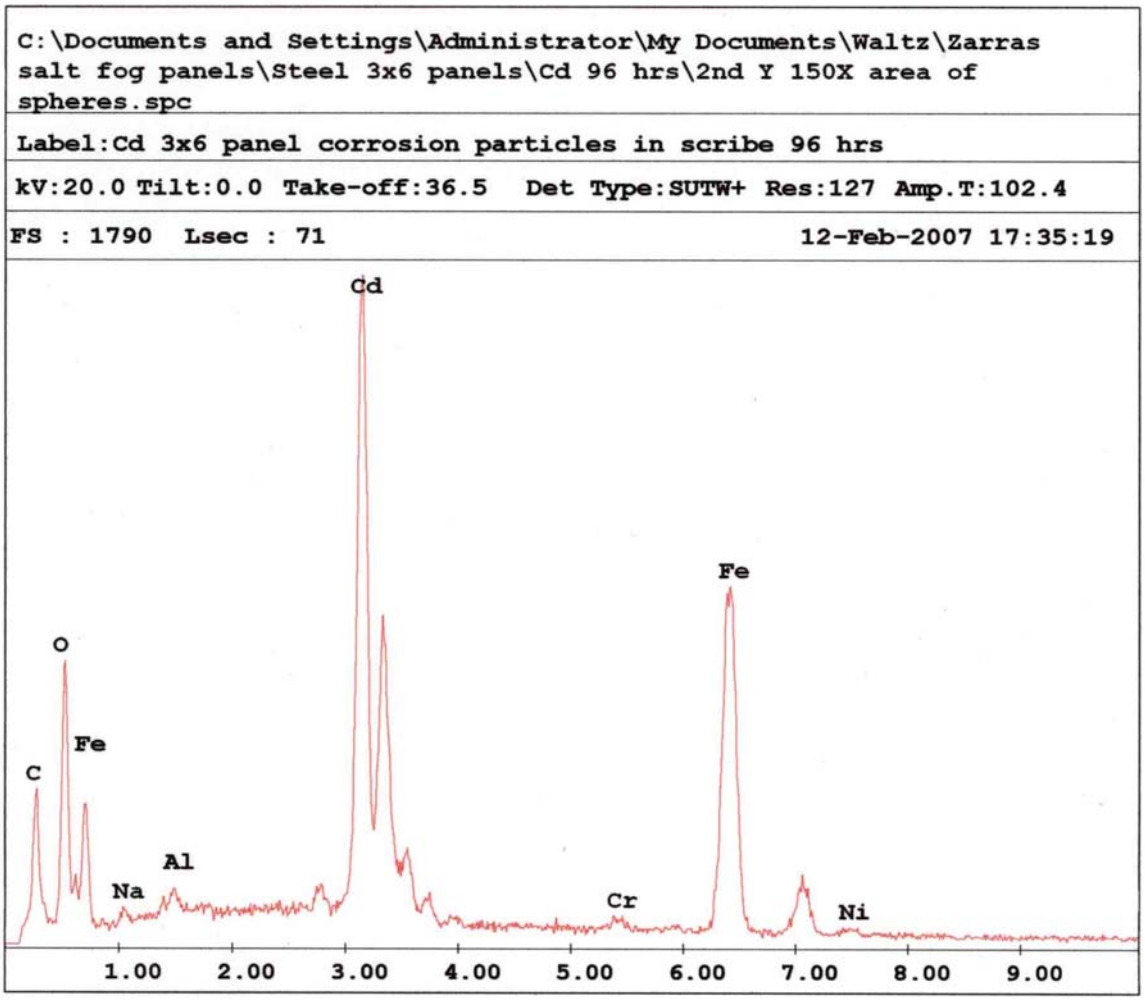

EDAX ZAF Quantification (Standardless)
Element Normalized
SEC Table : Default

Element	Wt %	At %	K-Ratio	Z	A	F
C K	13.19	35.65	0.0476	1.1579	0.3118	1.0002
O K	16.82	34.14	0.0340	1.1380	0.1776	1.0006
NaK	0.61	0.86	0.0014	1.0641	0.2138	1.0007
AlK	0.69	0.83	0.0031	1.0580	0.4250	1.0028
CdL	39.08	11.29	0.3525	0.8622	1.0405	1.0055
CrK	0.73	0.45	0.0067	0.9741	0.9166	1.0408
FeK	28.21	16.41	0.2627	0.9773	0.9520	1.0010
NiK	0.69	0.38	0.0064	0.9955	0.9400	1.0000
Total	100.00	100.00				

Figure 70: EDS Spectrum of Scribed Area of Cd-Plated Panel with Spheres Analyzed as Cadmium and Oxygen.

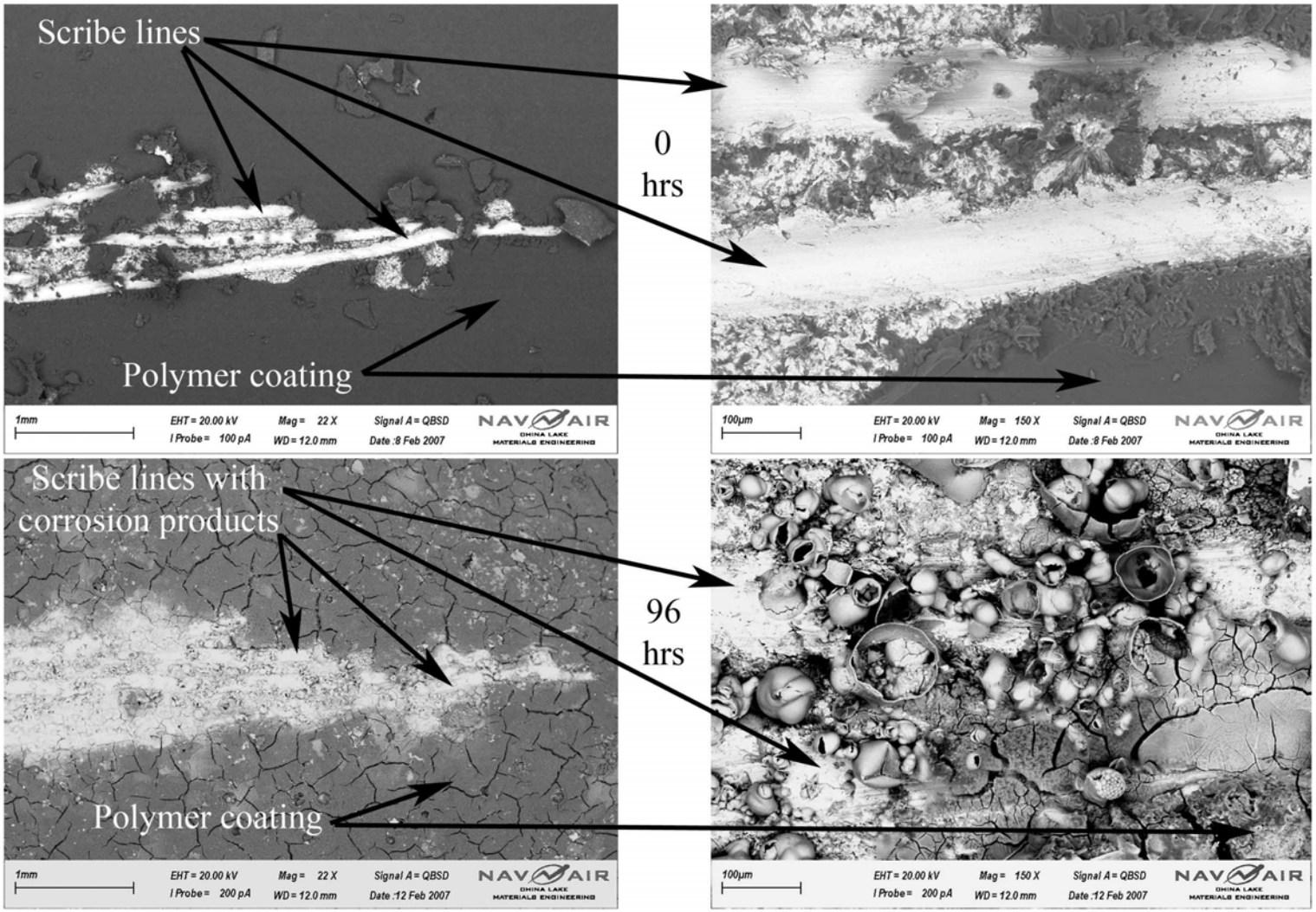

Figure 71: SEM Micrograph of Polymer Coated Panel (P(7-PHA)) As Compared to Cd-Plated Panel.

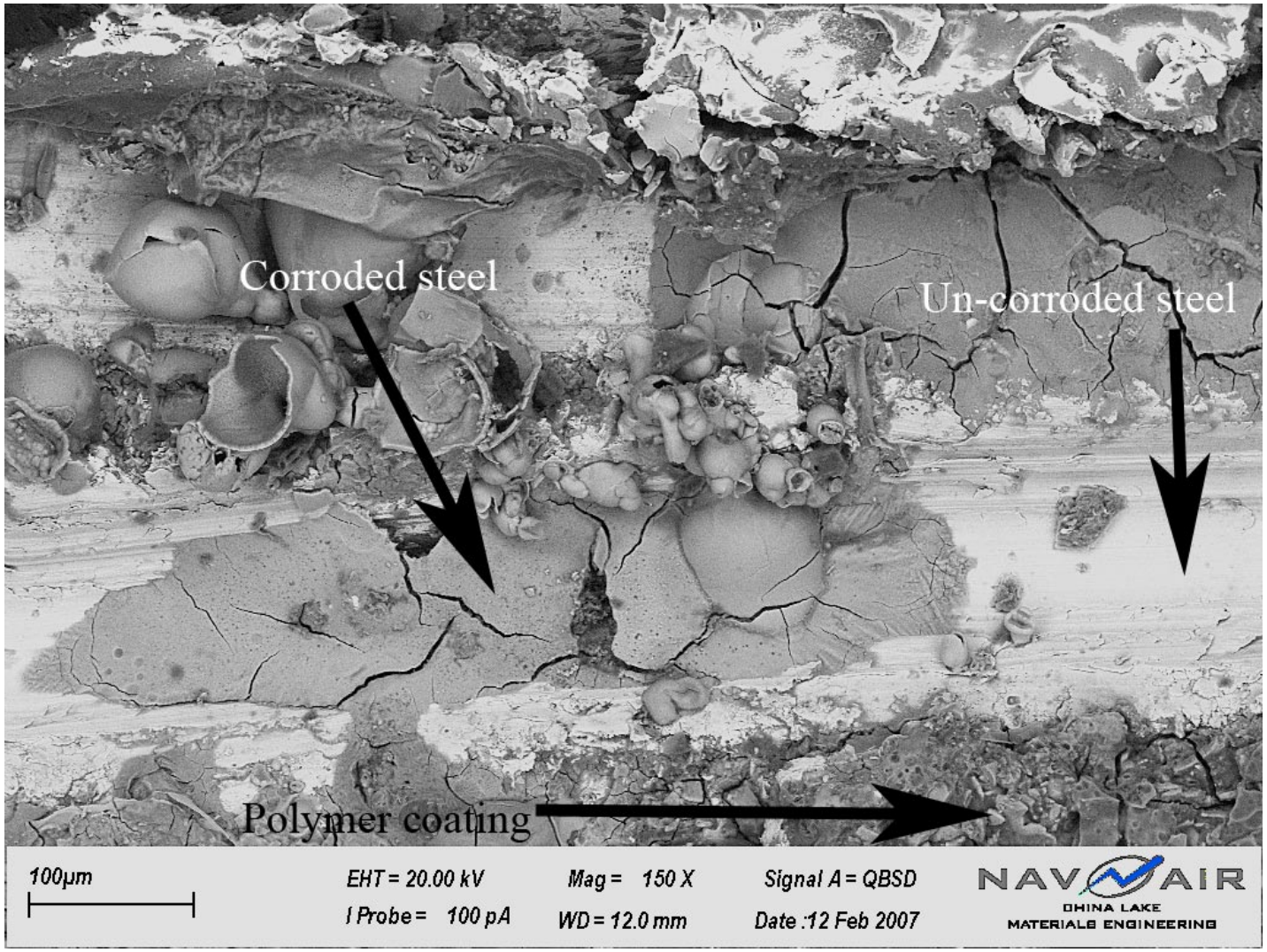

Figure 72: SEM Micrograph of Scribed Mark on P(-7PHA) Coated Panel.

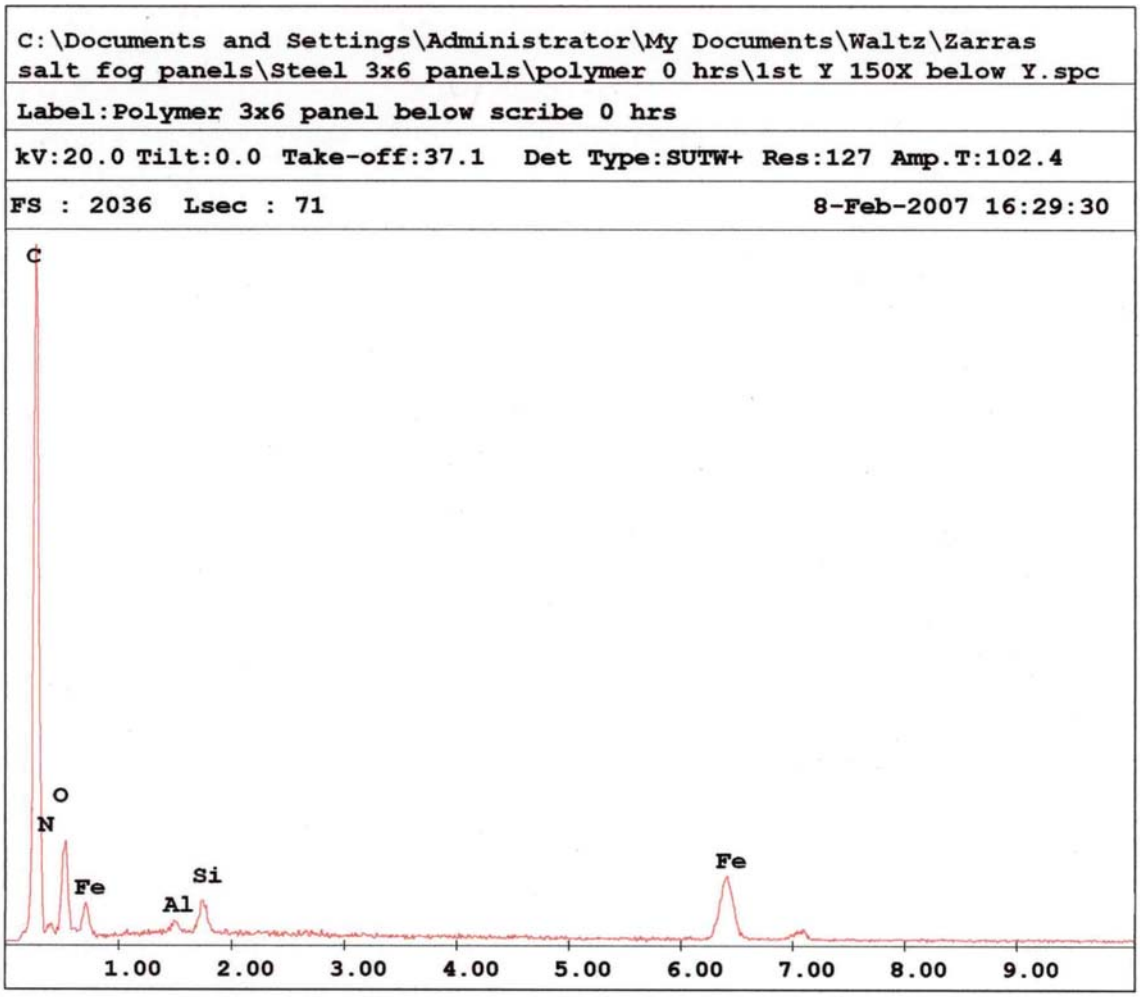

EDAX ZAF Quantification (Standardless)
Element Normalized
SEC Table : Default

Element	Wt %	At %	K-Ratio	Z	A	F
C K	68.61	78.54	0.3774	1.0173	0.5406	1.0002
N K	6.81	6.69	0.0074	1.0084	0.1072	1.0003
O K	13.66	11.74	0.0226	1.0003	0.1651	1.0003
AlK	0.38	0.19	0.0025	0.9321	0.7161	1.0006
SiK	0.98	0.48	0.0078	0.9594	0.8259	1.0003
FeK	9.55	2.35	0.0823	0.8428	1.0225	1.0000
Total	100.00	100.00				

Figure 73: EDS Spectrum of P(7-PHA) Coated Panel at 0 and 96 Hours Neutral Salt Fog Exposure.

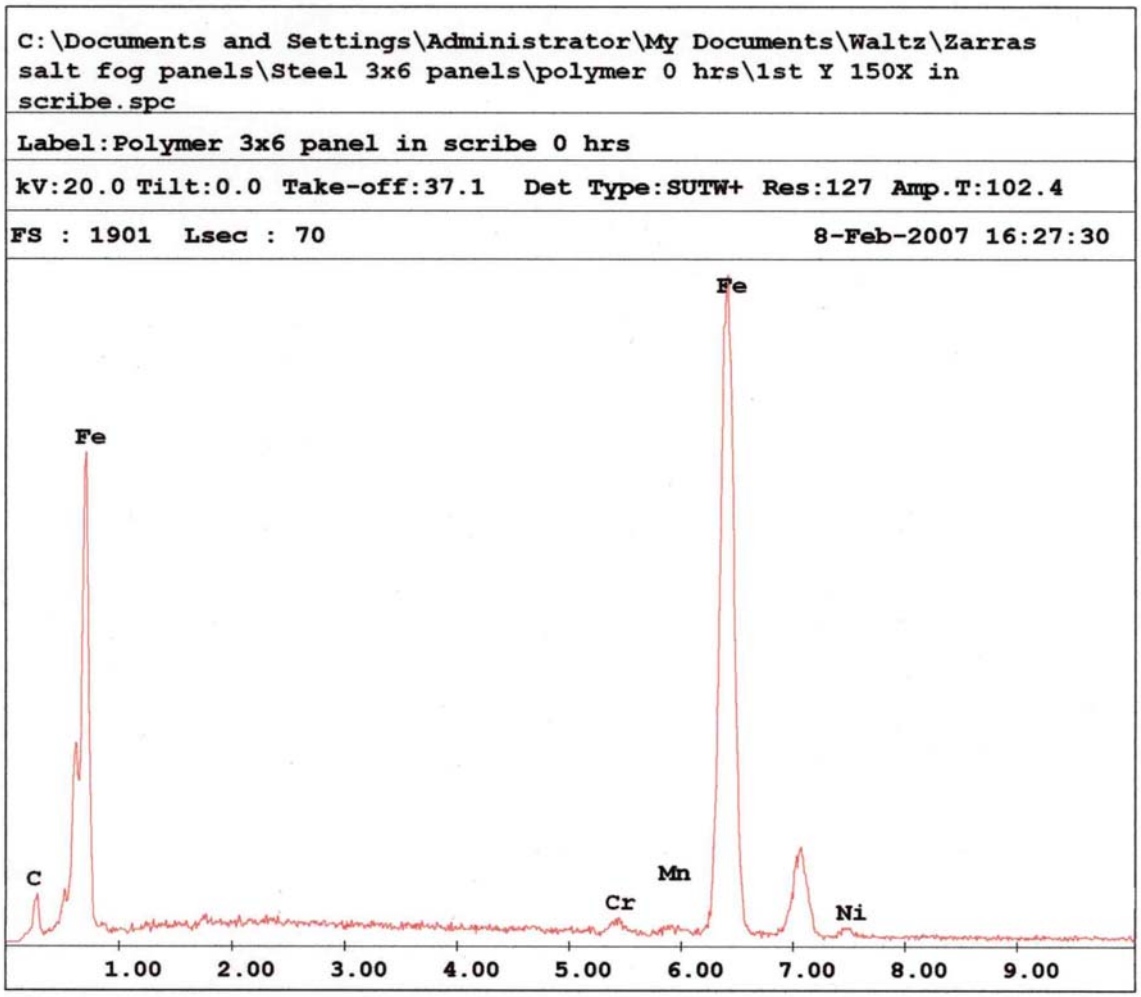

EDAX ZAF Quantification (Standardless)
Element Normalized
SEC Table : Default

Element	Wt %	At %	K-Ratio	Z	A	F
C K	10.50	35.29	0.0235	1.1613	0.1923	1.0005
CrK	0.78	0.61	0.0099	0.9745	0.9940	1.3060
MnK	0.54	0.40	0.0052	0.9575	0.9993	1.0011
FeK	87.03	62.91	0.8522	0.9762	1.0016	1.0016
NiK	1.15	0.79	0.0103	0.9928	0.9008	1.0000
Total	100.00	100.00				

Figure 74: EDS Spectrum of P(7-PHA) Before Neutral Salt Fog Exposure.

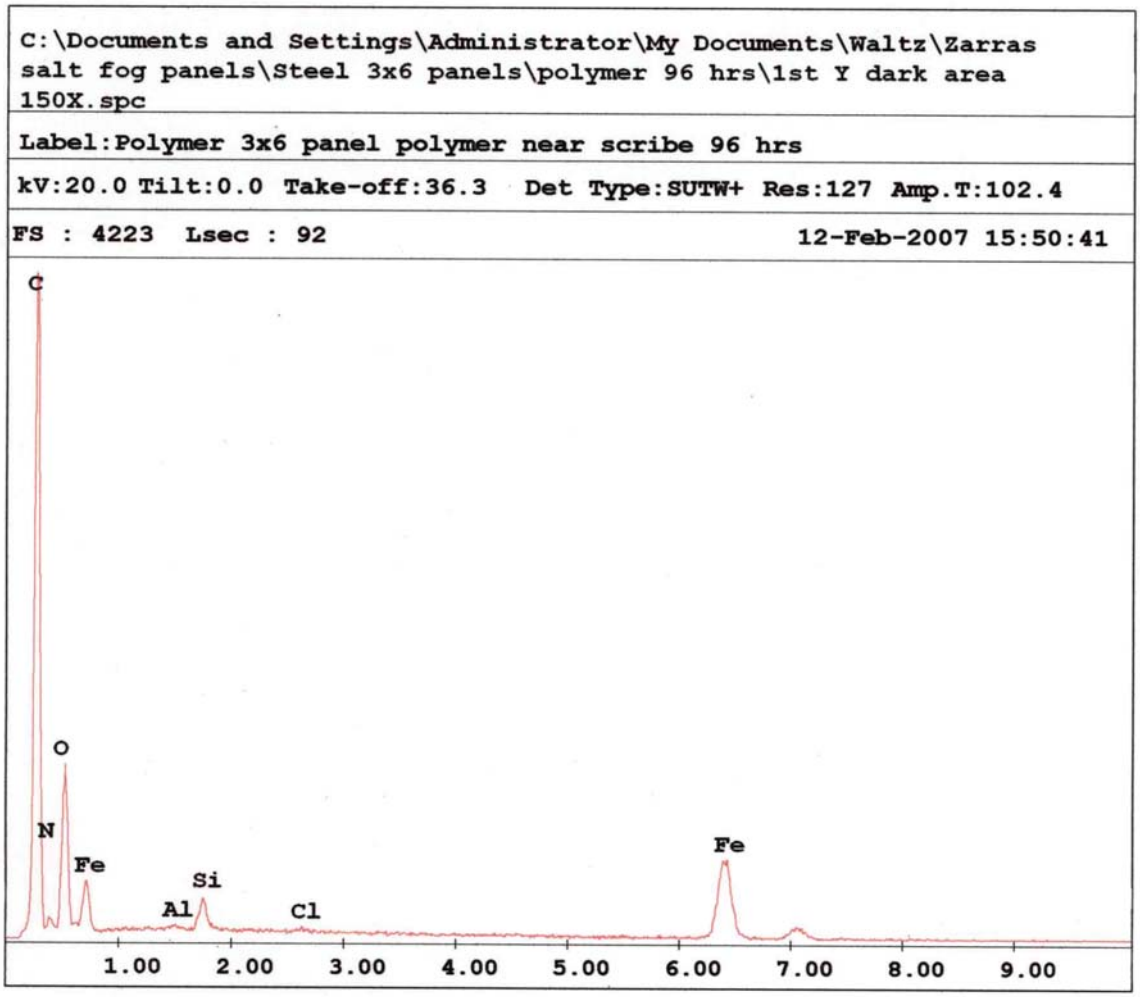

EDAX ZAF Quantification (Standardless)
Element Normalized
SEC Table : Default

Element	Wt %	At %	K-Ratio	Z	A	F
C K	63.34	74.14	0.3295	1.0196	0.5100	1.0002
N K	6.34	6.36	0.0073	1.0107	0.1136	1.0004
O K	18.55	16.30	0.0325	1.0027	0.1746	1.0003
AlK	0.10	0.05	0.0006	0.9342	0.6887	1.0005
SiK	0.77	0.38	0.0060	0.9616	0.8067	1.0004
ClK	0.13	0.05	0.0011	0.9015	0.9794	1.0026
FeK	10.77	2.71	0.0930	0.8450	1.0224	1.0000
Total	100.00	100.00				

Figure 75: EDS Spectrum of P(7-PHA) After 96 Hours Exposure to Neutral Salt Fog.

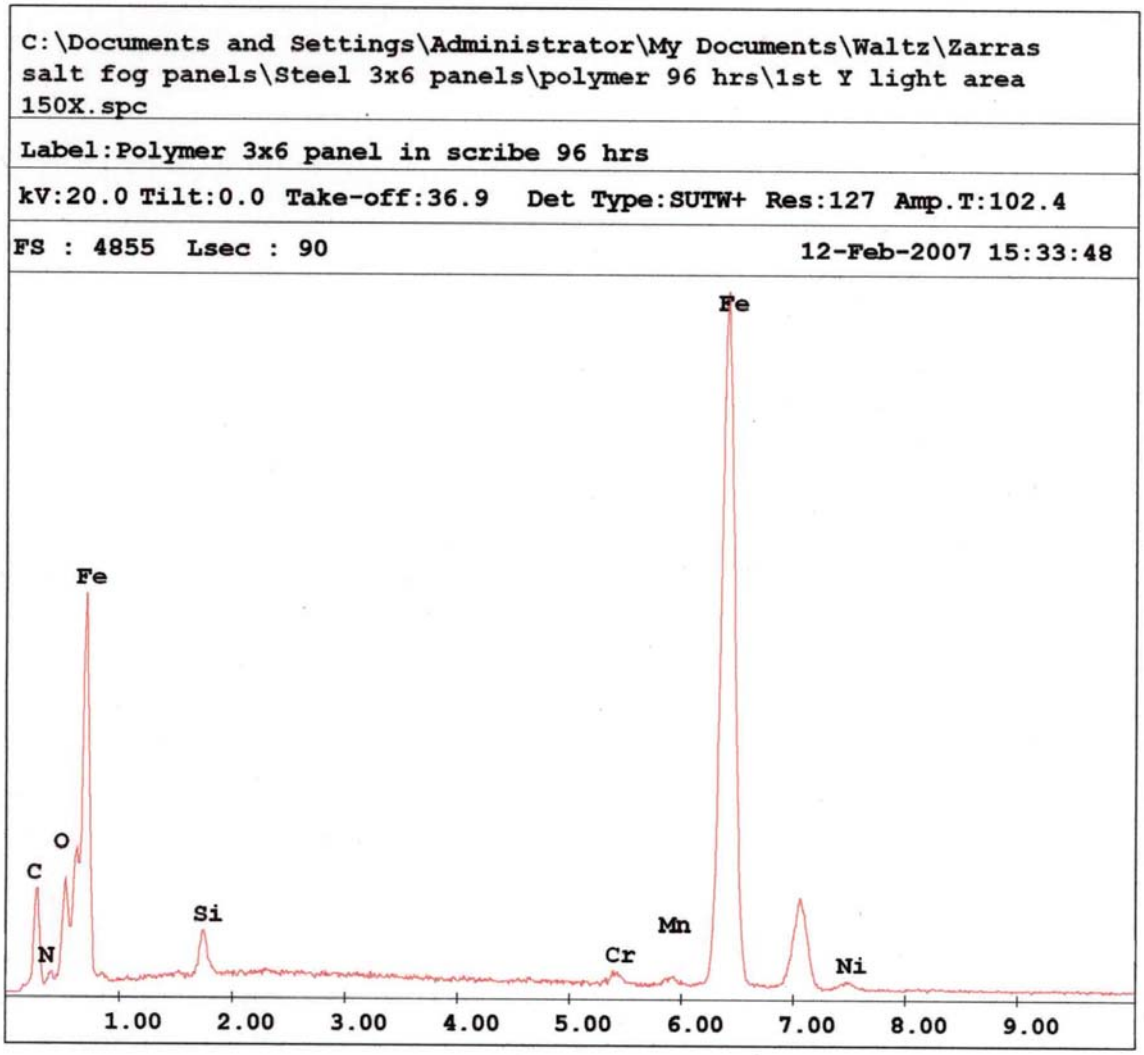

EDAX ZAF Quantification (Standardless)
Element Normalized
SEC Table : Default

Element	Wt %	At %	K-Ratio	Z	A	F
C K	17.48	43.77	0.0417	1.1279	0.2114	1.0005
N K	2.42	5.20	0.0054	1.1178	0.1996	1.0013
O K	5.33	10.02	0.0179	1.1087	0.3015	1.0031
SiK	1.38	1.48	0.0075	1.0611	0.5146	1.0012
CrK	0.72	0.41	0.0086	0.9445	0.9992	1.2775
MnK	0.71	0.39	0.0066	0.9277	1.0035	1.0013
FeK	70.80	38.13	0.6740	0.9455	1.0049	1.0019
NiK	1.16	0.60	0.0103	0.9610	0.9208	1.0000
Total	100.00	100.00				

Figure 76: EDS Spectrum of Uncorroded Areas of Sribe After 96 Hours Neutral Salt Fog Exposure.

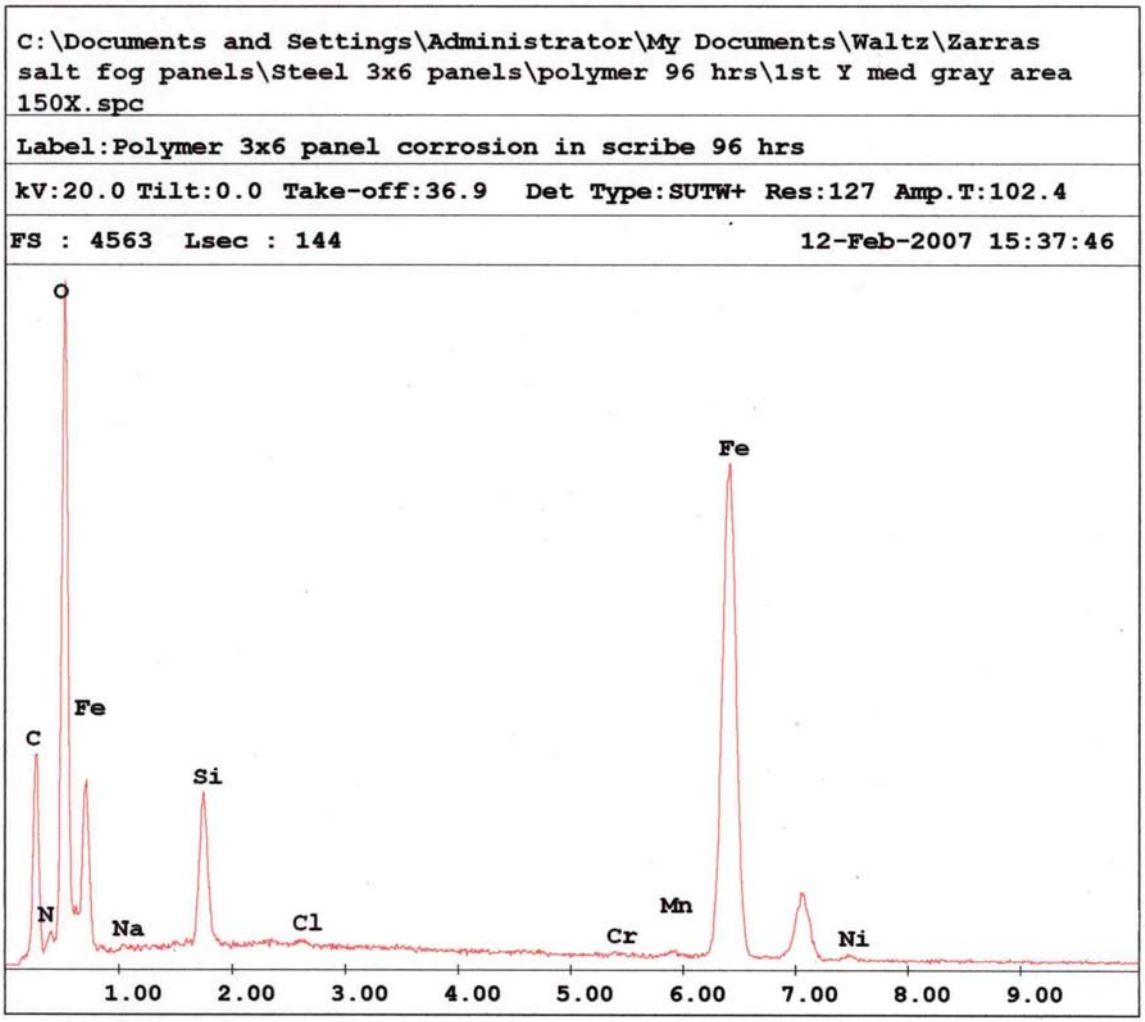

EDAX ZAF Quantification (Standardless)
Element Normalized
SEC Table : Default

Element	Wt %	At %	K-Ratio	Z	A	F
C K	23.67	41.03	0.0652	1.0736	0.2565	1.0005
N K	3.54	5.26	0.0073	1.0641	0.1940	1.0012
O K	27.23	35.44	0.0841	1.0555	0.2921	1.0013
NaK	0.14	0.13	0.0003	0.9877	0.2352	1.0002
SiK	3.22	2.38	0.0200	1.0112	0.6135	1.0009
ClK	0.10	0.06	0.0009	0.9561	0.8666	1.0057
CrK	0.16	0.07	0.0018	0.8954	1.0088	1.2110
MnK	0.38	0.15	0.0034	0.8789	1.0110	1.0008
FeK	41.07	15.31	0.3724	0.8953	1.0118	1.0012
NiK	0.49	0.17	0.0043	0.9088	0.9602	1.0000
Total	100.00	100.00				

Figure 77: EDS Spectrum of Uneven Corrosion Along Scribed Mark on P(7-PHA) Coated Steel Substrate.

Inductively Coupled Plasma Atomic Emission Spectroscopy (ICP-AES) and Ion Chromoatography (IC) Analysis of Salt Fog Panel Rinse Samples

Table 9 presents the results of both the ion and metals analyses. The first set of samples, those coated with P(7-PHA), were rinsings from four time intervals during which it was exposed to salt fog. The second set of samples were rinsings from the panel coated with cadmium taken at the same time intervals. The panel coated with cadmium was not analyzed for nitrate ions.

No chromium was detected in any of the samples. Only the rinsate taken at 96 hours from the polymer coated panel showed the presence of cadmium at 0.203 ppm. That same panel showed an increase in iron concentration in the rinsate over 72 hours, but then dropped off at the 96 hour mark. Nitrate was detected in all four washings. An initial value of 11.3 ppm was measured before the panel was even placed in the salt fog chamber. A high of 36.9 ppm was measured in the 19 hour rinse and successively dropped off in the next two samples to 25.6 and 14.3 ppm respectively. The nitrate ion is a known corrosion inhibitor. By coupling the redox properties of electroactive polymers with a known corrosion inhibitor, a controlled release mechanism of the nitrate ion into the scribed area is possible. A continuous release is averted due to the electroactive polymer system responding to the corroding metal and selectively releasing ions to prevent further corrosion.

The cadmium coated panel showed the presence of cadmium in all of the rinses. The cadmium concentration reached a high of 3.80 ppm in the 19 hour rinse, but then dropped off over the next two rinses to concentrations on the order of 0.5 ppm.

Table 9: Metal and Ion Results from Rinsates Before and After Exposure to Neutral Salt Fog Spray

Sample	Vol (ml)	Cadmium (mg/L)	Chromium (mg/L)	Iron (mg/L)	Nitrate as NO_3 (mg/L)
P(7-PHA) T=0 hours	20	nd	nd	nd	11.3
P(7-PHA) T=19 hours	20	nd	nd	4.72	36.9
P(7-PHA) T=72 hours	20	nd	nd	4.89	25.6
P(7-PHA) T=96 hours	20	0.203	nd	2.79	14.3
Cd Coated Steel T=0 hours	20	0.115	nd	nd	n/a
Cd Coated Steel T=19 hours	20	3.80	nd	nd	n/a
Cd Coated Steel T=72 hours	20	0.455	nd	nd	n/a
Cd Coated Steel T=96 hours	20	0.639	nd	nd	n/a

nd = non detect, < 100 ppb

Section VI

Conclusions:

The synthesis and characterization of novel polythiophenes and polypyrroles compounds for improved corrosion inhibition and lubricity was accomplished during this SERDP SEED study. A combination of NMR, IR, and cyclic voltametry was used to confirm that these materials were produced and attached onto the high strength steel surface. Application of the polymers onto steel substrates via air-brush and electroless deposition does not introduce toxic metals into the coated articles. The process has been shown to be an environmentally benign "green" alternative to the current use of Cd plating baths for high strength steel.

Several tests were performed on the EAP coated high strength steel specimens, with comparisons to Cd-based coatings and other alternative coating materials, in order to elucidate key structure-property relationships. Test results verified that no hydrogen embrittlement of the high strength steel samples results from using the electroless deposition process. Galling experiments showed that at least one EAP-based system containing a hard particle additive (embedded fumed silica) produced improved galling resistance when compared to IVD-Aluminum (though not cadmium), despite exhibiting limited lubricity. None of the EAP systems investigated provided corrosion protection exceeding cadmium-based coatings (>96 hours). One sample of pyrrole based system reached 96 hours of neutral salt fog exposure without significant corrosion. This specific polymer system did meet the minimum military requirement for alternatives to Cd replacement coatings on high strength steel substrates.

The corrosion inhibiting ability of the films was strongly correlated to film quality, with defects due to flaking or pin-holes limiting the corrosion inhibiting properties of the EAP-based systems. Improvements in film quality due to increased chain length on the pyrrole monomers produced films with significantly improved corrosion inhibition. EDS and SEM analysis of a scribed high strength steel panel coated with P(7-PHA) and doped with nitrate ions inhibited corrosion for 96 hours. The corrosion inhibiting qualities of the films were limited with several areas of the scribe showing signs of corrosion. In addition, the pretreatment silane compound was hydrophilic and slowly dissolved upon exposure to neutral salt fog spray. An improvement in the hydrophobicity of the silane group combined with the long chain-alkyl pyrrole polymer system would provide significantly improved corrosion inhibition on high strength steels.

Section VII

References:

1. IARC, "Beryllium, Cadmium, Mercury and Exposures in the Glass Manufacturing Industry," *IARC Monogr. Eval. Carcinog. Risks Hum*., **58**, 119-237 (1993).
2. Waalkes, M. P., Infante, P., and Huff, J., "The Scientific Fallacy of Route Specificity of Carcinogenesis with Particular Reference to Cadmium," *Regu. Toxicol. Pharmacol*., **20**, 119-121 (1994).
3. Cherian, M. G., Howell, S. B., Imura, N., Klaasaen, C. D., Koropatnick, J., Lazo, J. S., and Waakles, M. P., "Role of Meallothionein in Carcinogenesis," *Toxicol. Appl. Pharmacol.*, **126**, 1-5 (1994).
4. NIOSH 1997 -Cadmium –NS http://www.nsc.org/library/chemical/cadmium.htm.
5. Smith, C. J. E. and Baldwin, K. R., "Some Cadmium Replacements for Use on Aircraft Components, "*Product Finishing, (London) UK*, **45(6)**, 12-18, (1992).
6. FY98 Secretary of Defense Environmental Security Award, Award Category, Pollution Prevention–Weapons System Acquisition Team https:// www.denix.osd.mil/denix/public/news/earthday99/awards99/afaeronautical/aeronautical.html, referenced December 3, 2002.
7. *Guidance for Eliminating Cadmium from US Army Weapons Systems*, prepared by US Acquisition Pollution Prevention Support Office, April 1996.
8. *Alternative Surface Coatings and Surface Treatments for Hazardous Cadmium Plating of Small Parts*, prepared by Rosenblatt M. and Son, Inc., Arlington, VA September 30, 1995.
9. *Active JTEG Project Summaries*, Depot Maintenance Technology Projects, Project 020303, "Cadmium Alternatives for Fasteners, Updated March 2002. Http://www.jdmag.wpafb.af.mil/projects2.htm, referenced, December 3, 2002.
10. *The Pollution Prevention Pillar*, the Department of Defense Environmental Quality Technology Program (EQT), http://www.enviro.nfesc.navy.mil/p2library/cd/docs/dodoc/grnkpp.html, referenced December 3, 2002.
11. Shaw, G., *Long-Term Performance of Cadmium Alternatives*, US Army Tank Automotive and Armaments Command, Warren, MI, 48397-5000, February 1999, pp. 1-18.
12 Scheer, A., "Tin-Zinc as a Replacement for Cadmium," Burbank Plating Service Corp., Pacoima, CA 91331, January 2000, pp. 1-2.
13. Thompson, K. G., Byran, C. J., Benicewicz, B. C., and Wrobleski, D. A., Los Alamos National Laboratory Report, LA-UR-92-360 (1991).
14. Wrobleski, D. A., Benicewicz, B. C., Thompson, K. G., and Byran, B. J., "Corrosion Resistant Coatings from Conductive Polymers," *Polym. Prepr*., **35(1),** 265-266, (1994).
15. Jain, F. C., Rosato, J. J., Kolonia, K. S., and Argarwala, V. S., "Formation of an Active Electronic Barrier at Al/Semiconductor Interfaces: A Novel Approach in Corrosion Protection," *Corrosion-NACE*, **42(12**), 700-707 (1986).
16. Beard, B. C., and Spellane, P., "XPS Evidence of Redox Chemistry Between Cold Rolled Steel and Polyaniline, " *Chem. Mater*., **9**, 1949-1953 (1997).

17. Wessling, B., "From Conductive Polymers to Organic Metals," *Chemical Innovation,* pp. 35-40, January 2001.
18. Anderson, N., Irvin, D. J., Webber, C., Stenger-Smith, J. D., and Zarras, P., "Scale-up and Corrosion Inhibition of Poly (bis-(dialkylamino)phenylene vinylene)s," *Polym. Mater.: Sci. Eng*., **86**, 6-7, (2002).
19. Yang, S. C., Brown, R., Racicot, R., Lin, Y., and McClarnon, F., "Electroactive Polymer for Corrosion Inhibition of Aluminum Alloys," *Polymer Preprints*, **41(2**), 1776-1777 (2000).
20. Ren, S., and Barkey, D., "Electrochemically Prepared Poly(3-methylthiophene) Films for Passivation of 430 Stainless Steel," *J. Electrochem. Soc*., **139(4),** 1021-1026 (1992).
21. DeBerry, D. W., "Modification of the Electrochemical and Corrosion Behavior of Stainless Steels with an Electroactive Coating," *J. Electrochem. Soc*.: *Electrochemical Science and Technology*, **132(5),** 1022-1026, (1985).
22. Zarras, P. Anderson, N.,Webber, C., Guenthner, A., Prokopuk N. and Stenger-Smith, J. D., "Novel Conjugated Polymers Based on Derivatives of Poly(phenylene vinylene)s as Corrosion Protective Coatings in Marine Environments,"*PACE Conference Proceedings*, Chapter 14, p. 175-182, September 8-9, 2004, Cologne, Germany
23. Pickett, C. J. and Ryder, K. S., "Bioinorganic Reaction Centers on Electrodes. Modified Electrodes possessing Amino Acid, Peptide and Ferredoxin type Groups on a Poly(pyrrole) Backbone," *J. Chem. Soc., Dalton Trans*., **14**, 2181 (1994).
24. Blume, R. C. and Lindwall, H. G., Formylation and Cyanoethylation of Substituted Indoles, *J. Org Chem*., **10(3)**, 255 (1945).
25. Clemo, G. R. and Walton, E., "Some Properties and Reactions of β-chloroethyl, β-cyanoethyl, and β-carbethoxyethyl toluene-p-sulphonates Including an Extension of the Friedel-Crafts Reaction, " *J. Chem. Soc*., 723, (1928).
26. Willicut, R. J. and McCarley, R. L., "Surface-Confined Monomers on Electrode Surfaces 1. Electrochemical and Microscopic Characterization of ω-(N-Pyrrolyl)alkanethiol Self-Assembled Monolayers on Au," *Langmuir,* **11**, 296 (1995).
27. McCarley, R. L. and Willicut, R. J., Tethered Monolayers of Poly((N-pyrrolyl)alkanethiol) on Au, *J. Am. Chem. Soc*., **120**, 9296 (1998).
28. Friedman, L. and Shechter, H. "Preparation of Nitriles from Halides and Sodium Cyanide. An Advantageous Nucleophilic Displacement in Dimethyl Sulfoxide," *J. Org. Chem*., **25(6)**, 877 (1960).
29. Smiley, R. A. and Arnold, C., "Aliphatic Nitriles from Alkyl Chlorides," *J. Org Chem.*, **25,** 257 (1960).
30. Kim, B..-K., Chen, L., Gong, J., and Osada, Y., "Titration Behavior and Spectral Transitions of Water-Soluble Polythiophene Carboxylic Acids," *Macromolecules*, **32**, 3964 (1999).
31. Kuhn, H. H., Child, A. D. and Kimbrell, W. C., *Syn. Met*., **71**, 2139 (1995).
32. Zarras, P, Anderson, N, Webber, C, Guenthner, A, Prokopuk, N, and Stenger-Smith, J. D., "Novel Conjugated Polymers Based on Derivatives of Poly(Phenylene Vinylene)s as Corrosion Protecrtive Coatings in Marine Environments," *PACE 2004*, September 8-9, 2004, Cologne, Germany, Paper 14, p. 175.

33. Zarras, P., He, J., Tallman, D. E., Anderson, N., Guenthner, A., Webber, C., Stenger-Smith, J. D., Pentony, J. M., "Electroactive Polymer Coatings as Replacements for Chromate Conversion Coatings," in *Smart Coatings,* ed. T. Provder and J. Baghdachi, , ACS Symposium Book Series 957, American Chemical Society, Washington DC, 2007, Chapter 10, pp. 135-152.
34. Biallozor, S., and Kupniewska, A., *Syn. Met.*, **155,** 443, (2005).
35. Foitzik, R. C., Kaynak, A., and Pfeffer, F. M., and Beckman, J., *Syn. Met.*, **156**, 1333 (2006).
36. Snavely, C. A., Faust, C. L., *G: Oxide Removal, Chapter 3: Metal Surface Preparation and Cleaning*, in Electroplating Engineering Handbook, ed. Lawrence J. Durney, Van Nostrand Reinhold Company, New York, 1984, pp. 159-175.

Section VIII

List of Papers/Presentations:

1. P. Zarras, A. Guenthner, D. J. Irvin, S. Hawkins, M. Baronowski, J. Baronowski and J. Hibbs, *Microparticle Additives Embedded into Electroactive Polymer (EAP) Coatings for Improved Lubricity on High Strength Steel*, ACS Polymer Preprints, **47(2)**, 884-885 (2006).

2. P. Zarras, A. Guenthner, D. J. Irvin, S. Hawkins, M. Baronowski, J. Baronowski, J. Hibbs, F. Mansfeld, E. Kus, L. Raymond and T. Chao, *Electroactive Polymers As Environmentally Benign Coating Replacements for Cadmium Plating on High Strength Steels,* SERDP/ESTCP Technical Symposium and Workshop, Marriot Wardham Park Hotel, Washington DC, November 28-30, 2006.

3. Peter Zarras, Nicole Anderson, Cindy Webber, Andrew Guenthner, David J. Irvin, John D. Stenger-Smith, Samantha Hawkins, Lawrence Baldwin, Meghan Baronowski, John Baronowski and Joe Hibbs, *Electroactive Polymers (EAPs) As Alternatives Coatings for Chromium and Cadmium Based Pretreatment and Primer Coatings,* IUMACRO'07, Polytechnic University, Brooklyn, New York, June 10-13, 2007.

4. Peter Zarras, Nicole Anderson, Cindy Webber, Andrew Guenthner, David J. Irvin, John D. Stenger-Smith, Samantha Hawkins, Lawrence Baldwin, Meghan Baronowski, John Baronowski and Joe Hibbs, *Electroactive Polymers (EAPs) as Alternative Pretreatment Replacement Coatings for Chromium and Cadmium Based Coatings,* European Coatings Conference, Berlin, Germany June 14-15, 2007.